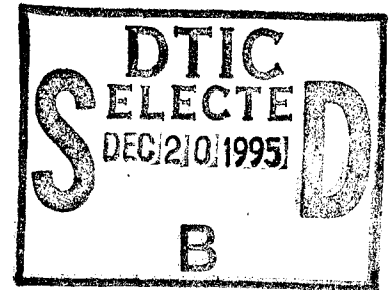


CHARACTERIZATION AND TESTING OF NOVEL TWO-PHASE WORKING FLUIDS FOR SPACECRAFT THERMAL MANAGEMENT SYSTEMS OPERATING BETWEEN 300°C AND 400°C

L.R. Grzyll
D.D. Back
C. Ramos
N.A. Samad

Chemical Systems Division
Mainstream Engineering Corporation
200 Yellow Place
Rockledge, FL 32955



December 1994

Final Report

19951218 131

Distribution authorized to U.S. Government Agencies and their contractors only; Critical Technology; December 1994. Other requests for this document shall be referred to AFMC/STI.

WARNING - This document contains technical data whose export is restricted by the Arms Export Control Act (Title 22, U.S.C., Sec 2751 *et seq.*) or The Export Administration Act of 1979, as amended (Title 50, U.S.C., App. 2401, *et seq.*). Violations of these export laws are subject to severe criminal penalties. Disseminate IAW the provisions of DoD Directive 5230.25 and AFI 61-204.

DESTRUCTION NOTICE - For classified documents, follow the procedures in DoD 5200.22-M, Industrial Security Manual, Section II-19 or DoD 5200.1-R, Information Security Program Regulation, Chapter IX. For unclassified, limited documents, destroy by any method that will prevent disclosure of contents or reconstruction of the document.

DTIC QUALITY INSPECTED 1



PHILLIPS LABORATORY
Space and Missiles Technology Directorate
AIR FORCE MATERIEL COMMAND
KIRTLAND AIR FORCE BASE, NM 87117-5776

PL-TR--95-1089

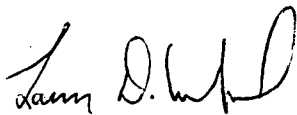
This final report was prepared by Chemical Systems Division Mainstream Engineering Corporation, Rockledge, FL under contract F29601-92-C-0049, Job Order 8809TF01. The Laboratory Project Officer-in-Charge was Larry Crawford (VTPT).

When Government drawings, specifications, or other data are used for any purpose other than in connection with a definitely Government-related procurement, the United States Government incurs no responsibility or any obligation whatsoever. The fact that the Government may have formulated or in any way supplied the said drawings, specifications, or other data, is not to be regarded by implication, or otherwise in any manner construed, as licensing the holder, or any other person or corporation; or as conveying any rights or permission to manufacture, use, or sell any patented invention that may in any way be related thereto.


This report has been authored by a contractor and an employee of the United States Government. Accordingly, the United States Government retains a nonexclusive, royalty-free license to publish or reproduce the material contained herein, or allow others to do so, for the United States Government purposes.

If your address has changed, if you wish to be removed from the mailing list, or if your organization no longer employs the addressee, please notify PL/VTPT, Kirtland AFB, NM 87117-5776, to help maintain a current mailing list.

This technical report has been reviewed and is approved for publication.



LARRY D. CRAWFORD
Project Officer



DAVID KRISTENSEN, Lt Col, USAF
Chief, Space Power and Thermal
Management Division

FOR THE COMMANDER



HENRY L. PUGH, JR., Col, USAF
Director of Space and Missiles Technology

DO NOT RETURN COPIES OF THIS REPORT UNLESS CONTRACTUAL OBLIGATIONS OR NOTICE ON A SPECIFIC DOCUMENT REQUIRES THAT IT BE RETURNED.

The following notice applies to any unclassified (including originally classified and now declassified) technical reports released to "qualified U.S. contractors" under the provisions of DoD Directive 5230.25, Withholding of Unclassified Technical Data From Public Disclosure.

NOTICE TO ACCOMPANY THE DISSEMINATION OF EXPORT-CONTROLLED TECHNICAL DATA

1. Export of information contained herein, which includes, in some circumstances, release to foreign nationals within the United States, without first obtaining approval or license from the Department of State for items controlled by the International Traffic in Arms Regulations (ITAR), or the Department of Commerce for items controlled by the Export Administration Regulations (EAR), may constitute a violation of law.
2. Under 22 U.S.C. 2778 the penalty for unlawful export of items or information controlled under the ITAR is up to two years imprisonment, or a fine of \$100,000, or both. Under 50 U.S.C., Appendix 2410, the penalty for unlawful export of items or information controlled under the EAR is a fine of up to \$1,000,000, or five times the value of the exports, whichever is greater; or for an individual, imprisonment of up to 10 years, or a fine of up to \$250,000, or both.
3. In accordance with your certification that establishes you as a "qualified U.S. Contractor", unauthorized dissemination of this information is prohibited and may result in disqualification as a qualified U.S. contractor, and may be considered in determining your eligibility for future contracts with the Department of Defense.
4. The U.S. Government assumes no liability for direct patent infringement, or contributory patent infringement or misuse of technical data.
5. The U.S. Government does not warrant the adequacy, accuracy, currency, or completeness of the technical data.
6. The U.S. Government assumes no liability for loss, damage, or injury resulting from manufacture or use for any purpose of any product, article, system, or material involving reliance upon any or all technical data furnished in response to the request for technical data.
7. If the technical data furnished by the Government will be used for commercial manufacturing or other profit potential, a license for such use may be necessary. Any payments made in support of the request for data do not include or involve any license rights.
8. A copy of this notice shall be provided with any partial or complete reproduction of these data that are provided to qualified U.S. contractors.

D E S T R U C T I O N N O T I C E

For classified documents, follow the procedures in DoD 5200.22-M, Industrial Security Manual, Section II-19 or DoD 5200.1-R, Information Security Program Regulation, Chapter IX. For unclassified, limited documents, destroy by any method that will prevent disclosure of contents or reconstruction of the document.

DRAFT SF 298

1. Report Date (dd-mm-yy) December 1994		2. Report Type Final		3. Dates covered (from... to) 6/92 to 12/94	
4. Title & subtitle Characterization and Testing of Novel Two-Phase Working Fluids for Spacecraft Thermal Management Systems Operating Between 300°C and 400°C				5a. Contract or Grant # F29601-92-C-0049	
				5b. Program Element # 62601F	
				5c. Project # 8809	
6. Author(s) L.R. Grzyl D.D. Back C. Ramos N.A. Samad				5d. Task # TF	
				5e. Work Unit # 01	
				8. Performing Organization Report #	
7. Performing Organization Name & Address Chemical Systems Division Mainstream Engineering Corporation 200 Yellow Place Rockledge, FL 32955				10. Monitor Acronym	
9. Sponsoring/Monitoring Agency Name & Address Phillips Laboratory 3550 Aberdeen SE Kirtland AFB, NM 87117-5776					
11. Monitor Report # PL-TR-95-1089				12. Distribution/Availability Statement Distribution authorized to U.S. Government agencies and their contractors only; Critical Technology; December 1994. Other requests for this document shall be referred to AFMC/STI.	
14. Abstract This project identified and characterized two-phase heat pipe working fluids in the 300°C to 400°C temperature range for thermal control of a sodium sulfur battery. This project involved the identification, selection, and extensive experimental evaluation of specific compounds from these two chemical families to determine their suitability for this application. Extensive literature reviews, thermophysical property surveys, and surveys of compound availability on the aromatic hydrocarbons and aromatic perfluorocarbons resulted in the selection of six promising compounds for experimental evaluation. Long term thermal stability tests were performed on each of these fluids in stainless steel gravity reflux heat pipes. Thermophysical property measurements were made for the fluids between 300°C and 400°C. Specific properties measured included liquid density, liquid viscosity, surface tension, vapor pressure, heat of vaporization, critical point, and melting point. A unique fabrication technique for stainless steel axial grooved heat pipes was also developed.					
15. Subject Terms Naphthalene, quinoline, biphenyl, o-terphenyl, decafluorobiphenyl, perfluoro-1,3,5 triphenbenzene, heat pipes, sodium sulfur battery, spacecraft thermal control.					
Security Classification of			19. Limitation of Abstract	20. # of Pages	21. Responsible Person (Name and Telephone #)
16. Report Unclassified	17. Abstract Unclassified	18. This Page Unclassified	Limited	152	Larry Crawford (505) 846-0477

CONTENTS

	<u>Page</u>
INTRODUCTION	1
SUMMARY	1
PROBLEM DESCRIPTION	3
PREVIOUS EFFORTS TO FIND SUITABLE TWO-PHASE WORKING FLUIDS	4
CONCEPTS THAT SOLVE THE PROBLEM	7
PROJECT OBJECTIVES	9
RESULTS AND DISCUSSION	11
CONTRACT KICK-OFF MEETING	11
TASK 1: LITERATURE SEARCH	11
Aromatic Hydrocarbons	11
Aromatic Perfluorocarbons	18
Figure-of-Merit	19
TASK 2: PREPARATION/PURCHASE OF COMPOUNDS	27
TASK 3: CONSTRUCT GRAVITY REFLUX HEAT PIPE APPARATUS	30
Heat Pipe Fabrication, Cleaning, and Assembly	30
Working Fluid Preparation, Evacuation, and Charging	31
Test Stand Hardware	33
Data Acquisition/Control System	33
TASK 4: GRAVITY REFLUX HEAT PIPE TESTS	35
Evaporator-Condenser Temperature Differences	37
Fluid Appearance	37
GC Analysis	38
DSC Analysis	39
UV/VIS Spectrometry	39
IR Spectrometry	40
Thermal Stability Test Conclusions	41

<input type="checkbox"/>	<input type="checkbox"/>
<input checked="" type="checkbox"/>	<input type="checkbox"/>
<input type="checkbox"/>	<input type="checkbox"/>

By _____	
Distribution/ _____	
Availability Codes	
Dist	Avail and/or Special
0-2	

CONTENTS (Concluded)

	<u>Page</u>
TASK 5: WORKING FLUID CHARACTERIZATION	42
Immersion Bath	42
Critical Point	42
Liquid Density	43
Liquid Viscosity	45
Surface Tension	54
Vapor Pressure and Heat of Vaporization	61
Liquid Thermal Conductivity	73
Figures-of-Merit	76
TASK 6: CONSTRUCT PROTOTYPE HEAT PIPE	81
Heat Pipe Test Stand Design Concept	81
Design and Fabrication of Prototype Heat Pipe	83
TASK 7: HEAT PIPE PERFORMANCE TESTING	85
TASK 8: PREPARATION OF TWO-PHASE DESIGN MANUAL	85
RECOMMENDATIONS FOR FURTHER WORK	91
CONCLUSIONS	93
REFERENCES	95
APPENDIXES	
A. GRAVITY REFLUX HEAT PIPE TEST RESULTS	102
B. SURFACE TENSION FORTRAN PROGRAM	111
C. PROTOTYPE HEAT PIPE DESIGNS	117
D. TWO-PHASE DESIGN MANUAL	127

FIGURES

<u>Figure</u>		<u>Page</u>
1.	Calculated liquid transport factor of candidate fluids.	22
2.	Calculated vapor pressure of candidate fluids.	23
3.	Calculated kinematic viscosity ratio of candidate fluids.	24
4.	Calculated liquid thermal conductivity of candidate fluids.	25
5.	Calculated wicking height factor of candidate fluids.	26
6.	Schematic of heat pipe filling station.	32
7.	Schematic of liquid density apparatus.	43
8.	Liquid density data and curve-fit for biphenyl.	47
9.	Liquid density data and curve-fit for naphthalene.	47
10.	Liquid density data and curve-fit for quinoline.	48
11.	Liquid density data and curve-fit for o-terphenyl.	48
12.	Liquid density data and curve-fit for decafluorobiphenyl.	49
13.	Schematic of liquid viscosity apparatus.	49
14.	Liquid viscosity and curve-fit for naphthalene.	52
15.	Liquid viscosity and curve-fit for biphenyl.	52
16.	Liquid viscosity and curve-fit for o-terphenyl.	53
17.	Liquid viscosity and curve-fit for quinoline.	53
18.	Liquid viscosity and curve-fit for decafluorobiphenyl.	54
19.	Schematic of surface tension apparatus.	55
20.	Surface tension data and curve-fit for biphenyl.	59

FIGURES (Concluded)

<u>Figure</u>		<u>Page</u>
21.	Surface tension data and curve-fit for o-terphenyl.	59
22.	Surface tension data and curve-fit for naphthalene.	60
23.	Surface tension data and curve-fit for decafluorobiphenyl.	60
24.	Surface tension data and curve-fit for quinoline.	61
25.	Schematic of experimental setup.	62
26.	DSC temperature scan for naphthalene at 47.6 kPa.	64
27.	DSC temperature scan for decafluorobiphenyl at 343.4 kPa.	64
28.	DSC temperature scan for biphenyl at 1.034 MPa.	65
29.	Antoine equation curve fits and DSC pressure-temperature data for naphthalene, biphenyl, and o-terphenyl.	68
30.	Antoine equation curve fits and DSC pressure-temperature data for decafluorobiphenyl, quinoline, and perfluoro-1,3,5-triphenylbenzene.	68
31.	Antoine equation curve fits and DSC pressure-temperature data for deionized water.	69
32.	DSC temperature scan for perfluoro-1,3,5-triphenylbenzene at 343.4 kPa.	70
33.	Liquid transport factor of candidate working fluids.	77
34.	Vapor pressure of candidate working fluids.	78
35.	Kinematic viscosity ratio of candidate working fluids.	79
36.	Wicking height factor of candidate working fluids.	80

TABLES

<u>Table</u>		<u>Page</u>
1.	Property information on naphthalene.	12
2.	Property information on biphenyl.	13
3.	Property information on o-terphenyl.	14
4.	Property information on m-terphenyl.	15
5.	Property information on p-terphenyl.	16
6.	Property information on perfluoronaphthalene.	18
7.	Property information on perfluorobiphenyl.	19
8.	Data acquisition/control system configuration.	36
9.	Liquid density measurements.	46
10.	Liquid viscosity measurements.	51
11.	Surface tension measurements.	58
12.	Non-linear least squares curve fits to the Antoine equation.	67
13.	Enthalpy of vaporization data from Antoine and Clapeyron.	72
14.	Comparison of measured melting points to literature values.	72
15.	Results of liquid thermal conductivity characterizations.	75
16.	Fitted constants for Antoine equation.	85
17.	Fitted constants for liquid density equation.	86
18.	Fitted constants for surface tension equation.	87
19.	Fitted constants for liquid viscosity equation.	88

INTRODUCTION

This project was funded under BAA 91-01 issued by the United States Air Force, Air Force Systems Command, Phillips Laboratory, Kirtland AFB, NM. The project involved the experimental characterization and testing of novel two-phase working fluids for spacecraft thermal management applications between 300°C and 400°C. The main application of these fluids will be for use in a heat pipe for thermal control of the sodium/sulfur battery (NASBAT).

SUMMARY

This project identified and characterized two-phase heat pipe working fluids in the 300°C to 400°C temperature range for thermal control of the sodium/sulfur battery. Previous work performed by Mainstream and other researchers recommended aromatic hydrocarbons and aromatic perfluorocarbons as compounds with suitable thermal stability and thermophysical property characteristics for use in this temperature range. This project involved the identification, selection, and extensive experimental evaluation of specific compounds from these two chemical families to determine their suitability for this application.

Extensive literature reviews, thermophysical property surveys, and surveys of compound availability on the aromatic hydrocarbons and aromatic perfluorocarbons resulted in the selection of six compounds for experimental evaluation under this effort: naphthalene, quinoline, biphenyl, o-terphenyl, decafluorobiphenyl, and perfluoro-1,3,5-triphenylbenzene. These compounds were procured from chemical manufacturers and were purified at Mainstream by either fractional distillation under vacuum or by multiple crystallizations from suitable solvents. The extensive purification was performed to maximize the thermal stability characteristics of the compounds.

Long-term thermal stability tests were performed on each of these fluids in stainless steel gravity reflux heat pipes. Each fluid was subjected to two temperature profiles: a constant temperature test at 350°C and a variable temperature test between 325°C and 380°C. Each test was

performed in duplicate to ensure that adequate data was collected. All fluids were tested for 230 days except for quinoline, which was tested for approximately 90 days, and perfluoro-1,3,5-triphenylbenzene, which underwent severe thermal decomposition during preliminary testing at 300°C. The heat pipe wall temperatures along the length of the pipe were monitored during the test to see if the temperature profiles changed with time, which is evidence of thermal decomposition. After the test, the fluid samples were analyzed for the presence of decomposition products by gas chromatography (GC), differential scanning calorimetry (DSC), infrared (IR) spectrometry, ultraviolet-visible (UV-VIS) spectrometry, and visual observation of fluid appearance before and after the test. Based on the results of these tests, the following thermal stability ranking was developed (from most stable to least stable): biphenyl, o-terphenyl, naphthalene, decafluorobiphenyl, quinoline, perfluoro-1,3,5-triphenylbenzene. No decomposition was detected for any of the biphenyl samples by any of the analysis methods.

Thermophysical property measurements were made for all fluids (except for perfluoro-1,3,5-triphenylbenzene) between 300°C and 400°C. Specific properties measured included liquid density, liquid viscosity, surface tension, vapor pressure, heat of vaporization, critical point, and melting point. Unique experimental methods were developed that allowed for these measurements to be made both below and above the normal boiling points of the fluids. Attempts were also made to measure liquid thermal conductivity, but these measurements resulted in large experimental errors and were therefore inconclusive. The thermophysical properties of the working fluid candidates were then used to calculate the figures-of-merit of the fluids in the 300°C-400°C temperature range.

A unique fabrication method for stainless steel axial-groove heat pipes was also developed. The fabrication method involves the use of stainless steel angle material, welded together to form a rectangular cross-section. The grooves were machined in the angle steel prior to welding. The normal method of fabricating axial grooves, extrusion, is not feasible with stainless steel. These heat pipes were manufactured, cleaned, and filled at Mainstream and delivered to the Phillips Lab for performance testing. This type of fabrication method is less costly and time-consuming

than other fabrication methods. The rectangular cross section also has heat transfer benefits over circular cross sections for heat sources and sinks with flat surfaces.

The fluid that will be performance tested in the heat pipe will be biphenyl. This fluid was selected because there were no references in the open technical literature regarding performance testing in commercial heat pipes. Biphenyl also had the highest thermal stability of all fluids tested.

Future work in this area should concentrate on three areas: 1) heat pipe performance testing of biphenyl in normal and reduced gravity, 2) refinement of the axial-groove heat pipe fabrication with stainless steel, and 3) optimization of the heat pipe design to maximize the performance of the fluids in the 300°C to 400°C temperature range. Concurrent work on all three areas will result in the demonstration of this technology to passively remove heat from the sodium/sulfur battery and transport it over a significant distance to a heat sink.

PROBLEM DESCRIPTION

In order to meet the increasingly stringent high-power, low-mass military spacecraft thermal management requirements, two-phase thermal management systems are used. These two-phase thermal management systems have lower masses, lower power requirements, and better thermal control than other types of thermal management systems. Examples of two-phase thermal management systems include heat pipes, Rankine cycles, heat pumps (reverse Rankine cycles), and two-phase pumped loops. These systems find spacecraft applications in thermal management of electronics, heat engines, other high-power devices, and in power distribution and environmental control and life support systems (ECLSS).

The various thermal management systems aboard spacecraft have many temperature ranges of operation, from cryogenic temperatures to temperatures of liquid metal use. One temperature range, 300°C to 400°C, presents problems for two-phase fluid use. No fluid has been characterized and suitably tested for this temperature range. Water, a common two-phase fluid

below 300°C, develops too high of a vapor pressure over the 300°C to 400°C temperature range and its thermal performance is low due to its approach to its critical point of 374°C. Metals are either solids in this temperature range or are liquids with too low of a vapor pressure for practical use in low-mass systems. Other fluids, such as common refrigerants or organic heat transfer fluids, suffer thermal decomposition in this temperature range.

The lack of a suitably tested and characterized two-phase working fluid for spacecraft thermal management systems in the 300°C to 400°C temperature range is adversely affecting many military and NASA projects. One specific area is thermal management of the NASBAT. The NASBAT normally operates at about 350°C and requires rejection of waste heat at this temperature to maintain its normal operating temperature. Both the Air Force and NASA are currently planning, or are in the process of, flight testing this battery. Another project being affected by the lack of a suitable two-phase for this temperature range is NASA's free-piston Stirling engine (FPSE) program. Thermal management of other high-power spacecraft components, such as thermionic or thermoelectric converters, are also being affected.

Thermal control technologies that have been considered for the NASBAT demonstration projects include systems such as liquid metal coolant loops (Ref. 1), direct heat rejection to space via louvers (Ref. 2), or cryogenic gas flooding (Ref. 3). These technologies impose weight, thermal control, and reliability penalties on the system. The use of cryogenic gas flooding or louvers may not allow the NASBAT to be radiation-hardened because it is exposed to space during heat rejection.

PREVIOUS EFFORTS TO FIND SUITABLE TWO-PHASE WORKING FLUIDS

A study by Saaski and others was performed in the late 1970s to try to find a suitable heat pipe working fluid for the 50°C to 350°C temperature range (Refs. 4-6). They investigated four classes of compounds: 1. aliphatic hydrocarbons, 2. aromatic hydrocarbons, 3. halogenated hydrocarbons, and 4. inorganic compounds. Their work investigated the theoretical aspects of working fluid decomposition, categorized and ranked compounds with similar stability

characteristics, and performed long-term reflux compatibility tests of several compounds in gravity reflux heat pipes. Their work determined that naphthalene, biphenyl, and the terphenyl isomers (ortho, meta, and para) had vapor pressure, thermal stability, and materials compatibility characteristics suitable for the 50°C to 350°C temperature range. Their work also concluded that fluorinated derivatives of these aromatic compounds offered even greater thermal stability than their hydrocarbon analogs and should be considered as heat pipe working fluids for this temperature range. Unfortunately, no thermophysical property characterizations were performed on the fluids considered.

Another study from the late 1970s performed by Kenney and coworkers (Ref. 7) involved the performance of heat pipe life tests with numerous working fluids. They studied various working fluids in stainless steel, carbon steel, and black iron gravity reflux heat pipes between 225°C and 475°C. Successful operation was obtained with biphenyl from 275°C to 400°C for over 1200 hours with no increase in the temperature difference along the length of the heat pipe. Operation above 400°C, however, resulted in fluid decomposition after 100 hours. They concluded that biphenyl would be a suitable heat pipe working fluid at temperatures below 400°C.

Mainstream has also been active in this area (Refs. 8 and 9), investigating aromatic hydrocarbons for heat pipes operating in the 175°C to 425°C temperature range. The kinematic viscosity, surface tension, corrosion properties, and thermal stability of phenol, p-cresol, aniline, biphenyl, and m-terphenyl were experimentally measured. Corrosion rates showed that biphenyl and m-terphenyl were compatible with all materials tested (aluminum 6061-T6, stainless steel T-316, nickel-200, Monel-400, Haynes-230, and titanium). Kinematic viscosity and surface tension measurements were used to calculate the liquid transport factor for the five compounds. Thermal stability results indicated that biphenyl and m-terphenyl had suitable characteristics over the 175°C to 425°C temperature range.

Thermal stability studies performed by others have shown that aromatic hydrocarbons, such as naphthalene, biphenyl, and the terphenyls, are the most stable organic compounds known. Experimental data generated by Monsanto (Ref. 10) has shown that at 350°C the amount of

liquid decomposition product generated for biphenyl is about 1 wt% over a ten-year period, and 5 wt% for m-terphenyl over a ten-year period. The decomposition products have been identified as higher-order polyphenyls and hydrogen (Refs. 11-13). The hydrogen generated during this period would diffuse through any material of construction over the ten-year period (Ref. 7). Other work has shown that 400°C is well below the thermal stability limit of naphthalene (570-650°C), biphenyl (510-540°C), and a biphenyl/terphenyl eutectic mixture (493°C) (Refs. 11-13). Polymerization rates for biphenyl were found to be insignificant at 343°C (Ref. 14). Other references show that biphenyl and terphenyl decomposition can be further minimized by using ultra-pure materials (Refs. 15 and 16).

Mainstream has also been active in the characterization and testing of novel perfluorinated hydrocarbons (perfluorocarbons) as heat transport fluids due to their high resistance to thermal decomposition (Refs. 17 and 18). Many perfluorocarbons are thermally stable to temperatures as high as 840°C, even in the presence of catalytic material, with no decomposition detected (Ref. 19). Perfluorination of a hydrocarbon has been shown to increase its thermal stability and make the compound nontoxic and nonflammable (Ref. 20). Other references have shown that perfluorinated aromatics are more thermally stable than their hydrocarbon analogs (Ref. 21), and are among the most stable organic compounds known (Ref. 13).

Further work in this area by Mainstream has shown that the thermal performance of biphenyl is superior to that of cesium for heat pipe applications at 350°C (Ref. 8). The study calculated the theoretical heat transport limitations of both fluids in an axial groove heat pipe. The theoretical heat transport limitations of both fluids were approximately equivalent. Cesium, however, has operational problems associated with its use. It has an extremely low vapor pressure at 350°C (0.9 kPa), which would favor leakage into the pipe and result in a high-mass containment structure. Cesium also reacts violently with water generating hydrogen, which would present catastrophic problem if moisture in the atmosphere leaked into the pipe. Cesium also has handling and toxicity problems that are not an issue with biphenyl.

CONCEPTS THAT SOLVE THE PROBLEM

The lack of a suitable, thermally-stable, characterized two-phase fluid for use in the 300°C to 400 °C temperature range is forcing the use of inferior thermal control technologies for spacecraft thermal management. As a solution to this problem, this project was performed to identify, test, and characterize novel compounds that have suitable characteristics for use as a two-phase working fluid in the 300°C to 400°C temperature range. Specifically, the ideal fluid would have the following characteristics.

1. The fluid should be thermally stable over the temperature range. This is the most critical characteristic. Any fluid decomposition would result in a shorter life for the thermal control system. Noncondensable gases that would be generated as a result of fluid decomposition would also result in a decrease in fluid performance and an increase in system pressure. The generation of liquid decomposition products would change the bulk thermophysical properties of the fluid over time, affecting system performance.
2. The fluid should be compatible with all construction materials of the thermal control system. Any incompatibilities can affect the lifetime and performance of the system.
3. The fluid should have suitable thermophysical properties over the temperature range. The critical properties of the fluid should allow for liquid-vapor phase change over the temperature range. The vapor pressure of the fluid should not be excessively high or low; both of which would result in high-mass containment structures. The heat of vaporization should be as high as possible to maximize the thermal performance of the fluid in the system. For heat pipe applications, the density, viscosity, and surface tension are critical in defining the heat transport capability of the fluid.
4. The fluid should preferably be nontoxic and nonflammable. For unmanned applications these characteristics are less critical, but would minimize logistical and handling concerns.

The above discussion shows that two families of compounds, aromatic hydrocarbons and aromatic perfluorocarbons, have suitable thermal stability and thermophysical characteristics for use in this temperature range. Compounds from these families were selected and experimentally investigated to determine their suitability for this temperature range. Specific aromatic hydrocarbons and perfluorocarbons of interest are naphthalene, biphenyl, the terphenyl isomers, perfluoronaphthalene, perfluorobiphenyl, the perfluorinated derivatives of the terphenyl isomers, and other perfluorinated aromatic compounds.

PROJECT OBJECTIVES

The goal of this project was to identify, test, and characterize aromatic hydrocarbons and aromatic perfluorocarbons for use as two-phase working fluids in the 300°C to 400°C temperature range. There were several technical objectives involved in the performance of this project.

1. A literature search was performed to collect as much information as possible on aromatic hydrocarbons and aromatic perfluorocarbons. The objective was to find any existing synthesis methods, thermophysical property information, thermal stability, toxicity, and handling information available on these families of compounds.
2. Vendors and custom chemical manufacturers were surveyed to identify suppliers of aromatic hydrocarbons and aromatic perfluorocarbons, or companies that could provide custom synthesis of these compounds. This information, along with the literature information collected, were used to make final selection of the compounds to be experimentally evaluated.
3. Gravity reflux heat pipes were fabricated to assess the materials compatibility and thermal stability characteristics of the compounds to be evaluated. Long-term gravity reflux heat pipe tests were performed at two temperature environments: a constant temperature test at 350°C and a variable-temperature test between 325°C and 380°C that simulated the temperature profiles of the NASBAT during operation.
4. Extensive thermophysical property characterizations were performed on the selected compounds. Properties that were experimentally characterized were vapor pressure, heat of vaporization, melting point, liquid density, liquid viscosity, and surface tension. Theoretical correlations were used to calculate vapor density, vapor viscosity, liquid thermal conductivity, and vapor thermal conductivity. A design manual, with tabular thermophysical property data, was then developed.

5. A prototype heat pipe was fabricated to performance test the most suitable fluid investigated on this project

The project was performed through nine tasks, listed below.

- Task 1: Literature Search
- Task 2: Preparation/Purchase of Compounds To Be Tested
- Task 3: Construct Gravity Reflux Heat Pipe Apparatus
- Task 4: Gravity Reflux Heat Pipe Tests
- Task 5: Working Fluid Characterization
- Task 6: Construct Prototype Heat Pipe
- Task 7: Performance Test Prototype Heat Pipe
- Task 8: Preparation of Two-Phase Design Manual
- Task 9: Report Documentation and Contract Direction

RESULTS AND DISCUSSION

CONTRACT KICK-OFF MEETING

A contract kick-off meeting was held on August 18, 1992 at the Phillips Lab. In attendance were:

- Larry Grzyll - Mainstream Engineering
- Mary Corrigan - Phillips Lab
- Bob Vacek - Phillips Lab

TASK 1: LITERATURE SEARCH

The open technical literature and commercial databases were searched to locate as much information as possible on aromatic hydrocarbons and aromatic perfluorocarbons. The objective was to find any existing synthesis methods, thermophysical property information, thermal stability, toxicity, and handling information available on these families of compounds. The open technical literature was searched using the online bibliographic and numeric databases.

Aromatic Hydrocarbons

Much information has been obtained on naphthalene, biphenyl, and the terphenyl isomers (Refs. 7-8, 11-16, and 22-44). References have been collected pertaining to properties and thermal stability of these compounds. Specific information collected on these compounds is given in Tables 1-5 along with specific references to the information. Much of the temperature-dependent data collected on these compounds was below the 300-400°C temperature range, however, theoretical correlations were used to extend the data into this temperature range. All five of these aromatic hydrocarbons are readily available commercially.

Table 1. Property information on naphthalene.

Constant Property	Value	Reference
Molecular Weight	128.17 g/mol	34
Critical Temperature	748.35 K	43
Critical Pressure	4.051 MPa	43
Melting Point	353.43 K	43
Boiling Point	491.14 K	43
Acentric Factor	0.30193	43
Flash Point	353.15 K	43
Lower Flammab. Limit	0.88 vol% in air	43
Upper Flammab. Limit	5.9 vol% in air	43
Autoignition Temp.	860.15 K	43
Oral LD ₅₀ child	100 mg/kg	58
Oral LD ₅₀ rat	1780 mg/kg	58
inhal. LD ₅₀ mouse	150 mg/kg	58
Temperature-Dependent Property	Type of Information	Reference
Liquid Density	Correlation	39, 43
Vapor Pressure	Data, Correlation	22-23, 33, 39, 43
Heat of Vaporization	Correlation	39, 43
Liquid Heat Capacity	Data, Correlation	24, 39, 43
Ideal Gas Heat Cap.	Correlation	39, 43
Liquid Viscosity	Correlation	39, 43
Vapor Viscosity	Correlation	39, 43
Liquid Thermal Cond.	Correlation	39, 43
Vapor Thermal Cond.	Correlation	39, 43
Surface Tension	Data, Correlation	36, 39, 43
Data- Experimental Data		
Correlation - Theoretical Correlation		

Table 2. Property information on biphenyl.

Constant Property	Value	Reference
Molecular Weight	154.21 g/mol	43
Critical Temperature	789.26 K	43
Critical Pressure	3.385 MPa	43
Melting Point	342.37 K	43
Boiling Point	528.15 K	43
Acentric Factor	0.36593	43
Flash Point	385.93 K	43
Lower Flammab. Limit	0.6 vol% in air	43
Upper Flammab. Limit	5.8 vol% in air	43
Autoignition Temp.	813.15 K	43
Oral LD ₅₀ rat	3280 mg/kg	58
inhal. TD _{LO} human	2400 mg/kg	58
Temperature-Dependent Property	Type of Information	Reference
Liquid Density	Correlation	14-15, 34, 43
Vapor Pressure	Data, Correlation	42-43
Heat of Vaporization	Correlation	42-43
Liquid Heat Capacity	Data, Correlation	26, 42-43
Ideal Gas Heat Cap.	Data, Correlation	42-43
Liquid Viscosity	Data, Correlation	8, 14-15, 34, 43
Vapor Viscosity	Estimation	34 43
Liquid Thermal Cond.	Data, Correlation	31-32, 34, 43
Vapor Thermal Cond.	Estimation	34, 43
Surface Tension	Data, Correlation	8, 36, 43
Data - Experimental Data		
Correlation - Theoretical Correlation		
Estimation - Theoretical Estimation Technique		

Table 3. Property information on o-terphenyl.

Constant Property	Value	Reference
Molecular Weight	230.31 g/mol	43
Critical Temperature	890.95 K	43
Critical Pressure	3.901 MPa	43
Melting Point	329.35 K	43
Boiling Point	609.00 K	43
Acentric Factor	0.46707	43
Flash Point	40.93 K	43
Lower Flammab. Limit	0.5 vol% in air	43
Upper Flammab. Limit	5.3 vol% in air	43
Autoignition Temp.	no information	
Toxicity	irritant	44
Temperature-Dependent Property	Type of Information	Reference
Liquid Density	Correlation	14, 34, 43
Vapor Pressure	Correlation	43
Heat of Vaporization	Correlation	43
Liquid Heat Capacity	Data, Correlation	35, 43
Ideal Gas Heat Cap.	Estimation	43
Liquid Viscosity	Data, Correlation	14, 34, 43
Vapor Viscosity	Estimation	34, 43
Liquid Thermal Cond.	Data, Correlation	14, 32, 34, 43
Vapor Thermal Cond.	Estimation	34, 43
Surface Tension	Correlation	43
Data - Experimental Data Correlation - Theoretical Correlation Estimation - Theoretical Estimation Technique		

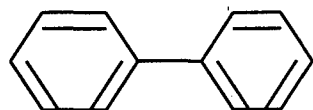
Table 4. Property information on m-terphenyl.

Constant Property	Value	Reference
Molecular Weight	230.31 g/mol	43
Critical Temperature	924.85 K	43
Critical Pressure	3.506 MPa	43
Melting Point	360.00 K	43
Boiling Point	650.00 K	43
Acentric Factor	0.55826	43
Flash Point	463.73 K	43
Lower Flammab. Limit	0.5 vol% in air	43
Upper Flammab. Limit	5.3 vol% in air	43
Autoignition Temp.	no information	
Toxicity	irritant	44
Temperature-Dependent Property	Type of Information	Reference
Liquid Density	Correlation	14, 34, 43
Vapor Pressure	Correlation	43
Heat of Vaporization	Correlation	43
Liquid Heat Capacity	Correlation	43
Ideal Gas Heat Cap.	Estimation	43
Liquid Viscosity	Data, Correlation	8, 14, 34, 43
Vapor Viscosity	Estimation	34, 43
Liquid Thermal Cond.	Data, Correlation	14, 32, 34, 43
Vapor Thermal Cond.	Estimation	34, 43
Surface Tension	Data, Correlation	8, 43
Data - Experimental Data		
Correlation - Theoretical Correlation		
Estimation - Theoretical Estimation Technique		

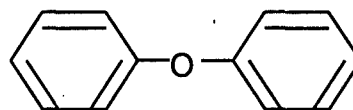
Table 5. Property information on p-terphenyl

Constant Property	Value	Reference
Molecular Weight	230.31 g/mol	43
Critical Temperature	925.95 K	43
Critical Pressure	3.324 MPa	43
Melting Point	485.00 K	43
Boiling Point	649.15 K	43
Acentric Factor	0.52805	43
Flash Point	480.37 K	43
Lower Flammab. Limit	0.5 vol% in air	43
Upper Flammab. Limit	5.3 vol% in air	43
Autoignition Temp.	no information	
Toxicity	irritant	44
Temperature-Dependent Property	Type of Information	Reference
Liquid Density	Correlation	14, 34, 43
Vapor Pressure	Correlation	43
Heat of Vaporization	Correlation	43
Liquid Heat Capacity	Correlation	43
Ideal Gas Heat Cap.	Estimation	43
Liquid Viscosity	Data, Correlation	14, 34, 43
Vapor Viscosity	Estimation	34, 43
Liquid Thermal Cond.	Data, Correlation	14, 32, 34, 43
Vapor Thermal Cond.	Estimation	34, 43
Surface Tension	Correlation	43
Data - Experimental Data Correlation - Theoretical Correlation Estimation - Theoretical Estimation Technique		

A discussion is warranted on the differences between biphenyl and the commercial heat transfer fluids Dowtherm A and Therminol VP-1. Biphenyl is a single chemical compound, while Dowtherm A and Therminol VP-1 are eutectic mixtures of biphenyl and diphenyl oxide. The structural differences between biphenyl and diphenyl oxide can be seen below:



Biphenyl



Diphenyl Oxide

Experimental data by Johns (Ref. 13) shows that biphenyl has a higher thermal stability limit than diphenyl oxide. Bond dissociation data also shows that the carbon-carbon bond connecting the phenyl rings of biphenyl is stronger than the carbon-oxygen bond connecting the phenyl rings of diphenyl oxide. The carbon-carbon bond has a dissociation energy of 94.5 kcal/mole (Ref. 30) while the carbon-oxygen bond has a dissociation energy of 73 kcal/mole (Ref. 38). The oxygen atom of diphenyl oxide also results in a larger number of possible decomposition products than with biphenyl. Many of the oxygen-containing decomposition products are tar-like, polymeric materials that could affect the bulk fluid properties. Biphenyl, on the other hand, decomposes into hydrogen and the terphenyl isomers only (Refs. 11-13).

Commercial heat transfer problems, such as Dowtherm A, have been tested in heat pipes and, as expected, their performance was not satisfactory (Ref. 5). Dowtherm A is a fluid mixture, and fluid mixtures are not well suited for use in heat pipes. This is due to the difference in volatility of the components of the mixture, which results in a temperature glide upon evaporation and condensation (at constant pressure). This is not the case with a pure fluid, which undergoes a constant-temperature evaporation and condensation at constant pressure.

Aromatic Perfluorocarbons

Only limited information on the perfluorocarbon derivatives of the above aromatic hydrocarbons has been obtained, primarily on synthesis, reactions, and thermal stability of perfluoronaphthalene and perfluorobiphenyl (Refs. 37 and 44-58). Specific information on perfluoronaphthalene and perfluorobiphenyl are given in Tables 6 and 7 along with references to the information. We have found a reference to preparation of perfluoro-o-terphenyl from a 1969 journal article (Ref. 50).

Table 6. Property information on perfluoronaphthalene.

Constant Property	Value	Reference
Molecular Weight	272.09 g/mol	44
Critical Temperature	673.05 K	49
Critical Pressure	2.0468 MPa	49
Melting Point	360-361 K	44
Boiling Point	482 K	41
Acentric Factor	0.4159	59 ¹
Flash Point	No Data	
Lower Flammab. Limit	No Data	
Upper Flammab. Limit	No Data	
Autoignition Temp.	No Data	
Toxicity	irritant	44

¹ Estimated Using Lee-Kesler Correlations

Table 7. Property information on perfluorobiphenyl.

Constant Property	Value	Reference
Molecular Weight	334.11 g/mol	44
Critical Temperature	No Data	
Critical Pressure	ND	
Melting Point	341-343 K	44
Boiling Point	479.15 K	44
Acentric Factor	No Data	
Flash Point	No Data	
Lower Flammab. Limit	No Data	
Upper Flammab. Limit	No Data	
Autoignition Temp.	No Data	
Toxicity	No Data	

Figure-of-Merit

One of the action items of the contract kick-off meeting was to develop a figure-of-merit for the 10 candidate working fluids. This figure-of-merit will be developed using existing literature data and suitable estimation algorithms where data does not exist. The intent of this figure-of-merit is to screen the 10 fluids to determine if any appear unsuitable for further testing and characterization. A variety of physical, chemical, and thermodynamic properties of the working fluid must be evaluated to determine the figure-of-merit. These properties are (Ref. 60):

1. operating temperature range
2. liquid transport factor
3. vapor phase properties
4. wicking capability in body-force field
5. thermal conductivity
6. fluid compatibility and stability

A working fluid should be chosen such that its operating temperature range is above the melting point and below the critical point. Ideally, the lowest temperature should be greater than a temperature corresponding to a vapor pressure of about 0.1 atm. The highest temperature should be below the critical temperature to avoid excessive pressure and to avoid low values of surface tension and latent heat of vaporization (which result in poor capillary pumping).

The capillary pumping ability of the working fluid is described by the liquid transport factor. The liquid transport factor is defined as the product of the surface tension and heat of vaporization divided by the kinematic viscosity of the liquid. A plot of the liquid transport factor of the working fluid versus temperature typically has a maximum near the normal boiling point of the fluid.

In the presence of body forces, the capillary head of the working fluid must overcome the body-force head to overcome fluid flow losses. This is a problem of surface tension forces against body forces, with the ratio termed the wicking height factor. The wicking height factor is defined as the surface tension divided by the product of liquid density and gravitational force. To minimize adverse body-force effects, this fluid should have a maximum value. The body-force effects diminish proportionally with decreasing gravity.

The relative merit of the vapor phase can be described by the kinematic viscosity ratio, defined as the ratio of vapor kinematic viscosity to liquid kinematic viscosity. This parameter defines the proportion of viscous vapor to liquid flow losses, and should be as low as possible to minimize adverse vapor effects.

It is desirable to choose a working fluid with the highest value of liquid thermal conductivity since the heat transfer coefficients are directly proportional to this property. Maximizing the thermal conductivity helps to minimize the temperature gradient in the heat pipe itself.

The compatibility of the working fluid with construction materials of the heat pipe is a major factor in working fluid selection. Incompatibility can result in chemical reaction or in outgassing

of the construction material, both of which generate noncondensable gases in the heat pipe that significantly affect heat pipe performance by causing condenser blockage. Corrosion of the construction material can cause damage to the heat pipe wick and other structural portions of the heat pipe.

A FORTRAN program was written to calculate the figure-of-merit for the 10 compounds. For the five aromatic hydrocarbons, the DIPPR property correlations (Ref. 43) were used to calculate the required properties. For the five aromatic perfluorocarbons, suitable property estimation techniques (Refs. 41 and 59) were used to estimate the required properties. Figures 1-5 show the figure-of-merit for the candidate fluids, water, mercury, and cesium. Water is not typically considered in this temperature range due to its critical temperature of 647 K. Mercury has been considered in the past but it is extremely toxic and presents fluid handling difficulties, has a poor contact angle that results in wick wettability and priming problems, and has a high liquid density that results in a heavy pipe. Cesium has also been considered but has an extremely low vapor pressure, has the same toxicity, handling, and density concerns as mercury, and is very reactive with atmospheric water generating hydrogen in an exothermic reaction.

Figure 1 shows that the calculated liquid transport factor of the ten candidate working fluids is about 2 orders of magnitude less than that of mercury and about 1 order of magnitude less than cesium. The liquid transport factor of water decreases rapidly with increasing temperature, dropping below all candidate fluids above 640 K due to its approach to the critical point. The aromatic hydrocarbons have consistently higher values of liquid transport factor than the aromatic perfluorocarbons.

Figure 2 shows that the vapor pressure of water is excessively high (greater than 10 MPa) and the vapor pressure of cesium is excessively low (around 1 kPa) over this temperature range. The vapor pressures of the 10 candidate fluids are in the range of 100 kPa to 2 MPa. A common heat pipe rule-of-thumb states that the vapor pressure in the heat pipe should be between 10 kPa and 1 MPa (0.1 to 10 atm.). Generally, the vapor pressure of the aromatic perfluorocarbons is greater than their aromatic hydrocarbon analogs.

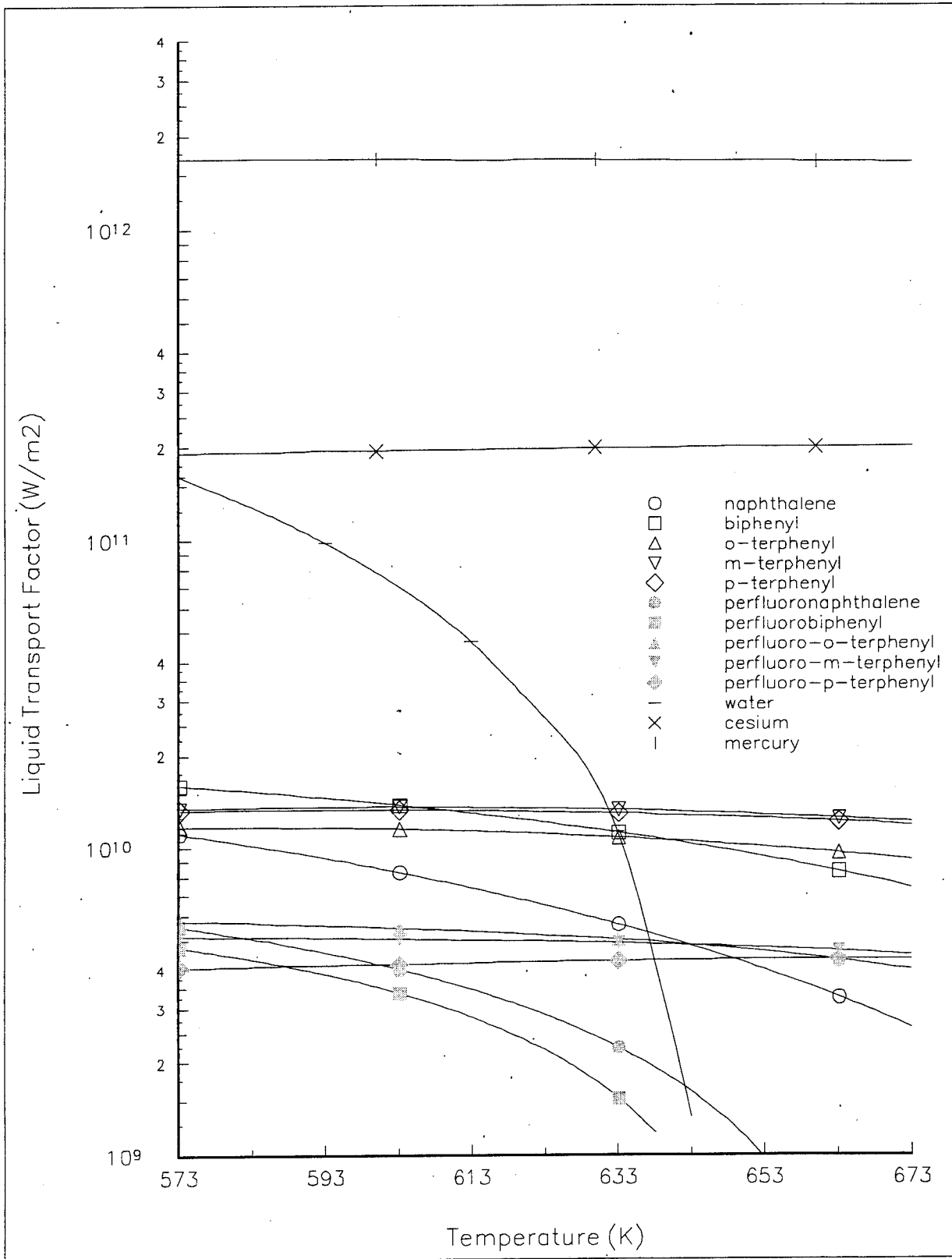


Figure 1. Calculated liquid transport factor of candidate fluids.

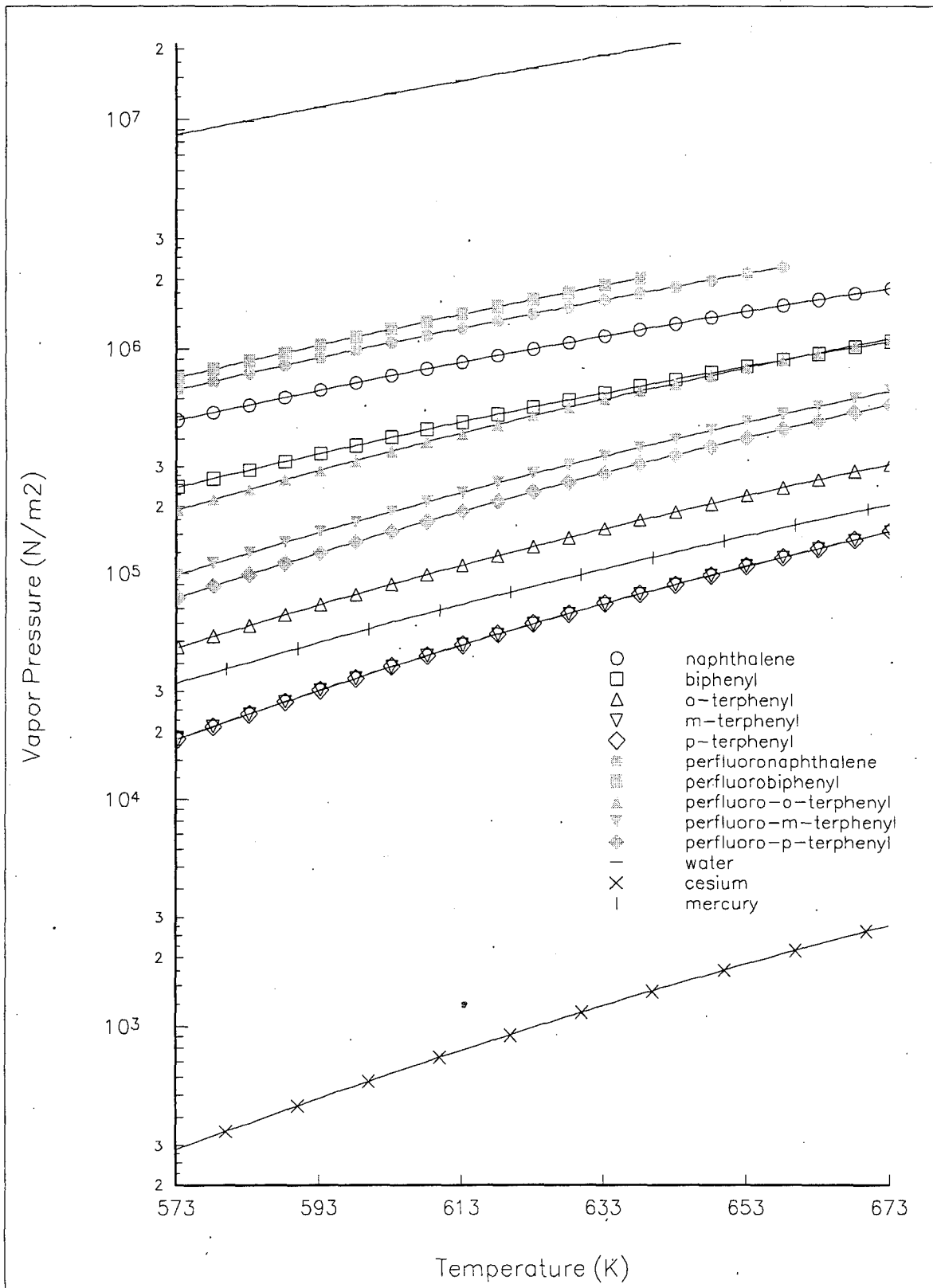


Figure 2. Calculated vapor pressure of candidate fluids.

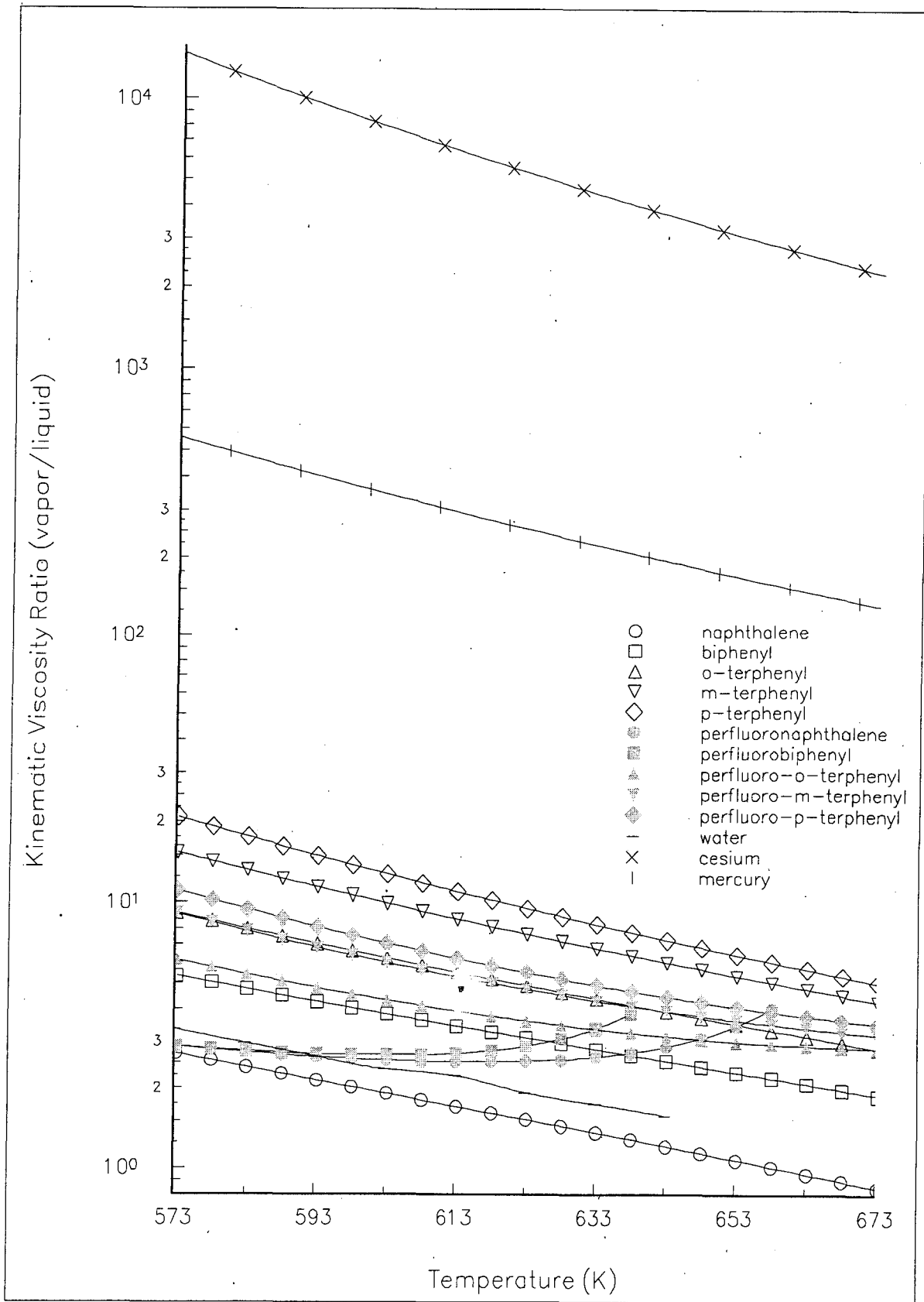


Figure 3. Calculated kinematic viscosity ratio of candidate fluids.

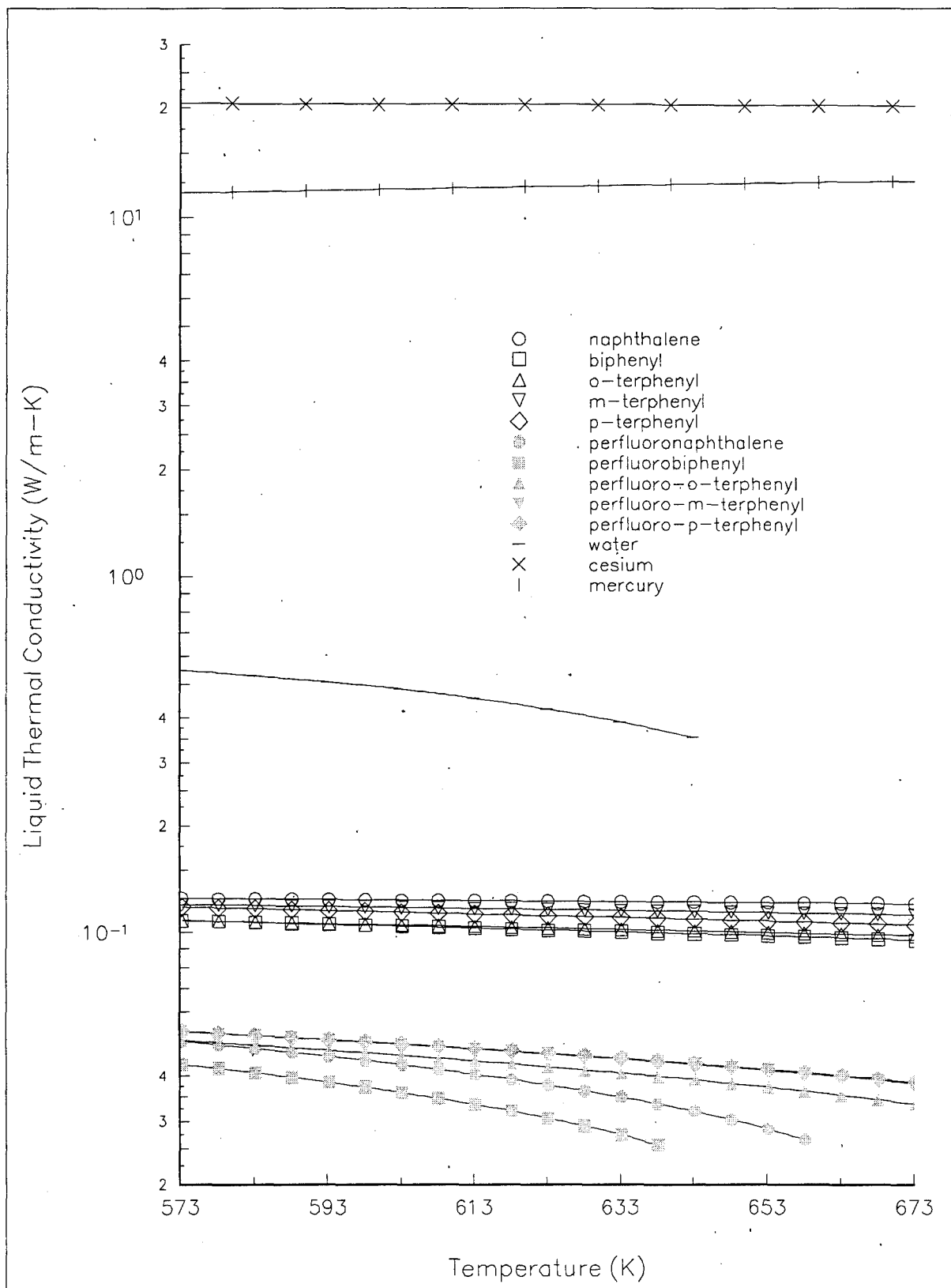


Figure 4. Calculated liquid thermal conductivity of candidate fluids.

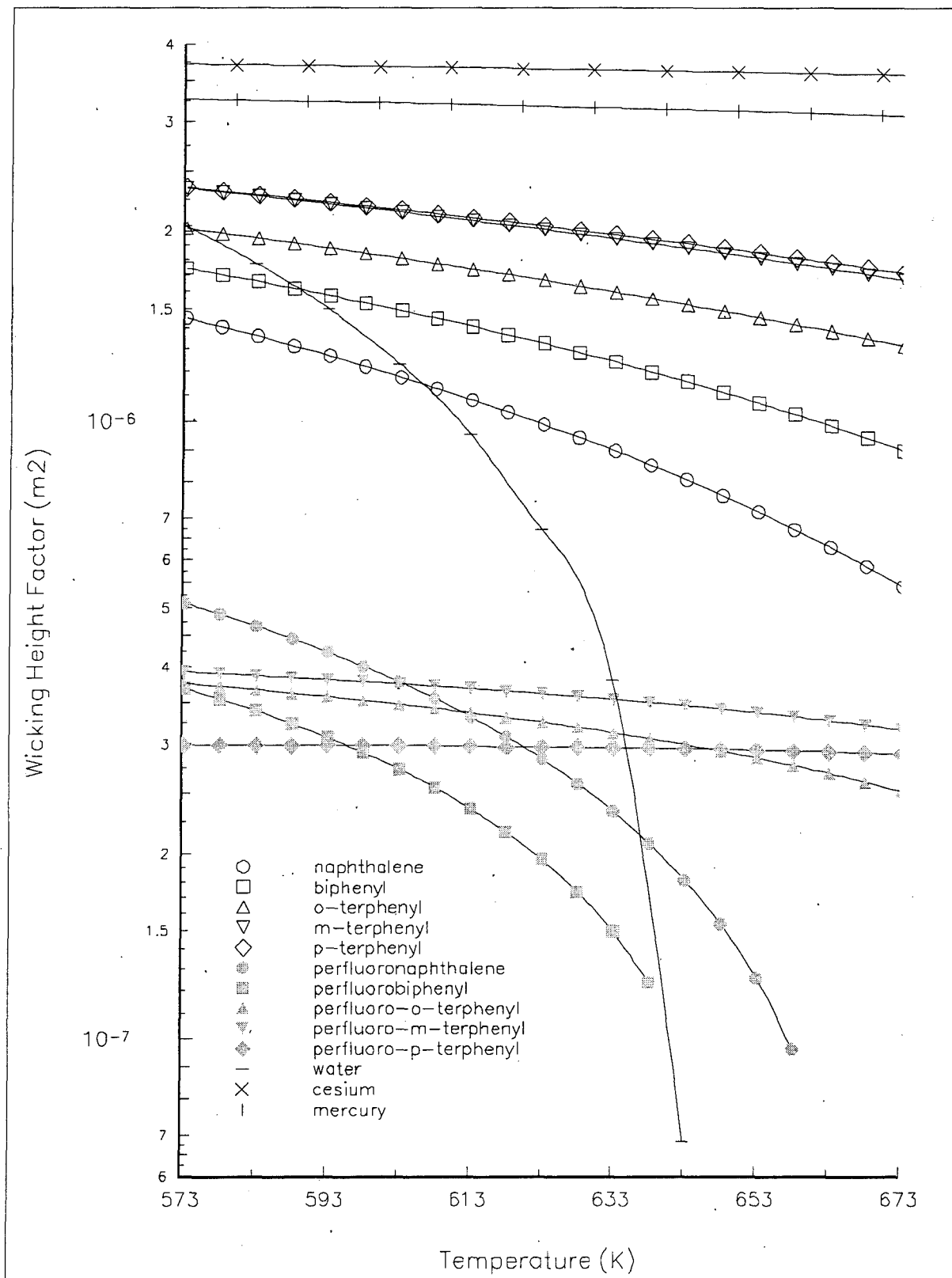


Figure 5. Calculated wicking height factor of candidate fluids.

Figure 3 shows the kinematic viscosity ratio for the candidate fluids. It is desirable to have a minimum value of this ratio to minimize adverse vapor effects. Figure 3 shows that all candidate fluids have lower values of this factor than cesium or mercury.

Figure 4 shows that the liquid thermal conductivity of the candidate fluids are much lower than the liquid metals and water. Generally, the aromatic hydrocarbons have higher values of thermal conductivity than the aromatic perfluorocarbons.

Figure 5 shows that the wicking height factor of the aromatic hydrocarbons approaches that of the two liquid metals and is greater than that of water. The wicking height factor for the aromatic perfluorocarbons is about an order of magnitude less than their hydrocarbon analogs. This factor becomes less important in the absence of gravity.

Based on the information compiled in this task, five compounds were selected for testing and characterization: naphthalene, biphenyl, o-terphenyl, perfluorobiphenyl, and one of the perfluorinated terphenyl isomers (depending on availability).

TASK 2 - PREPARATION/PURCHASE OF COMPOUNDS

We surveyed various chemical supplier catalogs and custom chemical manufacturers to identify suppliers of the five compounds that were targeted for this project. Naphthalene, biphenyl, and o-terphenyl (all 99%) were purchased from Aldrich Chemical Company. Perfluorobiphenyl (decafluorobiphenyl) was purchased from Ryan Scientific (99%). No suppliers of the perfluorinated terphenyl isomers were found. An online search for the three perfluorinated terphenyl isomers showed that none of these compounds had a Chemical Registry Number, which implies that little, if any, work has been performed on synthesizing these compounds. One reference to perfluoro-o-terphenyl was found in the open technical literature (Ref. 50), however, no manufacturer of this material was found.

Because the perfluorinated terphenyl isomers were not available commercially, we developed synthesis approaches for these compounds that could be used by a custom chemical

manufacturer. These approaches could be used to supply laboratory samples and could provide a manufacturing procedure for commercial quantities. During the literature search into the preparation of the perfluoroterphenyls, preparations for perfluorotriphenylene and perfluoro-1,3,5-triphenylbenzene, two other perfluorinated aromatic compounds, were identified. The hydrocarbon analogs to these two compounds have thermal stability characteristics similar to naphthalene, biphenyl, and the terphenyls (Ref. 13). The synthesis approaches to the perfluorinated aromatic compounds are provided below.

The synthesis of perfluoro-p-terphenyl starts with p-terphenyl which is perfluorinated to give the corresponding perfluorocycloalkane. The perfluorocycloalkane is then defluorinated to yield perfluoro-p-terphenyl. Barbour et al. (Ref. 61) and Coe (Ref. 62) converted aromatic hydrocarbons to perfluorocycloalkanes by passing them through a reactor with a bed of CoF_3 at 250-350°C or potassium tetrafluorocobaltate at 250°C. The perfluorocarbon was washed with ice-water to remove the HF formed in the reaction. The perfluorocycloalkane is then defluorinated using one of the following methods. Gethig et al. (Ref. 63) used iron or nickel gauze which was heated to 400-600°C to defluorinate the perfluorocycloalkane. Hu et al. (Ref. 64) used zinc in dioxane, acetonitrile, dimethylformamide, or methanol at 60-100°C to defluorinate the perfluorocycloalkane. Marsella et al. (Ref. 65) used sodium or lithium with bezophenone under reducing conditions in the -75-75°C temperature range to defluorinate the perfluorocycloalkane.

The preparation of perfluoro-1,3,5-triphenylbenzene is accomplished by reacting perfluorobenzonium ions with four equivalents of pentafluorobenzene in SbF_5 (Ref. 66). The reported yield is 70-80%. The preparation of the perfluorobenzonium ion from the reaction of perfluorobenzene and SbF_5 is reported in literature (Ref. 67).

Perfluorotriphenylene can be synthesized by reacting the perfluorobenzonium ion with 2,2-di-H-ocatfluorodiphenyl in SbF_5 (Ref. 66). The reported yield is 50-60%.

After contacting several custom chemical manufacturers, we decided to subcontract the synthesis of perfluoro-1,3,5-triphenylbenzene to FAR Research, Inc. (Palm Bay, FL). They produced an initial amount of 11 g on a laboratory-scale, and subsequently scaled-up their process to produce approximately 300 g.

Initial tests of the perfluoro-1,3,5-triphenylbenzene in a pressure differential scanning calorimeter (DSC) indicated the occurrence of material decomposition between melting point of the material (about 155°C) and the boiling point. No distinct endotherm corresponding to an isothermal boiling point could be detected at elevated pressures, and examination of the sample cell following the DSC scan showed the presence of black char material (evidence of severe decomposition). Since the material was off-white, it was speculated that impurities caused the material to decompose above its melting point. After several crystallizations of the material from ethanol, the material became white, fluffy, and crystalline (as opposed to an off-white powder), a sign that the material was significantly purer. This material was heated in a glass ampule to about 300°C, where only slight discoloration was seen. The material appeared to evaporate at this temperature. Further crystallization (a total of four crystallizations) did not seem to improve this phenomena. Even after four crystallizations the material discolored and charred around 300°C. Thus, this compound appeared unsuitable due to its thermal decomposition. This experimental result was not expected, as many investigators in past work have suggested that perfluorination of an aromatic compound results in increased stability over the hydrocarbon analog (Refs. 12-13 and 21). These papers state that the most stable aromatics are perfluorinated. References to 1,3,5-triphenylbenzene show its thermal stability limit to be 499°C (Ref. 12), therefore, it was expected that perfluorination of the molecule would further increase stability. This, however, was not observed in this study.

We discussed the decomposition problems of perfluoro-1,3,5-triphenylbenzene with the Air Force technical monitor. During these discussions, it was suggested to drop further characterization of perfluoro-1,3,5-triphenylbenzene and consider another candidate compound, quinoline. This compound has thermodynamic properties suitable for use in the 300-400°C range, with a boiling point of 237.7°C and a critical temperature of 509°C. Its melting point is -

16°C, which will eliminate any problems associated with frozen start-up of the heat pipe. Technical literature indicates this compound has thermal stability characteristics equal to biphenyl and naphthalene (Ref. 12), however, it is toxic. We procured this compound from Aldrich Chemical Company (99%).

TASK 3: CONSTRUCT GRAVITY REFLUX HEAT PIPE APPARATUS

The gravity reflux heat pipe apparatus consisted of several components. The main component was the heat pipes themselves. A filling station was constructed to bake out the heat pipes and fill with working fluid. A heating block was configured to provide a heat load at the evaporator section of each pipe. A data acquisition and control system was used to control the temperature of the heat pipe and monitor the temperature of the exterior wall of the heat pipe at various locations.

Heat Pipe Fabrication, Cleaning, and Assembly

In the fabrication of the gravity reflux heat pipes, standard heat pipe manufacturing procedures obtained from accepted references were followed (Refs. 60 and 68-70). Standard commercial stainless steel 316 seamless tubing, with an OD of 0.625 in., a length of 17.5 in., and a wall thickness of 0.065 in. was selected for the heat pipe envelope. The evaporator and adiabatic sections of the pipe were each 6 in. long, and the condenser section was 5.5 in. long. The fill tube of the heat pipe stainless steel 316 seamless tubing, 3.2 in. long, 0.25 in. OD, and 0.035 in. wall thickness. The end caps were machined from 0.625 in. OD stainless steel 316 round stock and were 0.2 in. long. The end caps and envelope ends were machined with a deep 90-degree V-groove butt joint for connection. The fill tube was connected to the end cap with a fillet joint. A wick of 100 mesh stainless steel screen was used in the evaporator section of the heat pipe. A stainless steel 316 bellows valve was attached to the end of the fill tube.

All heat pipe materials were cleaned using standard procedures for stainless steel heat pipes (Refs. 60 and 68-70). All parts were initially cleaned in 1,1,1-trichloroethane with a bristle brush

and dried with filtered air. The parts were then immersed in a passivating solution of 35-65% nitric acid for 1-2 hours, rinsed with tap water for 2 minutes, and dried with filtered air. A final rinse in isopropyl alcohol was performed, followed by drying with filtered air. All cleaned parts were stored in a plastic bag.

The first step in the assembly process was to insert the wick into the evaporator section pipe with a custom insertion tool. The end caps were then inserted, and all joints were TIG welded. After welding, all joints were inspected using X-ray to verify the adequacy of the joints. Pre-charging leak detection was performed using a halogen leak detector (with a leak sensitivity of 10^{-7} ml/sec) and HCFC-22 (chlorodifluoromethane).

Working Fluid Preparation, Evacuation, and Charging

A heat pipe filling station was constructed for working fluid degassing (freeze/thaw cycles), heat pipe degassing (bakeout), working fluid metering, and working fluid filling. The filling station consisted of stainless steel tubing, fittings, bellows valves, and a sample bottle. A schematic of the filling station is provided in Figure 6.

The working fluid was fractionally distilled prior to use to ensure as high a purity as possible. Several freeze/thaw cycles under vacuum were also performed to remove noncondensibles from the working fluid. Each heat pipe was degassed prior to filling by heating it to approximately 400°C under vacuum on the filling station. The fluid was charged to the heat pipe orthobarically on the filling station. The filling station was designed to charge a constant volume to each pipe. Once filled, the heat pipes and their fill valve were removed from the filling station. The fill tube was flattened and crimped between the fill valve and the heat pipe using a 100-ton press, and the crimped area was cut and TIG-welded for a final seal.

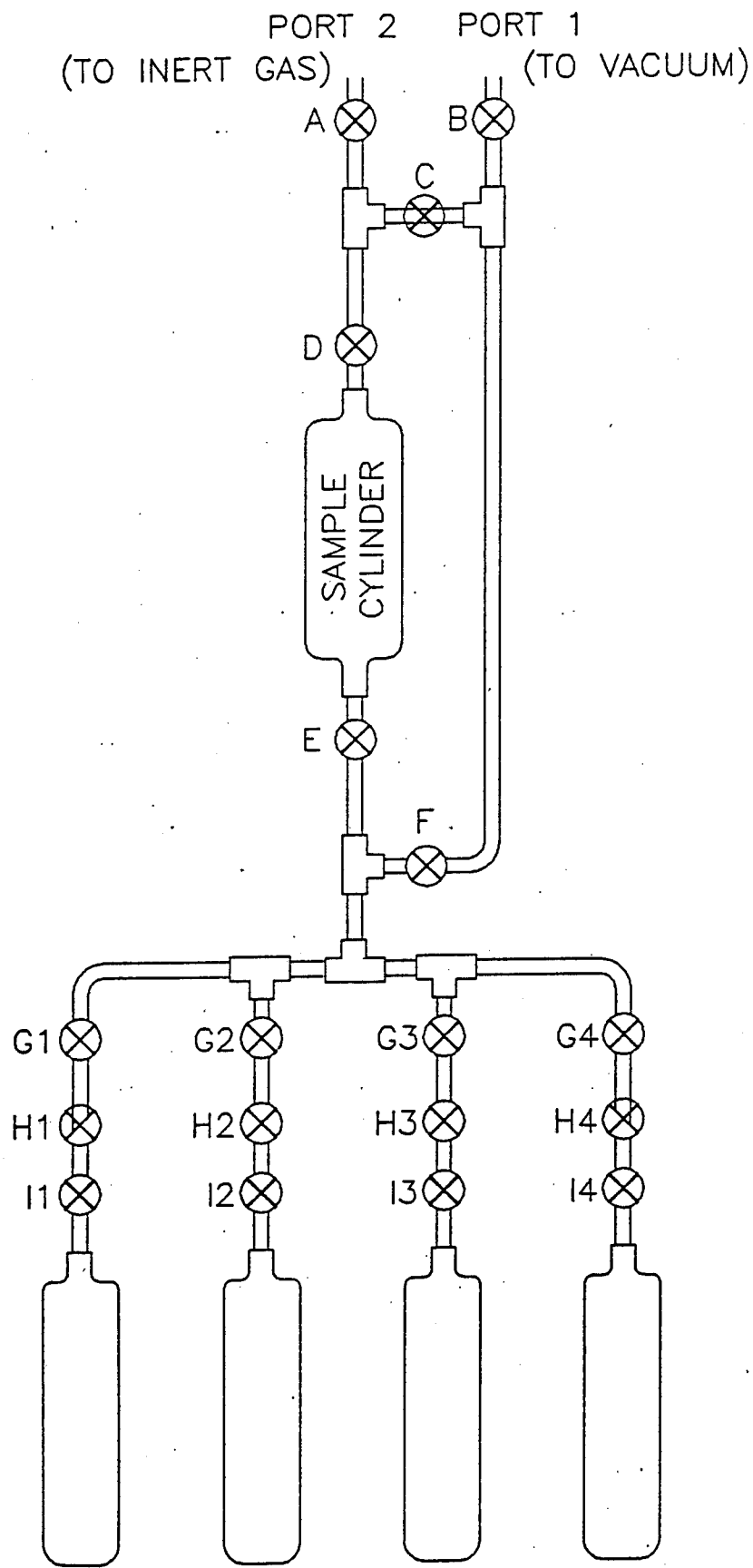


Figure 6. Schematic of heat pipe filling station.

Test Stand Hardware

The test stand hardware consisted of heating blocks for the heat pipe evaporators, insulation for the evaporator and adiabatic sections, and thermocouples to monitor the heat pipe wall temperatures.

The heating blocks on the evaporator section of the heat pipe were cylindrical aluminum blocks (3 in. OD by 6" tall) with 400 W stainless steel band heaters on the outside surface of the aluminum block. The band heaters were bonded to the aluminum blocks using heat transfer cement. The evaporator section of the heat pipe was inserted into a pre-drilled hole in the aluminum block. The pipes were coated with a zirconium/water paste prior to insertion into the block to aid conduction of heat from the block to the pipe. The heating blocks and adiabatic section of the heat pipe were surrounded with ceramic insulation (approximately 4 inches thick) to minimize heat losses and keep the container at a safe temperature. The experimental setup was placed in a high-bay area of Mainstream's facility away from any electronic equipment.

Type-K thermocouple wire, with high-temperature fiberglass insulation, was used for temperature measurement. The thermocouples had welded junctions and were held to the exterior heat pipe wall using stainless steel hose clamps and ceramic cloth insulation. Each pipe had five thermocouples; one on the evaporator, one on the adiabatic section, and three on the condenser section. Each heating block had a thermocouple inserted inside of it to monitor block temperature.

Data Acquisition/Control System

The data acquisition system that was used for temperature control and measurement was the HELIOS I by John Fluke Mfg. Co. Inc., LABTECH CONTROL by Laboratory Technologies Corporation and a personal computer. The HELIOS I operated as the front end of the system and received thermocouple (TC) data and sent various signals to control the heating block

temperature. The commands and data were sent and received to the HELIOS I through a standard serial interface (RS-232) from a personal computer.

The HELIOS I is a highly accurate measurement and control system. It can adapt to a very broad spectrum of applications, with a capacity ranging from a single channel to 1500 channels in a fully expanded system. The HELIOS I consists of the main chassis and an extender chassis to accommodate the amount of thermocouples and digital to analog converters. There is a total of 10 option boards - two high performance A/D converters that can host up to 5 option boards each, six isothermal input boards for the thermocouples that can accommodate 20 TCs per board, and two analog output boards to control the heaters.

The LABTECH Control software package includes a Proportional-Integral-Derivative (PID) control algorithm to support the heater controls. This software allows detail configuration and fully supports all functions of the HELIOS I. The software can be configured to control multiple systems on a single interface. For example, process 1 begins immediately where as process 2 begins at a later date, it can also analyze data and allow full usage of the PC while it is receiving and sending information to the hardware. The main advantage of this package is the PID control which receives a preset temperature and compares it with the current temperature to determine the value of the output signal required to maintain the system at its setpoint. Other advantages such as real-time display of all data on a graph or spreadsheet, data recording to hard copy and as well as to magnetic media, and the use of ICONs for configuring the system.

The heaters used for this project were controlled by the HELIOS I via a Solid State Relay Power Control unit (VPAC). The VPAC provides output power proportional to the input command signal from the HELIOS I. The VPAC used in this project also had an option board which allows 4-20 mA input source (compatible output with HELIOS I). For safety precautions a 10 A inline fuse and a switch is used to prevent excess current draw and access to the heater and VPAC respectively. Each heater and VPAC was supplied by an individual power source that has backup power supplied by a generator. The data acquisition system was on a separate uninterrupted power supply.

TASK 4: GRAVITY REFLUX HEAT PIPE TESTS

There were two temperature environments that each fluid would be subjected to in this task. Each of these temperature environments was programmed into the control logic of the data acquisition software. The first temperature environment was a constant temperature test at a block temperature of 350°C. The second test was a variable temperature test to simulate the temperature profile of the NASBAT during operation. This test starts at 325°C, with a temperature increase to 380°C within 0.8 hours. The temperature is maintained at 380°C for 1.2 hours, after which it is allowed to cool to 325°C where it is held for 22 hours. This 24 hour cycle is then repeated. All of the heating blocks had an initial temperature gradient programmed to bring the blocks to the starting temperature in a 24-hour period. After this startup period, the control logic for the two temperature environments took over.

In order to assure quality and quantity of data that was acquired during the gravity reflux heat pipe tests, each test was performed in duplicate. Since there were two temperature environments for each fluid, each performed in duplicate, there were a total of four heat pipes per fluid. For data acquisition, a total of 110 TCs and 8 heaters were utilized. The channels assigned to the thermocouples were 0-110 and the channels assigned to the heaters were 120-123 and 130-133. Table 8 presents the configuration used with the Helios system. The constant temperature tests were blocks 3, 4, 7, and 8. The variable temperature tests were blocks 1, 2, 5, and 6.

The fluids naphthalene, biphenyl, o-terphenyl, and decafluorobiphenyl were tested for a total time of 230 days. Data was initially logged to a file 4 times a day, but was reduced to once a day to avoid computer memory problems and system crashes (which did not affect the heater control, but did affect data logging). During the course of this period, occasional failure of thermocouples or thermocouple channels on the data acquisition occurred. This did not affect the overall test results. Quinoline was tested for durations ranging from 81-98 days, the shorter of which resulted from heating block failure after 81 days (heating block #6). Block #5 was a duplicate test of block #6. Heating block #8 was disabled shortly after startup due to a fluid leak in the fill tube of the pipe. Block #7 was a duplicate test of block #8.

Table 8. Data acquisition/control system configuration.

Block 1	Heat Pipe 16 Heat Pipe 12 Heat Pipe 10 Heat Pipe 2	TC channels 1-5 TC channels 6-10 TC channels 11-15 TC channels 16-20	o-terphenyl decafluorobiphenyl naphthalene biphenyl
Block 2	Heat Pipe 14 Heat Pipe 19 Heat Pipe 9 Heat Pipe 4	TC channels 21-25 TC channels 26-30 TC channels 31-35 TC channels 36-40	decafluorobiphenyl o-terphenyl naphthalene biphenyl
Block 3	Heat Pipe 20 Heat Pipe 15 Heat Pipe 3 Heat Pipe 7	TC channels 41-45 TC channels 46-50 TC channels 51-55 TC channels 56-60	o-terphenyl decafluorobiphenyl biphenyl naphthalene
Block 4	Heat Pipe 6 Heat Pipe 18 Heat Pipe 13 Heat Pipe 8	TC channels 61-65 TC channels 66-70 TC channels 71-75 TC channels 76-80	biphenyl o-terphenyl decafluorobiphenyl naphthalene
Block 5	Heat Pipe 17	TC channels 81-85	quinoline
Block 6	Heat Pipe 21	TC channels 86-90	quinoline
Block 7	Heat Pipe 22	TC channels 91-95	quinoline
Block 8	Heat Pipe 23	TC channels 96-100	quinoline
Block 1	temperature reference	TC channel 101	
Block 2	temperature reference	TC channel 102	
Block 3	temperature reference	TC channel 103	
Block 4	temperature reference	TC channel 104	
Block 5	temperature reference	TC channel 105	
Block 6	temperature reference	TC channel 106	
Block 7	temperature reference	TC channel 107	
Block 8	temperature reference	TC channel 108	
	ambient temperature	TC channels 109-110	
Heater 1	heater control	AO channel 120	
Heater 2	heater control	AO channel 121	
Heater 3	heater control	AO channel 122	
Heater 4	heater control	AO channel 123	
Heater 5	heater control	AO channel 130	
Heater 6	heater control	AO channel 131	
Heater 7	heater control	AO channel 132	
Heater 8	heater control	AO channel 133	

After the tests were completed, the pipes were removed from their heating blocks, cut open, and the candidate fluids were melted and collected in glass containers. Six parameters were used to determine if fluid pyrolysis could be detected:

1. the evaporator-condenser temperature differences over time during the tests
2. the appearance of the fluid when removed from the heat pipes
3. gas chromatography (GC) analysis of the fluids
4. differential scanning calorimeter (DSC) analysis of the fluids
5. ultraviolet (UV) absorption spectrometry analysis of the fluids
6. infrared (IR) absorption spectrometry analysis of the fluids

The evaporator-condenser temperature profiles, the appearance of the fluid after the test, and the DSC analysis results are presented in Appendix A. The following paragraphs will provide a summary of the results of each of the parameters used to assess fluid pyrolysis.

Evaporator-Condenser Temperature Differences

In general, inconsistent temperature readings were obtained, due most likely to improper contact of the thermocouple with the heat pipe. However, the data collected did suggest that quinoline did undergo pyrolysis due to the consistent increase in the evaporator-condenser temperature difference for all pipes tested. Similar behavior was seen with the decafluorobiphenyl heat pipe in heater block #2. No other consistent increases in the evaporator-condenser temperature difference were observed. The evaporator-condenser temperature differences for all pipes tested are provided in Appendix A.

Fluid Appearance

The fluid appearance after the test, when compared to the appearance before the test, is a valuable indicator of whether pyrolysis took place. Pyrolysis products of compounds of this type are usually non-condensable gases (which would not be collected when the pipes were cut open)

and high molecular weight materials (i.e. tars and chars). The high molecular weight tars and chars will usually cause the color of the fluid sample to darken. The appearance of the fluids after the test is noted in Appendix A. This table shows that all of the quinoline samples were dark brown liquids with solid precipitate, which is evidence of pyrolysis and which also agrees with the conclusions of the evaporator-condenser temperature difference data. All of the decafluorobiphenyl samples collected changed color slightly, from white crystals initially to light magenta crystals after the test. Unfortunately, no decafluorobiphenyl was collected from block #2, which had a continuous increase in the evaporator-condenser temperature difference over time. The naphthalene samples collected from blocks #2 and #3 were light brown crystals (compared to white crystals initially), but the naphthalene samples from blocks #1 and #4 were white crystals and needles, evidence that little or no pyrolysis took place. The biphenyl samples from blocks #1, #2, and #4 were white crystals and needles (very similar to the fluid before testing), while the sample from block #3 had only a slight amber discoloration. The o-terphenyl samples from blocks #2 and #4 were white crystals (similar to the fluid before testing), while the samples from blocks #1 and #3 had only a slight amber discoloration.

GC Analysis

The GC analysis was performed to determine if any decomposition products were detected in the fluid samples, and were compared to GC analysis of the fluid prior to testing. All samples collected were dissolved in HPLC chloroform and injected in a Gow-Mac GC to determine if decomposition products could be detected. The column used was an 8-foot column packed with 10% SP-2100 (methyl fluid) on Supelcoport. Each fluid was injected at a column temperature below and above the normal boiling temperature of the candidate fluid in order to detect the presence of impurities that had either lower or higher boiling points than the candidate fluid itself. A pyrolysis product impurity was only detected for one of the fluid samples, quinoline from block #7. No pyrolysis product was detected for any of the other samples.

DSC Analysis

The DSC analysis was performed to detect any change in either the melting or boiling points of the fluid samples before and after testing (the resolution of the DSC is $\pm 0.5-1^\circ\text{C}$). Such a change can be attributed to the presence of impurities in the sample (i.e. pyrolysis products). None of the samples analyzed had melting points that differed from the untested fluid by greater than 0.5°C . Five of the samples analyzed had boiling points that differed from the untested fluid by greater than 0.5°C ; these were naphthalene (blocks #2 and #3), biphenyl (block #4), decafluorobiphenyl (block #1), and quinoline (block #5). The naphthalene from blocks #2 and #3 and the quinoline from block #5 also had broader boiling peaks than the untested fluid, suggesting non-isothermal boiling (the presence of impurities). The quinoline from block #5 was the only quinoline sample tested because the other quinoline samples were completely used in the GC analysis.

UV/VIS Spectrometry

Since some compounds have shown a certain degree of discoloration after the test, a UV/VIS spectrum of these compounds should show some absorption at specific wavelengths where there was no absorption prior to the test. This method of detection will confirm the presence of a decomposition product and will give a rough approximation of its concentration in the compound. Using the Beer's law ($A = \epsilon b c$, where A is the absorbance, ϵ is the molar absorptivity, b is the length of the cell, and c is the concentration), a range of concentrations can be determined. This approximation is based on assuming a minimum and maximum value of the molar absorptivity ϵ . The concentration for all compounds used in this method was 0.01 Molar, and the wavelength range was from 190 to 820 nm. Quinoline was not analyzed using UV/VIS spectrometry due to the visual presence of solid decomposition products.

o-Terphenyl Results. All four o-terphenyl compounds showed two additional peaks at approximately 480 and 580 nm when compared to the distilled o-terphenyl. The maximum absorbance value of 0.002 was detected for heat pipe # 20, which results in an extremely low

concentration of impurity in the sample. However, the additional absorbance peaks do explain the resultant slight amber color in the samples.

Naphthalene Results. Naphthalene from heat pipe #9 showed two additional peaks. Heat pipe # 9 was subjected to variable temperature and showed a dark brown color. The two peaks were at approximately 337 and 350 nm, and the absorbances were 0.31 and 0.18 respectively. Typical minimum and maximum values of ϵ are 1000 and 100000 cm. mole^{-1} . Therefore, the minimum and maximum concentration of the impurity are: 0.00031 M and 0.0000031 M. This corresponds to 3.1 and 0.031 mole % impurity.

Decafluorobiphenyl Results. A magenta discoloration was observed for all decafluorobiphenyl samples. As a result, an absorbance peak at approximately 520 nm was detected for all samples. In order to better estimate the concentration of the peak, the concentration was increased from 0.01 M to 0.06 M. The maximum absorbance of 0.04 was observed for the decafluorobiphenyl in heat pipe #13. This corresponds to a minimum and maximum concentration of 0.0004 M to 0.000004 M, which in turn corresponds to 0.07 and 0.0007 mole % impurity.

Biphenyl Results. No significant difference was observed between the distilled and the tested biphenyls.

IR Spectrometry

This method is used to detect any difference between the distilled compound and the tested compounds IR spectrum. The wavelength ranges for the analysis were from 2.5 to 25 μm (wavenumber from 400 to 4000 cm^{-1}). The size of the peak has no implication on the amount of impurity. Quinoline was not analyzed using IR spectrometry due to the visual presence of solid decomposition products.

o-Terphenyl Results. The results showed no extra or missing peaks between the distilled and the tested o-terphenyl. However, the o-terphenyl from heat pipes # 16 and 19 (both of which were

subjected to the variable temperature test) showed an increase in size of two peaks, one of which is at 2367.8 cm^{-1} .

Naphthalene Results. Here again, the IR of the naphthalene from heat pipe # 9 confirm the presence of an impurity that is not present in the other naphthalene samples. Heat pipe #9 was subjected to the variable temperature test. The extra peak observed in the spectrum of heat pipe #9 was around 2367.8 cm^{-1} , the same wavenumber as one of the o-terphenyl impurities.

Decafluorobiphenyl Results. The decafluorobiphenyl spectrum from heat pipe # 13 did not show any significant difference compared to the distilled decafluorobiphenyl. On the other hand, additional peaks were observed in the decafluorobiphenyl from heat pipes # 12 and 15 around 2367.8 cm^{-1} . The peaks of heat pipe # 12 were greater in magnitude than those of heat pipe #15.

Biphenyl Results. All biphenyl samples after the test showed the same peaks as the distilled biphenyl.

Thermal Stability Test Conclusions

Based on the qualitative results of the thermal stability tests, we have concluded the following order of thermal stability of the candidate fluids, from most stable to least stable:

1. biphenyl
2. o-terphenyl
3. naphthalene
4. decafluorobiphenyl
5. quinoline
6. perfluoro-1,3,5-triphenylbenzene

TASK 5: WORKING FLUID CHARACTERIZATION

This task involved the experimental measurement of key thermophysical properties of the candidate working fluids. The specific properties that were measured included liquid density, liquid viscosity, surface tension, melting point, vapor pressure, heat of vaporization, critical point, and liquid thermal conductivity (this measurement was not successful). Also involved in this task was the design and fabrication of a constant-temperature immersion bath for the thermophysical property measurements.

Immersion Bath

A constant temperature bath and temperature control system was designed and fabricated for the thermophysical property measurements. The bath was a 12" OD x 12" high Pyrex jar surrounded with ceramic insulation and contained in an aluminum housing with two 3" x 8.5" openings for visual inspection of the bath interior. The bath fluid was Tempering A heat transfer salt supplied by Heatbath Corp., which is a mixture of potassium nitrate (40-50%), sodium nitrite (40-50%), and sodium nitrate (1-10%). The bath was heated by four 12.5" long, 1500 W cartridge heaters (Whatlow Electric) and was stirred with a mechanical stirrer. Temperature measurements were made using a type-K thermocouple and the bath temperature was controlled using a PID controller (Whatlow Electric) with a temperature accuracy of $\pm 0.1\%$ of the set point.

Critical Point

The critical temperature of decafluorobiphenyl was experimentally determined since this property was unknown. The critical temperatures of all other candidate working fluids were found in literature. We employed a method described in literature (Ref. 71) that involves the observation of appearance and disappearance of the meniscus of the fluid contained in a heavy walled, sealed glass ampule immersed in the constant temperature bath. The fluid was loaded into the ampule, frozen, and the ampule was evacuated and sealed so that the fluid was under its own vapor pressure. The sample was heated and cooled, so as to pass the material through the

critical temperature and detect the appearance and disappearance of the meniscus. The tube was carefully loaded so that just below the critical temperature approximately equal volumes of liquid and vapor coexisted.

The critical temperature of decafluorobiphenyl was determined to be 367°C (640 K) $\pm 1^{\circ}$ by the repeated appearance and disappearance of the meniscus as the fluid passed through this temperature. The critical pressure of decafluorobiphenyl was calculated by determining the vapor pressure at the critical temperature using the Antoine equation derived from pressure DSC measurements (discussed later). The critical temperature was calculated to be 2134.9 kPa .

Liquid Density

The liquid density measurements were performed using a modified pycnometric technique that yields an absolute value for liquid density. This technique has been used on recent alternative refrigerant measurements (Ref. 72). In this technique, liquid density is determined directly by dividing the mass difference between the full and evacuated sample cylinder by the total sample cylinder volume. A schematic of the experimental apparatus is given in Figure 7.

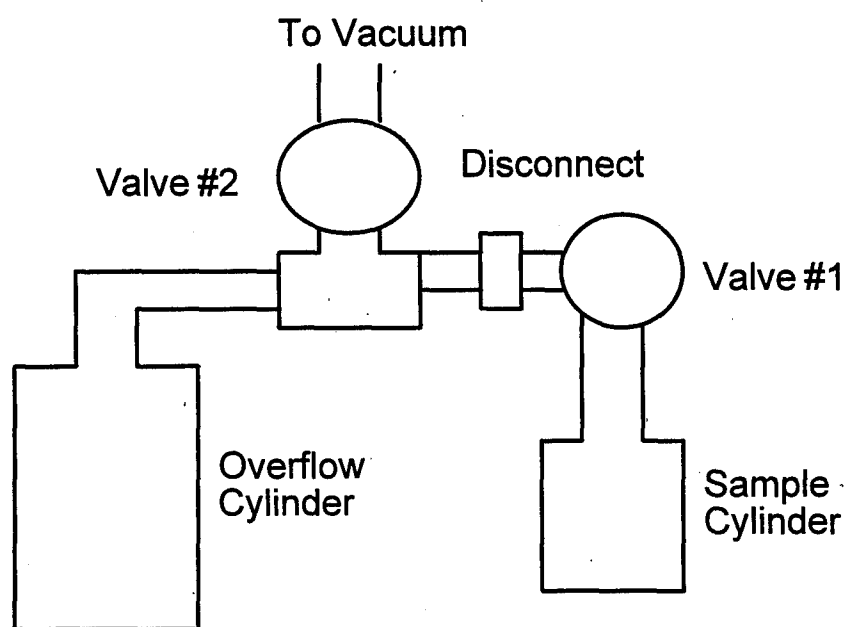


Figure 7. Schematic of the liquid density apparatus.

To perform a liquid density measurement, the stainless steel constant-volume sample cylinder is initially disconnected from the apparatus and filled completely in the liquid phase with the compound to be measured. The filled sample cylinder is then reconnected to the apparatus, valve #1 is opened, and the system is frozen and thawed under vacuum. The sample cylinder is then pressurized with nitrogen just above the vapor pressure of the fluid at the test temperature to suppress vaporization and valve #2 is closed. The system is then immersed completely in the constant temperature bath and allowed to reach thermal equilibrium. Since the temperature at which the liquid density measurement will take place is greater than the temperature at which the sample cylinder was filled, an overflow cylinder is present to provide the necessary volume for the fluid expansion at the elevated temperature. Once thermal equilibrium has been achieved, valve #1 is closed and the system is removed from the constant temperature bath. The sample cylinder is then cooled, disconnected from the apparatus, cleaned of excess fluid between the disconnect and the valve, and weighed to determine the weight of the compound in the constant volume sample cylinder. Duplicate measurements for each temperature were made.

The volume of the constant-volume cylinder was determined with deionized water in a constant-temperature bath accurate to $\pm 0.1^\circ\text{C}$. Due to the significant temperature difference between the measurement temperature and the calibration temperature, a correction for expansion of the constant-volume cylinder was included in the cylinder volume calculation (given below).

$$V_{cal} = \pi D^2 L / 4$$

$$V_{test} = \pi [D(1+\alpha)]^2 L(1+\alpha) / 4 = \pi D^2 L(1+\alpha)^3 / 4 = V_{cal}(1+\alpha)^3$$

$$\alpha = \alpha_o \Delta T$$

where:

α_o = thermal expansion coefficient of sample cylinder (1.7×10^{-5} m/m)

ΔT = measurement and calibration temperature difference

The experimental liquid density data was fit to a second-order polynomial using linear-least-squares procedures within AXUM software (TriMetrix, Inc.) for the 300°C to 400°C temperature

range except for decafluorobiphenyl, which was measured from 261°C to 341°C. The form of the second order polynomial is:

$$\rho = A + BT + CT^2$$

where:

ρ = liquid density (g/ml)

T = temperature (K)

A, B, C = fitted constants

The observed liquid densities, the average density values for each temperature, the calculated values from the curve fit, the residual error of the curve fit, and percent error of the curve fit are given in Table 9. Figures 8-12 are plots of the experimental liquid density and the polynomial curve fits for the five candidate fluids tested.

Liquid Viscosity

The liquid kinematic viscosity was measured using a closed, modified Cannon-Fenske, capillary glass viscometer. A schematic of the apparatus is given in Figure 13. This method has been used by others (Refs. 73 and 74) and is a modification of ASTM method. The kinematic viscosity of the fluid is determined by measuring the time it takes the fluid to flow from the upper to lower timing mark on the viscometer. The working equation for this viscometer includes a correction for the vapor density, which may buoy up the liquid:

$$\nu = C(1.0 - \rho_v / \rho_l)t$$

where:

ν = kinematic viscosity (cSt)

C = viscometer constant (cSt/s)

ρ_l = liquid density (g/ml)

ρ_v = vapor density (g/ml)

t = flow time (s)

Table 9. Liquid density measurements.

Temp (C)	Temp (K)	Liquid Density (g/ml)			Curve Fit Regression		
		Cyl #1	Cyl #2	Avg.	Calculated	Residual	% Error
Biphenyl				$d=1.721-0.002051*T+7.395e-7*t^2$			
301	574.15	0.785	0.791	0.788	0.787	2.52E-04	0.032
311	584.15	0.774	0.779	0.777	0.775	1.15E-03	0.149
321	594.15	0.771	0.762	0.767	0.764	2.90E-03	0.380
331	604.15	0.752	0.745	0.748	0.752	-3.76E-03	0.500
341	614.15	0.734	0.741	0.737	0.740	-3.17E-03	0.428
351	624.15	0.725	0.728	0.726	0.729	-2.92E-03	0.400
361	634.15	0.720	0.718	0.719	0.718	1.19E-03	0.166
371	644.15	0.712	0.708	0.710	0.707	3.14E-03	0.444
381	654.15	0.703	0.699	0.701	0.696	5.04E-03	0.724
400	673.15	0.670	0.673	0.672	0.676	-3.82E-03	0.565
Average % Error =							0.379
Naphthalene				$d=-0.7018+0.00591*T-5.842e-6*T^2$			
301	574.15	0.773	0.763	0.768	0.766	1.99E-03	0.260
321	594.15	0.751	0.737	0.744	0.747	-3.10E-03	0.415
341	614.15	0.729	0.717	0.723	0.724	-1.11E-03	0.153
361	634.15	0.704	0.693	0.699	0.697	2.01E-03	0.289
380	653.15	0.673	0.663	0.668	0.666	1.68E-03	0.252
401	674.15	0.628	0.624	0.626	0.627	-1.47E-03	0.235
Average % Error =							0.267
Quinoline				$d=2.755-0.004885*T+2.739e-6*T^2$			
301	574.15	0.856	0.840	0.848	0.853	-4.85E-03	0.569
321	594.15	0.822	0.835	0.829	0.819	9.72E-03	1.187
341	614.15	0.782	0.786	0.784	0.788	-3.21E-03	0.407
361	634.15	0.757	0.759	0.758	0.758	-1.92E-04	0.025
381	654.15	0.733	0.720	0.727	0.731	-4.62E-03	0.632
401	674.15	0.708	0.711	0.709	0.706	3.15E-03	0.446
Average % Error =							0.544
o-Terphenyl				$d=-0.1711+0.003956*T-3.833e-6*T^2$			
301	574.15	0.837	0.838	0.838	0.836	1.11E-03	0.133
321	594.15	0.829	0.817	0.823	0.826	-2.73E-03	0.331
341	614.15	0.815	0.814	0.814	0.812	1.73E-03	0.213
361	634.15	0.794	0.798	0.796	0.796	8.62E-05	0.011
381	654.15	0.773	0.779	0.776	0.776	2.22E-05	0.003
400	673.15	0.750	0.759	0.754	0.755	-2.17E-04	0.029
Average % Error =							0.120
Decafluorobiphenyl				$d=-1.48+0.01248*T-1.383e-5*T^2$			
261	534.15	1.246	1.233	1.240	1.239	8.38E-04	0.068
281	554.15	1.189	1.186	1.187	1.188	-3.10E-04	0.026
301	574.15	1.125	1.116	1.121	1.125	-4.10E-03	0.364
321	594.15	1.057	1.057	1.057	1.052	5.77E-03	0.549
341	614.15	0.977	0.952	0.965	0.967	-2.20E-03	0.228
Average % Error =							0.247

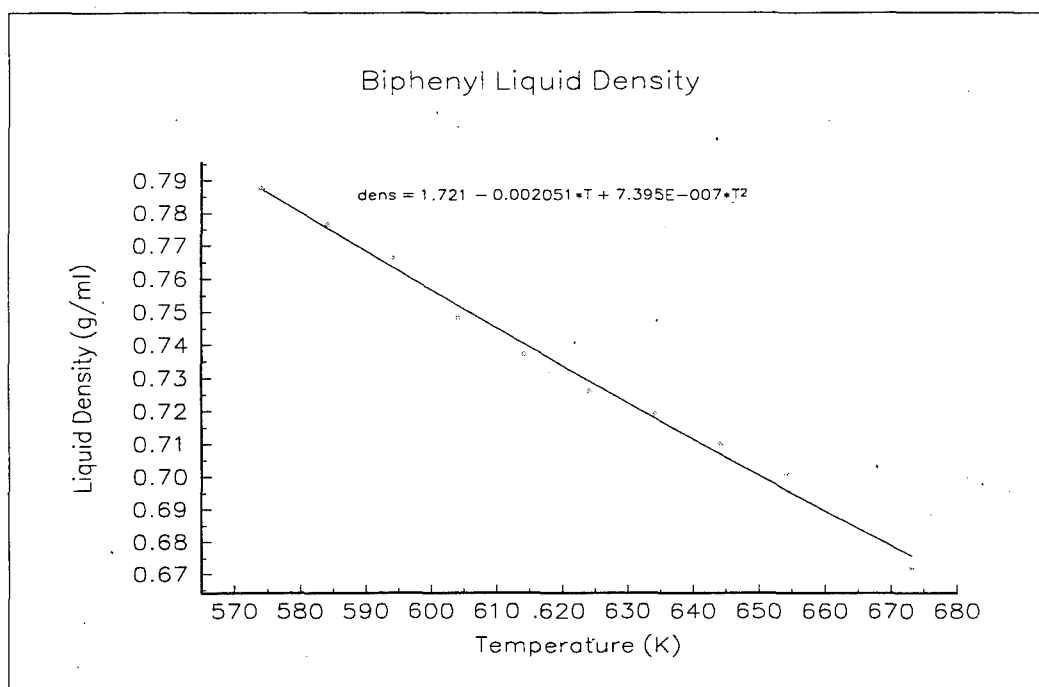


Figure 8. Liquid density data and curve-fit for biphenyl.

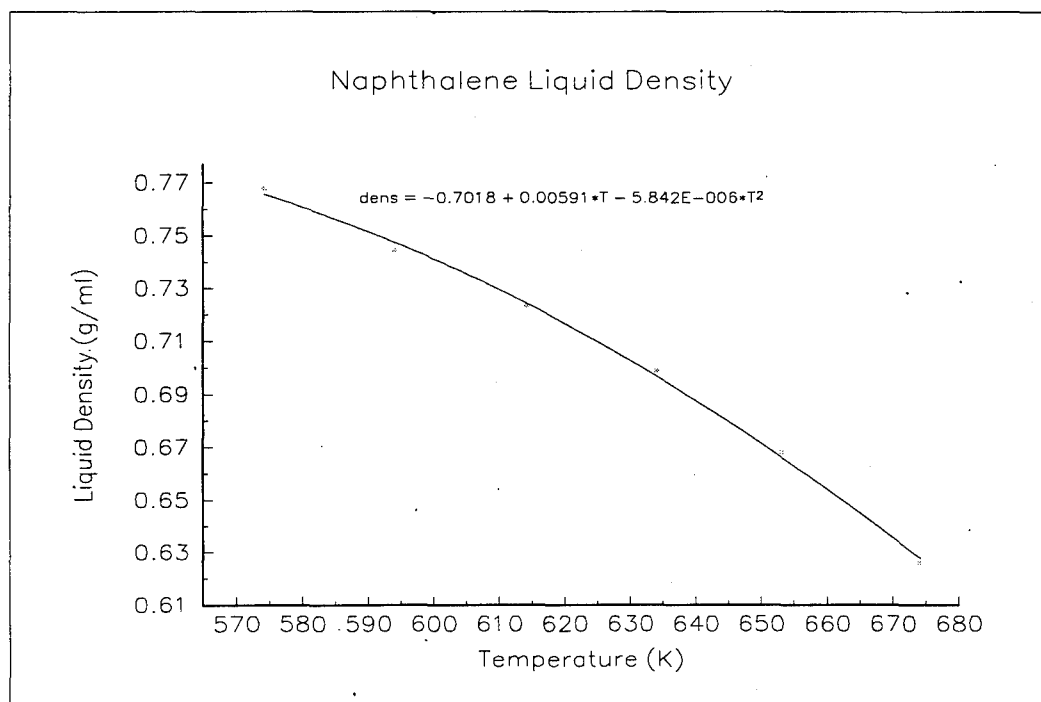


Figure 9. Liquid density data and curve-fit for naphthalene.

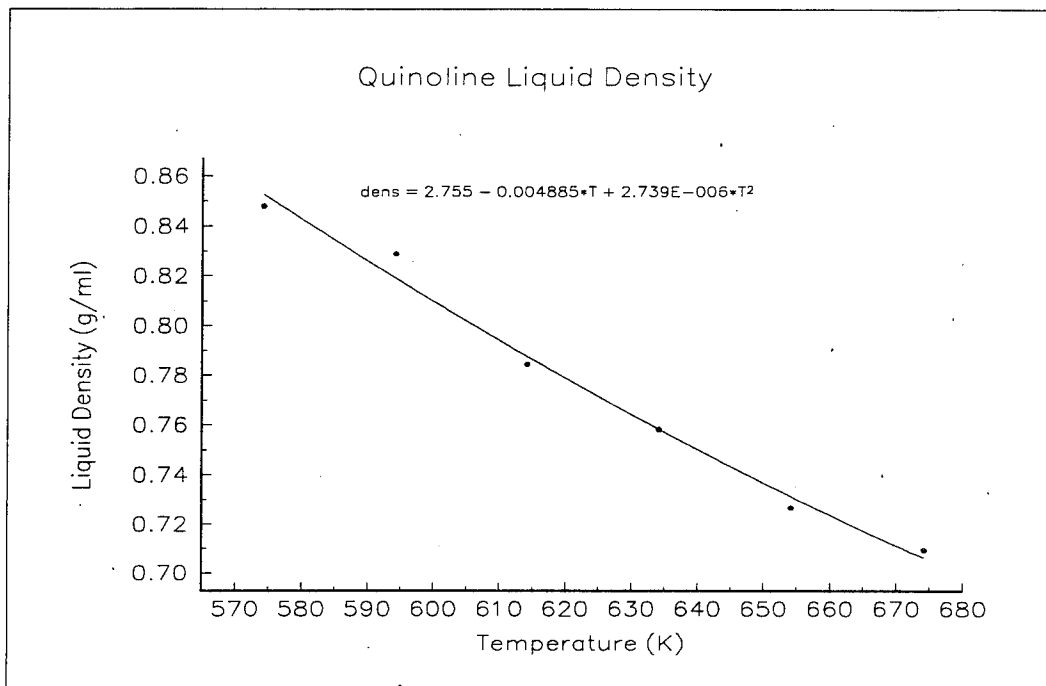


Figure 10. Liquid density data and curve-fit for quinoline.

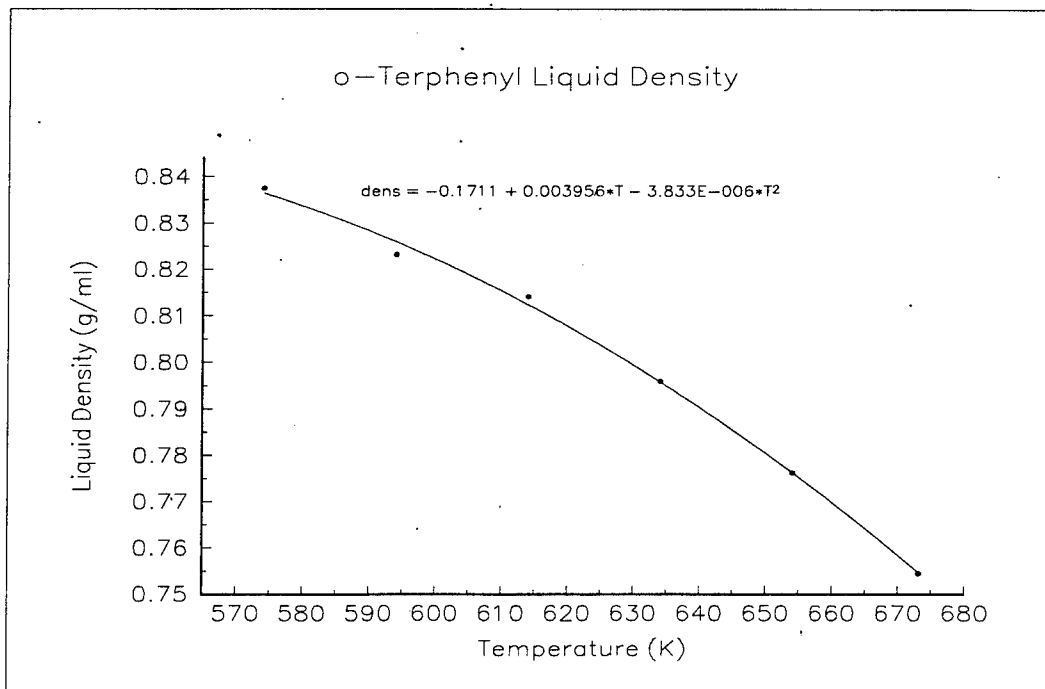


Figure 11. Liquid density data and curve-fit for o-terphenyl.

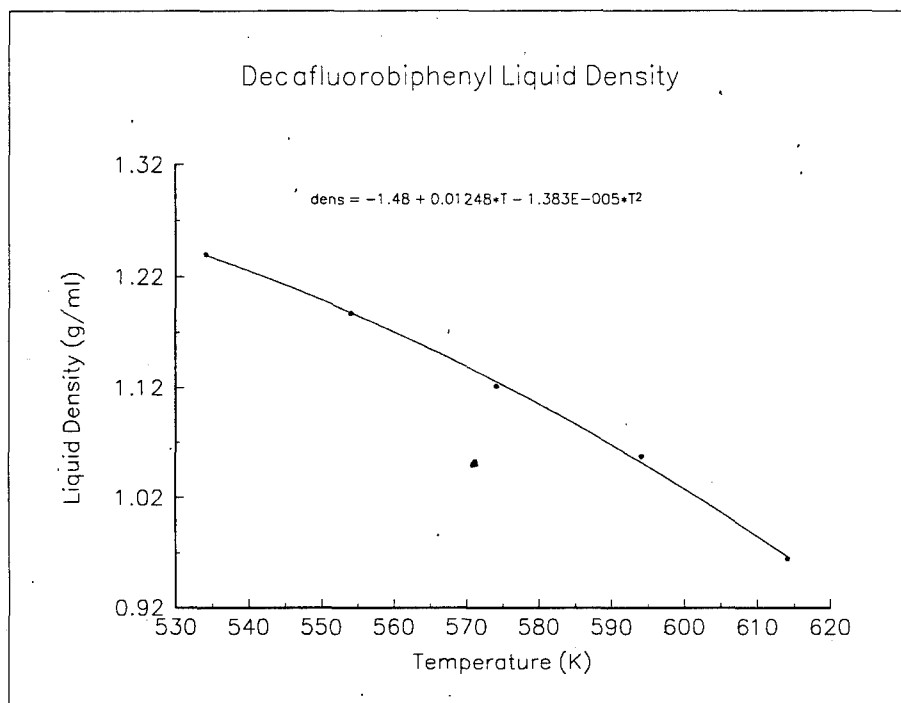


Figure 12. Liquid density data and curve-fit for decafluorobiphenyl.

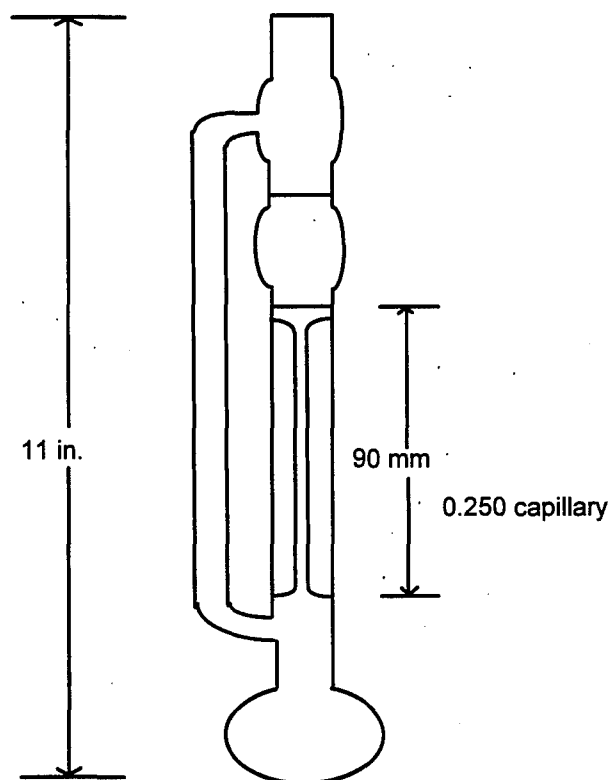


Figure 13. Schematic of liquid viscosity apparatus.

The viscometer was filled with molten working fluid, frozen and thawed under vacuum to remove noncondensibles, evacuated, and sealed with a torch so that the fluid was at its vapor pressure at all times (no air is in the viscometer). A stopwatch was used to determine the flow time in the viscometer. The apparatus was then fastened to its holding fixture and immersed in the lab bath where it was allowed to reach thermal equilibrium with at the test temperature. The viscometer holding fixture was then used to invert the viscometer, which allowed liquid to flow into the upper portion above the top timing mark. The viscometer was then re-inverted to its initial position and the flow time was recorded. This procedure was repeated three times for each temperature and the average flow time was calculated. Each viscometer was calibrated at 40°C (±0.1°C) to determine the viscometer constant using Cannon viscosity standard N1.0.

To use the kinematic viscosity working equation, liquid density was determined using the above experimental measurements and vapor density was determined using the Lee-Kesler correlations (Ref. 59). Absolute viscosity was determined by multiplying the kinematic viscosity by the liquid density. These values were then fit to the Andrade equations using Marquardt-Levenberg (Ref. 75) non-linear least squares regression software (AXUM by TriMetrix, Inc.) for the temperature range of 300°C to 400°C, except for decafluorobiphenyl, which was measured from 251°C to 321°C :

$$\ln \eta = A + B / T$$

where:

- η = absolute viscosity (cP) = ν / ρ_l
- A, B = fitted constants
- T = temperature (K)

The experimental data and curve fit information for the candidate working fluids are given in Table 10. Figures 14-18 are plots of the experimental liquid viscosities and the Andrade equation curve fits for the five candidate fluids tested.

Table 10. Liquid viscosity measurements.

Temp (C)	Temp (K)	Time (sec)			Average Time (s)	Liq. Dens. (g/ml)	Vap. Dens. (g/ml)	Kin. Visc. (cSt)	Abs. Visc. (cP)	Regression Curve Fit		
		1	2	3						Calc.	Residual	% Error
Naphthalene		constant =			4.963E-04							
301	574.15	539	556	546	547.00	0.766	1.51E-02	0.266	0.204	0.206	-0.002	0.961
311	584.15	514	516	521	517.00	0.757	1.76E-02	0.251	0.190	0.190	0.000	0.144
321	594.15	488	485	496	489.67	0.747	2.04E-02	0.236	0.177	0.176	0.001	0.380
331	604.15	469	459	453	460.33	0.736	2.37E-02	0.221	0.163	0.163	-0.001	0.340
341	614.15	439	443	438	440.00	0.724	2.73E-02	0.210	0.152	0.152	0.000	0.093
351	624.15	425	419	423	422.33	0.711	3.14E-02	0.200	0.142	0.142	0.001	0.422
361	634.15	410	407	406	407.67	0.697	3.60E-02	0.192	0.134	0.133	0.001	0.771
371	644.15	383	390	399	390.67	0.681	4.13E-02	0.182	0.124	0.124	0.000	0.169
381	654.15	380	384	383	382.33	0.664	4.73E-02	0.176	0.117	0.117	0.000	0.380
391	664.15	370	373	371	371.33	0.646	5.41E-02	0.169	0.109	0.110	-0.001	0.500
400	673.15	361	363	359	361.00	0.629	6.13E-02	0.162	0.102	0.104	-0.002	2.185
						Average % Error =						
						0.577						
Biphenyl		constant =			4.277E-04							
301	574.15	855	831	859	848.33	0.787	8.67E-03	0.359	0.282	0.275	0.007	2.642
311	584.15	798	805	786	796.33	0.775	1.03E-02	0.336	0.261	0.253	0.007	2.821
321	594.15	715	719	714	716.00	0.763	1.21E-02	0.301	0.230	0.234	-0.004	1.595
331	604.15	681	684	679	681.33	0.752	1.42E-02	0.286	0.215	0.216	-0.001	0.671
341	614.15	638	643	644	641.67	0.740	1.66E-02	0.268	0.199	0.201	-0.002	1.101
351	624.15	613	616	615	614.67	0.729	1.93E-02	0.256	0.187	0.187	0.000	0.122
361	634.15	580	577	581	579.33	0.718	2.24E-02	0.240	0.172	0.174	-0.002	1.072
371	644.15	536	548	545	543.00	0.707	2.58E-02	0.224	0.158	0.163	-0.005	2.906
381	654.15	525	531	533	529.67	0.696	2.97E-02	0.217	0.151	0.152	-0.001	0.971
391	664.15	512	504	510	508.67	0.685	3.41E-02	0.207	0.142	0.143	-0.001	0.935
400	673.15	496	488	490	491.33	0.675	3.86E-02	0.198	0.134	0.135	-0.001	0.999
						Average % Error =						
						1.440						
o-Terphenyl		constant =			4.196E-04							
301	574.15	1020	1015	1023	1019.33	0.837	2.57E-03	0.426	0.357	0.356	0.001	0.162
311	584.15	971	977	980	976.00	0.832	3.17E-03	0.408	0.339	0.335	0.004	1.152
321	594.15	936	925	931	930.67	0.826	3.88E-03	0.389	0.321	0.317	0.005	1.420
331	604.15	879	880	879	879.33	0.820	4.71E-03	0.367	0.301	0.299	0.001	0.477
341	614.15	836	839	837	837.33	0.813	5.68E-03	0.349	0.284	0.284	0.000	0.003
351	624.15	797	799	802	799.33	0.805	6.79E-03	0.333	0.268	0.269	-0.001	0.521
361	634.15	763	760	758	760.33	0.796	8.08E-03	0.316	0.251	0.256	-0.004	1.712
371	644.15	745	735	744	741.33	0.787	9.55E-03	0.307	0.242	0.243	-0.002	0.703
381	654.15	718	710	707	711.67	0.777	1.12E-02	0.294	0.229	0.232	-0.004	1.566
391	664.15	697	700	696	697.67	0.766	1.31E-02	0.288	0.220	0.222	-0.001	0.612
400	673.15	676	676	673	675.00	0.755	1.51E-02	0.278	0.210	0.213	-0.003	1.549
						Average % Error =						
						0.898						
Quinoline		constant =			4.963E-04							
301	574.15	537	539	540	538.67	0.853	1.05E-02	0.264	0.225	0.226	-0.001	0.402
311	584.15	518	518	518	518.00	0.836	1.24E-02	0.253	0.212	0.211	0.001	0.254
321	594.15	496	498	499	497.67	0.819	1.45E-02	0.243	0.199	0.198	0.001	0.567
331	604.15	478	477	479	478.00	0.803	1.69E-02	0.232	0.187	0.185	0.001	0.616
341	614.15	459	458	458	458.33	0.788	1.98E-02	0.222	0.175	0.174	0.000	0.264
351	624.15	441	442	442	441.67	0.773	2.27E-02	0.213	0.164	0.164	0.000	0.180
361	634.15	426	429	427	427.33	0.759	2.62E-02	0.205	0.155	0.155	0.000	0.277
371	644.15	413	411	412	412.00	0.745	3.00E-02	0.196	0.146	0.146	0.000	0.205
380	653.15	402	401	403	402.00	0.733	3.40E-02	0.190	0.139	0.139	0.000	0.003
391	664.15	391	390	391	390.67	0.719	3.94E-02	0.183	0.132	0.132	0.000	0.143
401	674.15	382	382	380	381.33	0.707	4.49E-02	0.177	0.125	0.125	0.000	0.204
						Average % Error =						
						0.283						
Decafluorobiphenyl		constant =			4.277E-04							
251	524.15	549	547	544	546.67	1.262	2.65E-02	0.229	0.289	0.282	0.007	2.542
261	534.15	518	520	515	517.67	1.240	3.27E-02	0.216	0.267	0.260	0.008	2.940
271	544.15	496	489	483	489.33	1.216	4.02E-02	0.202	0.246	0.240	0.006	2.505
281	554.15	438	459	450	449.00	1.189	4.92E-02	0.184	0.219	0.223	-0.004	1.670
291	564.15	433	430	435	432.67	1.159	6.01E-02	0.175	0.203	0.207	-0.003	1.699
301	574.15	406	414	423	414.33	1.126	7.34E-02	0.166	0.187	0.193	-0.006	3.321
311	584.15	385	379	387	383.67	1.091	8.96E-02	0.151	0.164	0.180	-0.016	9.601
						Average % Error =						
						3.468						

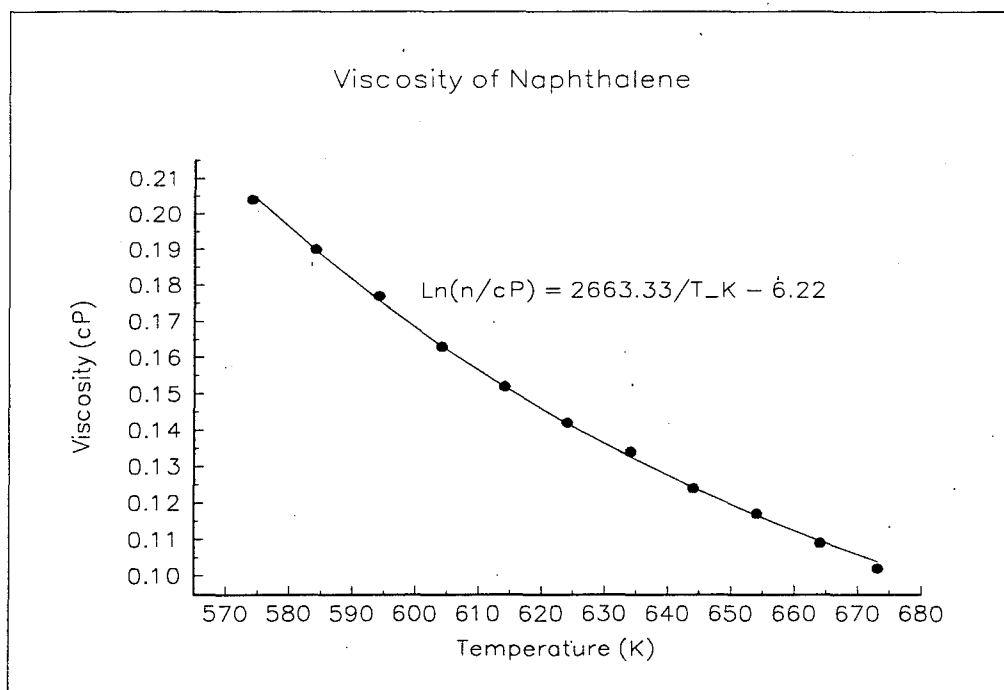


Figure 14. Liquid viscosity data and curve-fit for naphthalene.

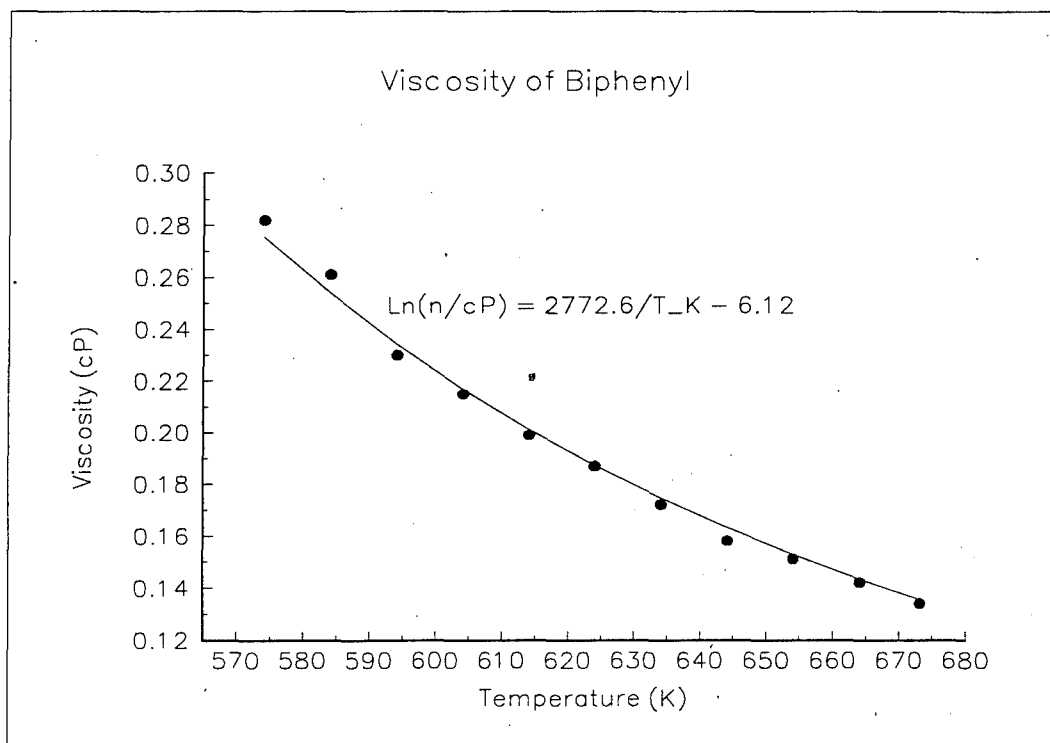


Figure 15. Liquid viscosity data and curve-fit for biphenyl.

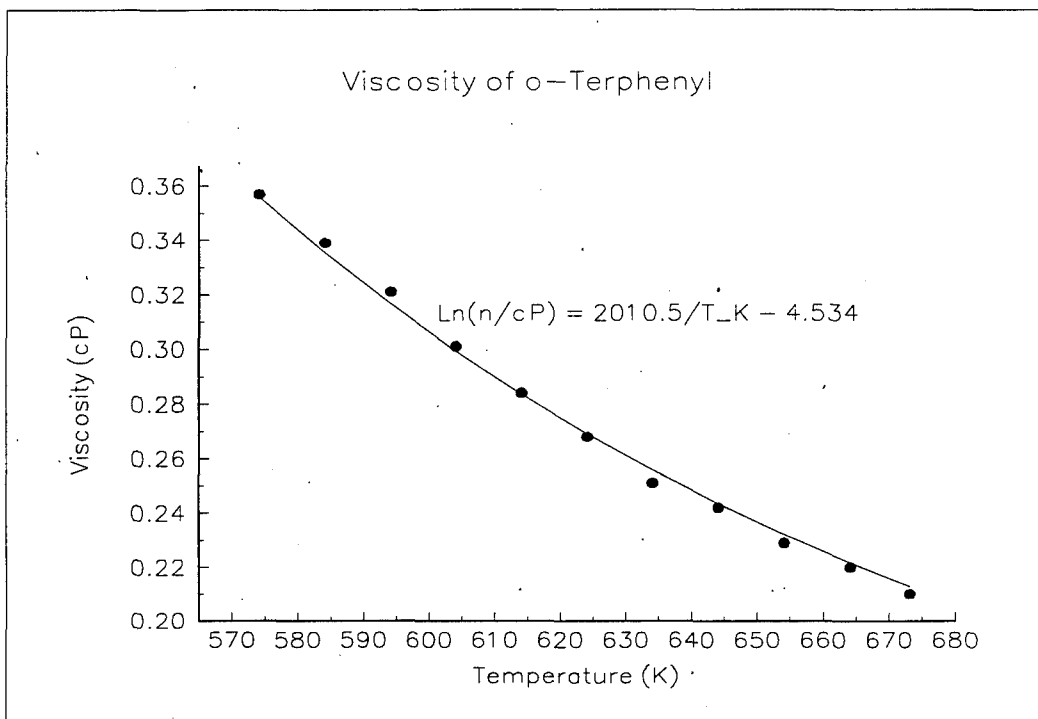


Figure 16. Liquid viscosity data and curve-fit for o-terphenyl.

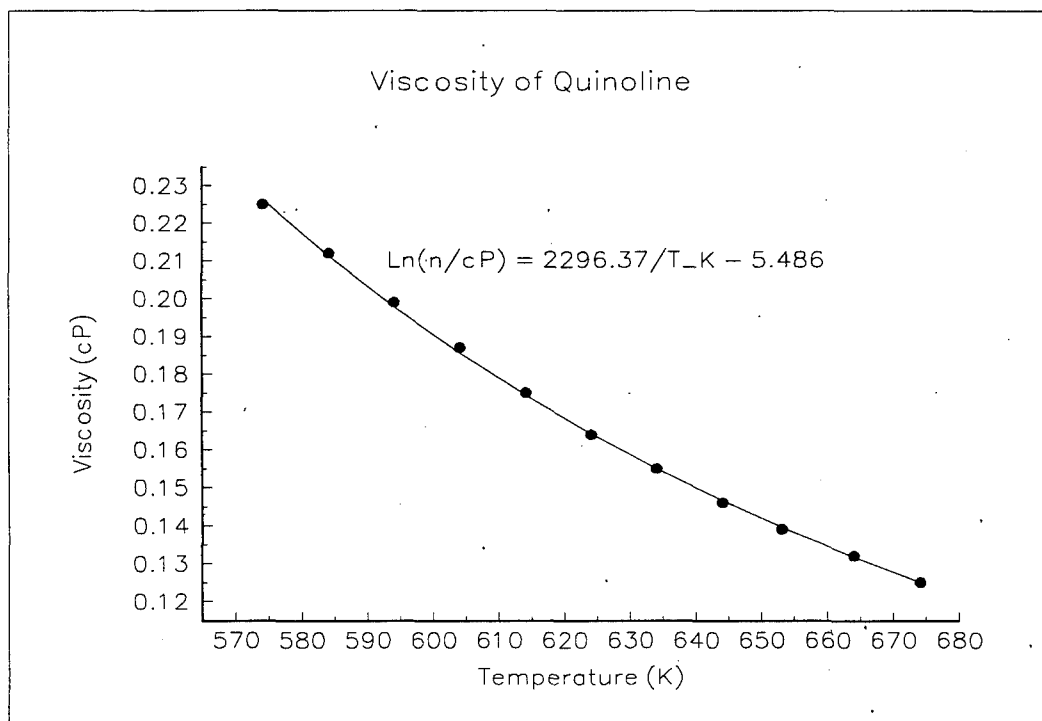


Figure 17. Liquid viscosity data and curve-fit for quinoline.

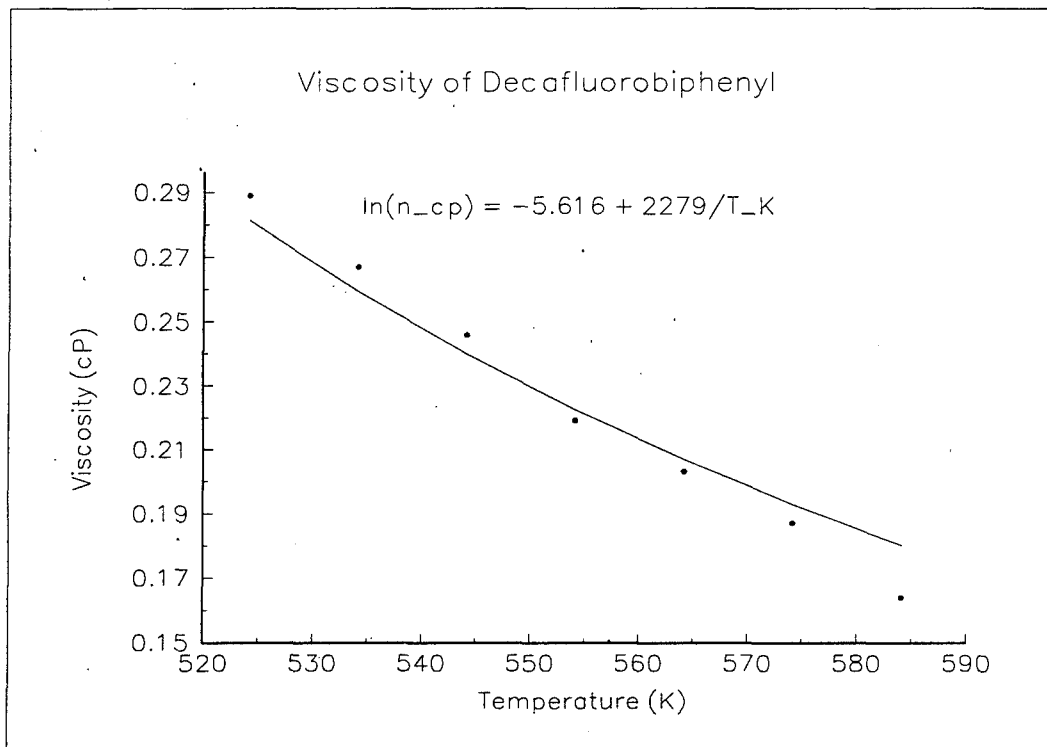


Figure 18. Liquid viscosity data and curve-fit for decafluorobiphenyl.

Surface Tension

The surface tension of the candidate working fluids was measured using the differential capillary rise technique in a closed glass vessel. This technique has been used on recent alternative refrigerant characterizations (Ref. 76). In this method, surface tension is determined directly from the capillary length parameter through the following equation.

$$\sigma = a^2(\rho_l - \rho_v)g/2$$

where:

- σ = surface tension
- α = capillary length parameter
- ρ_l = liquid density
- ρ_v = vapor density
- g = acceleration due to gravity

The capillary length parameter is determined by measuring the differential height (Δh) of the liquid menisci in two different capillaries with larger and smaller radii r_L and r_S respectively. The differential height of the candidate fluids was measured with a capillary glass apparatus consisting of three capillary tubes of different radii; 0.276 mm, 0.320 mm, and 0.574 mm (Tudor Scientific Glass). This apparatus is shown in Figure 19.

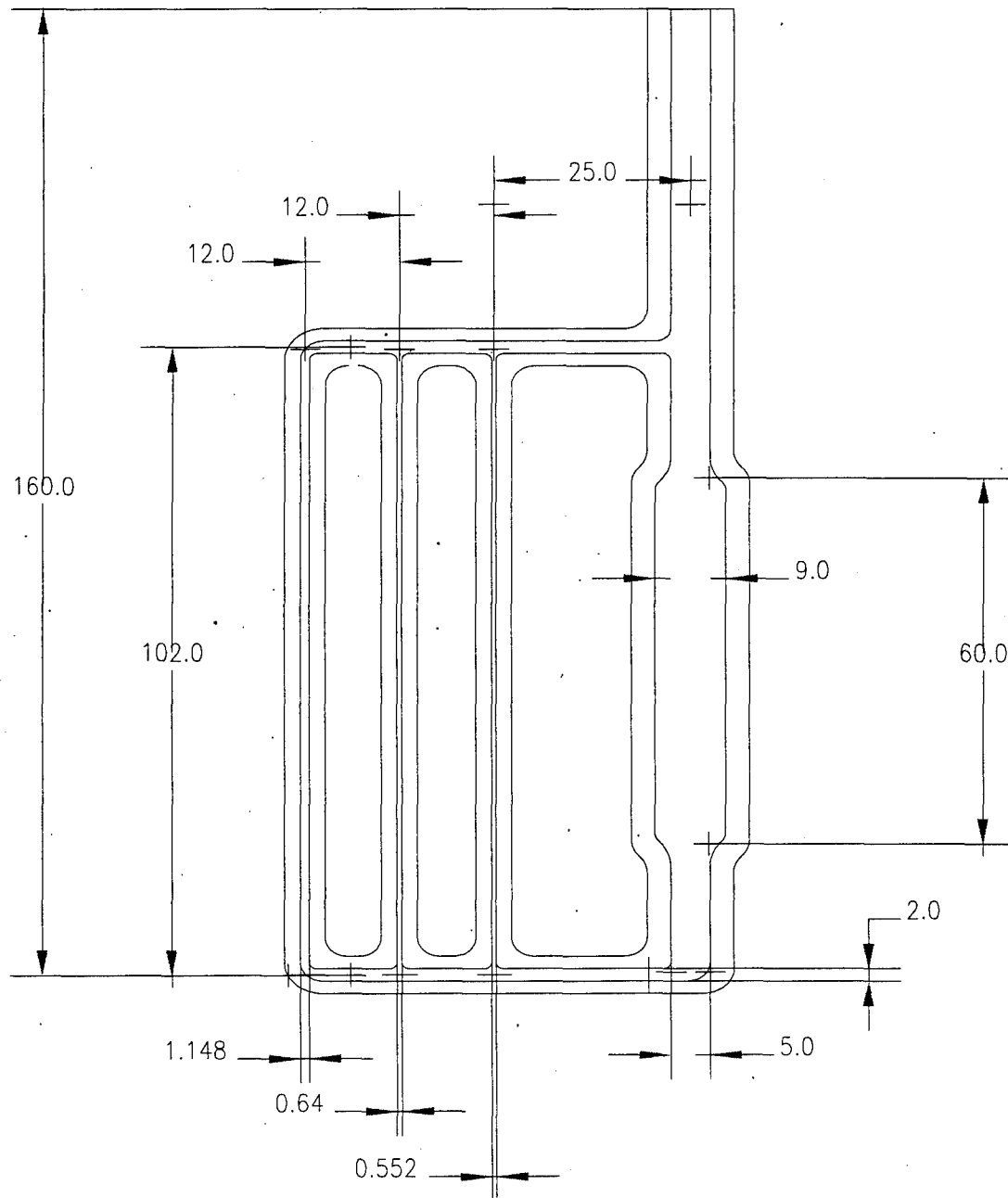


Figure 19. Schematic of the surface tension apparatus.

To perform a measurement, the apparatus was filled with working fluid, frozen and thawed under vacuum, evacuated, and sealed with a torch so that the fluid is at its own vapor pressure at all times. Therefore, the surface tension determined was the liquid/vapor interfacial tension of the fluid (no air is in the apparatus). The laboratory bath described above was used with an appropriate fixture to hold the apparatus. A cathetometer was used to measure Δh ($\pm 0.0005''$). Once the apparatus was filled and sealed, it was immersed in the lab bath and allowed to reach thermal equilibrium at the test temperature. The differential height between each of the capillaries was then measured with the cathetometer and the computer program determined the capillary length parameter from the Δh measurements.

Determination of the capillary length parameter is an iterative process using polynomial functions (Ref. 77). The first approximation to the capillary length parameter α is given by

$$\alpha_j^2 = \Delta h r_s$$

This first approximation of the capillary length parameter is then used to determine the capillary rise in the larger tube h_L .

$$h_L = \frac{\alpha_{ij}^2}{r_L} \frac{1}{F(r_L / \alpha_{ij})} \quad \text{for } \frac{r_L}{\alpha_{ij}} < 2$$

$$h_L = \frac{\alpha_{ij}^2}{r_L} \Phi(r_L / \alpha_{ij}) \quad \text{for } \frac{r_L}{\alpha_{ij}} > 2$$

with

$$F\left(X = \frac{r}{\alpha}\right) = 1 + a_2 X^2 + a_3 X^3 - a_4 X^4 + a_5 X^5 - a_6 X^6 + a_7 X^7 - a_8 X^8$$

$$\Phi\left(X = \frac{r}{\alpha}\right) = X^{3/2} \exp(b_1 X + b_2 - b_3 X^{-1} + b_4 X^{-2})$$

This value of h_L is then used to obtain a better estimate of α^2

$$\alpha_{ij}^2 = r_s (h_L + \Delta h_{ij}) F(r_s / \alpha_{ij}) \quad \text{for } \frac{r_s}{\alpha_{ij}} < 2$$

$$\alpha_{ij}^2 = r_s (h_L + \Delta h_{ij}) \frac{1}{\Phi(r_s / \alpha_{ij})} \quad \text{for } \frac{r_s}{\alpha_{ij}} > 2$$

This procedure is iterated until the solution converges. The final value of α^2 is then used to determine σ . A FORTRAN computer program was used to perform the calculation of α^2 . A copy of this program and an example output from the program is given in Appendix B.

The surface tension data was fit using Marquardt-Levenberg (Ref. 75) non-linear least squares regression software (AXUM by TriMetrix, Inc.) to an equation that accounts for the variation of surface tension with temperature (Ref. 41), for the temperature range of 300°C to 400°C (except for decafluorobiphenyl, which was measured from 251°C to 321°C):

$$\sigma = c(1 - T_r)^{4n}$$

where:

n, c = fitted constants

$$T_r = T/T_c$$

σ = surface tension (dyne/cm)

The capillary length parameters (determined from Δh measurements), the average capillary length parameter, the surface tension of the fluids, the calculated surface tension from the curve fit, the residual error of the curve fit, and the percent area of the curve fit are presented in Table 11. In this table, α_{23} refers to the medium and large capillaries, and α_{13} refers to the small and large capillaries (see Figure 19). Figures 20-24 are plots of the surface tension data and curve-fits for the five candidate fluids.

Table 12. Surface tension measurements.

Temp (C)	Temp (K)	Reduced Temp	Alpha 2-3 (mm)	Alpha 1-3 (mm)	Avg. Alpha (mm)	Liq. Dens. (g/ml)	Vap. Dens. (g/ml)	Surf. Tens. (dyne/cm)	Curve Fit Regression			
									Calc.	Residual	% Error	
Biphenyl												
			Tc= 789.000		K							
300	573.15	0.726	1.843	1.834	1.838	0.788	0.009	12.915	12.80	0.112	0.869	
310	583.15	0.739	1.799	1.800	1.799	0.776	0.010	12.158	12.13	0.030	0.243	
321	594.15	0.753	1.784	1.764	1.774	0.763	0.012	11.586	11.39	0.193	1.667	
331	604.15	0.766	1.722	1.707	1.715	0.752	0.014	10.629	10.73	-0.100	0.941	
341	614.15	0.778	1.694	1.665	1.680	0.740	0.017	10.003	10.07	-0.067	0.666	
351	624.15	0.791	1.632	1.611	1.622	0.729	0.019	9.144	9.42	-0.272	2.977	
361	634.15	0.804	1.603	1.593	1.598	0.718	0.022	8.702	8.77	-0.066	0.757	
371	644.15	0.816	1.557	1.559	1.558	0.707	0.026	8.095	8.12	-0.030	0.366	
381	654.15	0.829	1.515	1.537	1.526	0.696	0.030	7.599	7.49	0.111	1.456	
391	664.15	0.842	1.468	1.486	1.477	0.685	0.034	6.960	6.86	0.101	1.452	
400	673.15	0.853	1.429	1.440	1.435	0.675	0.039	6.424	6.30	0.126	1.964	
											Average % Error =	1.214
o-Terphenyl												
			Tc= 891.000		K							
301	574.15	0.644	2.055	2.057	2.056	0.837	0.003	17.274	17.27	0.000	0.001	
310	583.15	0.654	2.024	2.030	2.027	0.832	0.003	16.697	16.58	0.120	0.721	
321	594.15	0.667	1.984	1.992	1.988	0.826	0.004	15.922	15.74	0.186	1.170	
331	604.15	0.678	1.945	1.957	1.951	0.820	0.005	15.198	14.98	0.214	1.409	
341	614.15	0.689	1.893	1.909	1.901	0.813	0.006	14.290	14.24	0.048	0.337	
351	624.15	0.701	1.850	1.878	1.864	0.805	0.007	13.583	13.51	0.071	0.521	
361	634.15	0.712	1.823	1.838	1.830	0.796	0.008	12.933	12.79	0.139	1.073	
371	644.15	0.723	1.768	1.796	1.782	0.787	0.010	12.088	12.09	0.000	0.003	
381	654.15	0.734	1.734	1.763	1.748	0.777	0.011	11.464	11.39	0.070	0.612	
391	664.15	0.745	1.698	1.722	1.710	0.766	0.013	10.783	10.71	0.070	0.653	
400	673.15	0.755	1.672	1.686	1.679	0.755	0.015	10.222	10.11	0.113	1.102	
											Average % Error =	0.691
Naphthalene												
			Tc= 748.800		K							
301	574.15	0.767	1.866	1.878	1.872	0.766	0.015	12.887	12.91	-0.024	0.184	
311	584.15	0.780	1.826	1.817	1.822	0.757	0.018	12.022	12.06	-0.042	0.351	
321	594.15	0.793	1.768	1.775	1.772	0.747	0.020	11.178	11.23	-0.047	0.423	
331	604.15	0.807	1.704	1.720	1.712	0.736	0.024	10.234	10.39	-0.160	1.565	
341	614.15	0.820	1.654	1.669	1.661	0.724	0.027	9.427	9.57	-0.145	1.543	
351	624.15	0.834	1.625	1.623	1.624	0.711	0.031	8.783	8.76	0.023	0.262	
361	634.15	0.847	1.563	1.569	1.566	0.697	0.036	7.936	7.96	-0.021	0.264	
371	644.15	0.860	1.493	1.516	1.504	0.681	0.041	7.095	7.16	-0.068	0.964	
380	653.15	0.872	1.454	1.452	1.453	0.666	0.047	6.408	6.46	-0.052	0.814	
390	663.15	0.886	1.388	1.395	1.391	0.648	0.053	5.644	5.69	-0.046	0.812	
400	673.15	0.899	1.320	1.337	1.329	0.629	0.061	4.916	4.93	-0.016	0.330	
											Average % Error =	0.683
Decafluorobiphenyl												
			Tc= 640.450		K							
251	524.15	0.818	1.014	0.975	0.995	1.262	0.026	5.987	6.06	-0.076	1.271	
261	534.15	0.834	0.983	0.942	0.963	1.240	0.033	5.485	5.35	0.134	2.447	
271	544.15	0.850	0.930	0.877	0.903	1.216	0.040	4.703	4.66	0.038	0.809	
281	554.15	0.865	0.871	0.834	0.853	1.189	0.049	4.059	4.01	0.054	1.330	
291	564.15	0.881	0.804	0.734	0.769	1.159	0.060	3.181	3.38	-0.194	6.105	
301	574.15	0.896	0.770	0.700	0.735	1.126	0.073	2.788	2.78	0.012	0.419	
311	584.15	0.912	0.733	0.678	0.705	1.091	0.090	2.440	2.21	0.228	9.352	
321	594.15	0.928	0.613	0.543	0.578	1.053	0.110	1.543	1.69	-0.143	9.268	
											Average % Error =	3.875
Quinoline												
			Tc= 782.150		K							
301	574.15	0.734	1.945	1.929	1.937	0.853	0.011	15.492	15.22	0.271	1.752	
311	584.15	0.747	1.912	1.861	1.886	0.836	0.012	14.361	14.26	0.096	0.669	
321	594.15	0.760	1.849	1.809	1.829	0.819	0.015	13.191	13.32	-0.133	1.007	
331	604.15	0.772	1.813	1.759	1.786	0.803	0.017	12.290	12.40	-0.109	0.889	
341	614.15	0.785	1.753	1.713	1.733	0.788	0.020	11.309	11.49	-0.182	1.609	
351	624.15	0.798	1.701	1.667	1.684	0.773	0.023	10.428	10.60	-0.171	1.640	
361	634.15	0.811	1.661	1.622	1.642	0.759	0.026	9.674	9.73	-0.052	0.536	
371	644.15	0.824	1.614	1.567	1.590	0.745	0.030	8.858	8.87	-0.012	0.139	
381	654.15	0.836	1.560	1.523	1.542	0.732	0.034	8.117	8.03	0.083	1.018	
391	664.15	0.849	1.484	1.458	1.471	0.719	0.039	7.203	7.22	-0.015	0.209	
400	673.15	0.861	1.464	1.430	1.447	0.708	0.044	6.805	6.50	0.302	4.435	
											Average % Error =	1.264

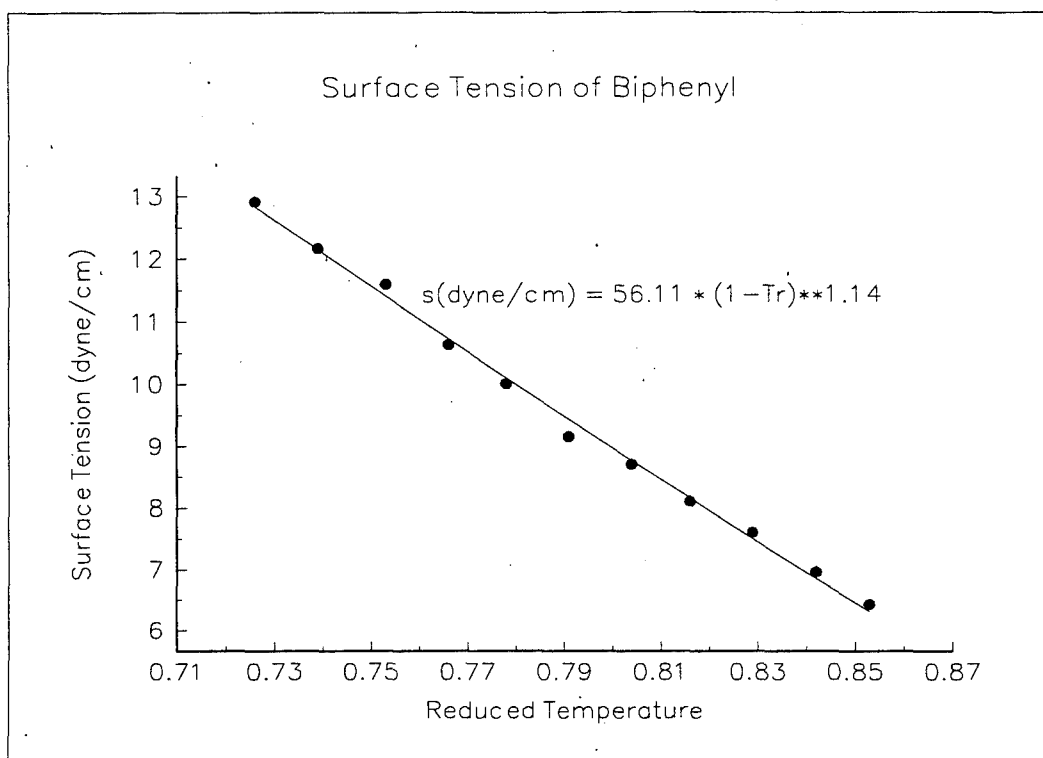


Figure 20. Surface tension data and curve-fit for biphenyl.

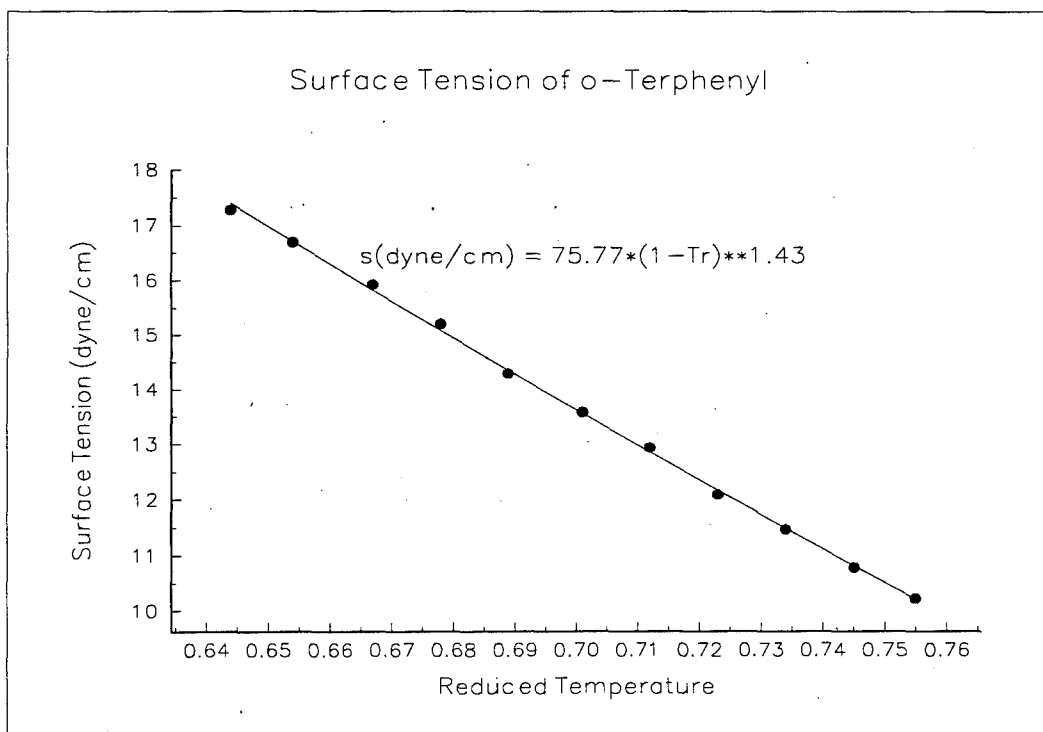


Figure 21. Surface tension data and curve-fit for o-terphenyl.

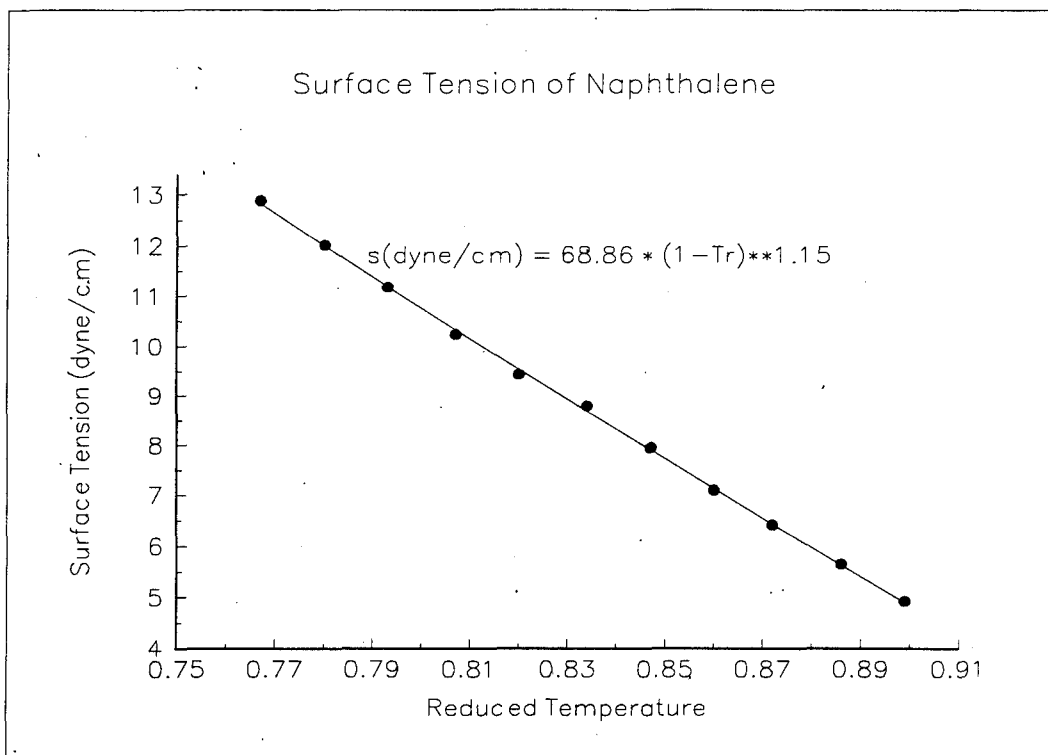


Figure 22. Surface tension data and curve-fit for naphthalene.

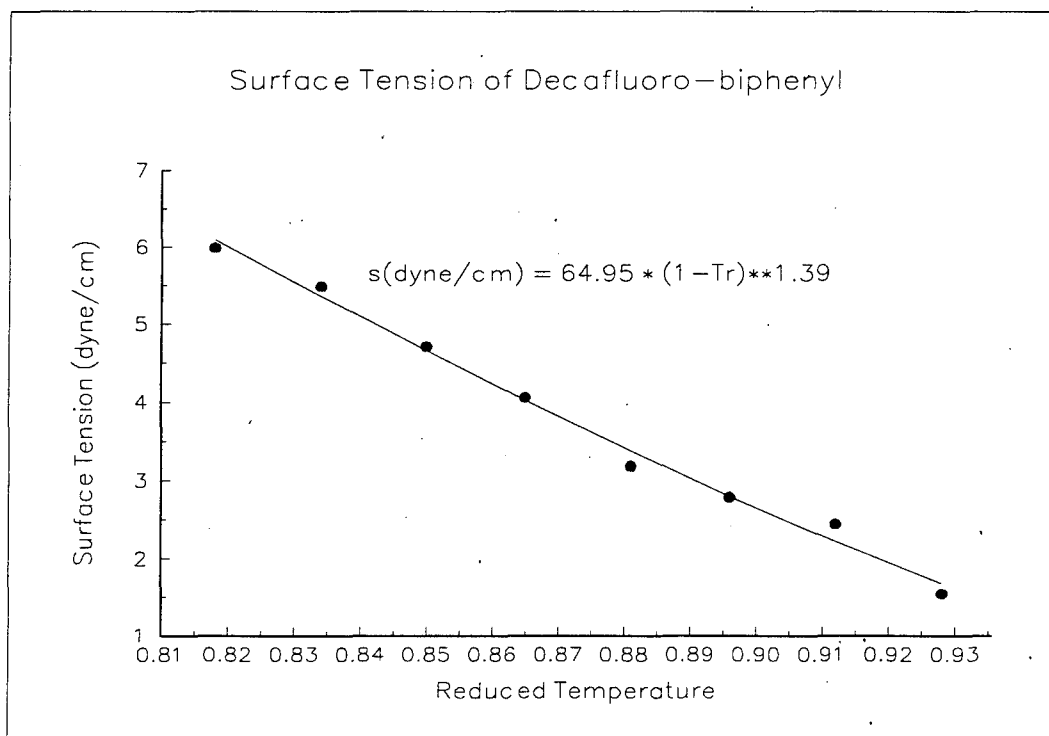


Figure 23. Surface tension data and curve-fit for decafluorobiphenyl.

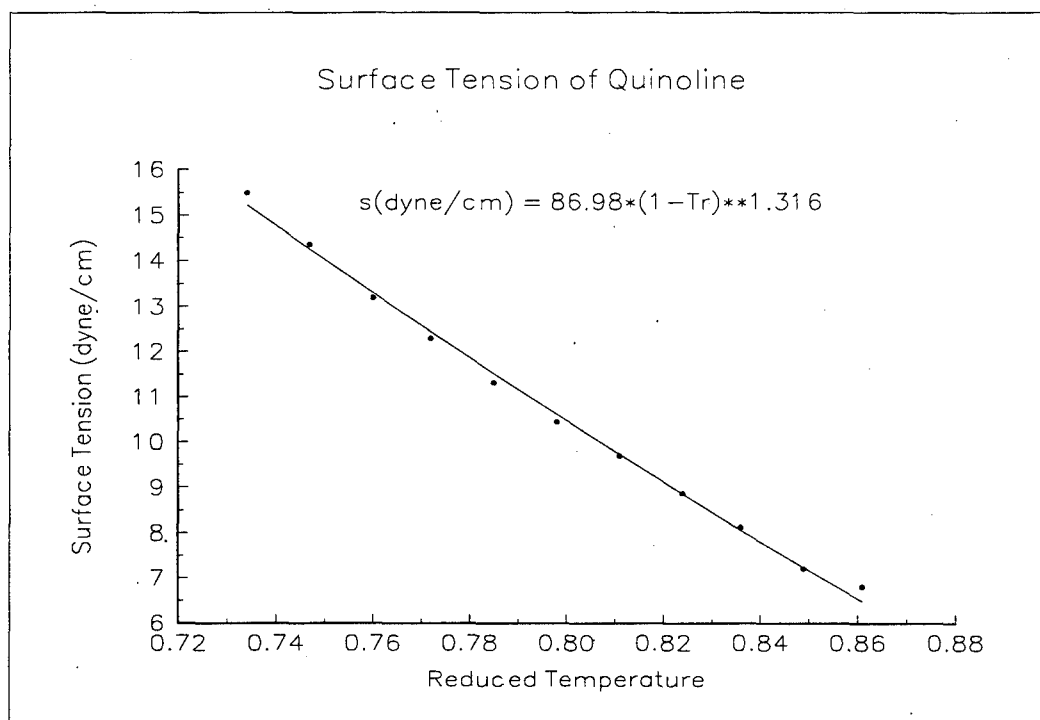


Figure 24. Surface tension data and curve-fit for quinoline.

Vapor Pressure and Heat of Vaporization

The objective of these measurements was to evaluate the vaporization thermodynamic properties of the working fluids candidates using Differential Scanning Calorimetry (DSC). The specific thermodynamic properties measured included melting points, vaporization temperatures, and enthalpies of vaporization. These properties were all measured at various pressures.

Mainstream began developing a technique in this effort utilizing high-pressure DSC and sample vaporization with the objective of measuring enthalpies of vaporization directly over a pressure range from vacuum to several atmospheres. However, the difficulties associated with mass uncertainties through the vaporization endotherm and pressure uncertainties associated with sealed samples pans made this task non-trivial. In developing an alternate approach of indirectly calculating the enthalpy of vaporization with pressure-temperature points and an Antoine equation, it was learned that ASTM's E37 (Thermal Measurements) task group was in the final

stages of detailing such a method (Ref. 77). The general procedures under development by ASTM's E37 task group were integrated into the working-fluid measurements of this effort.

A Mettler 27HP DSC and TC11 Controller was used for the vaporization measurements. The pressure in the DSC cell was controlled by a Brooks 5866 Pressure Controller downstream of the DSC module. The DSC cell was continuously purged with N_2 between 0.5 and 1 l/min (STP) while the cell was maintained at constant pressure. A schematic of the experimental setup is shown in Figure 25. The pressure controller is rated at an accuracy of 0.5% full scale (± 6.9 kPa) and 0.1% repeatability (± 1.5 kPa). Temperature scan rates (β) of 5 K/min were used for all calibration and experimental runs. The temperature accuracy of the DSC system and repeatability are assumed to be ± 0.5 -1.0 K as measured by standard-material checks during the experimental runs and also from correspondence with Mettler application specialists.

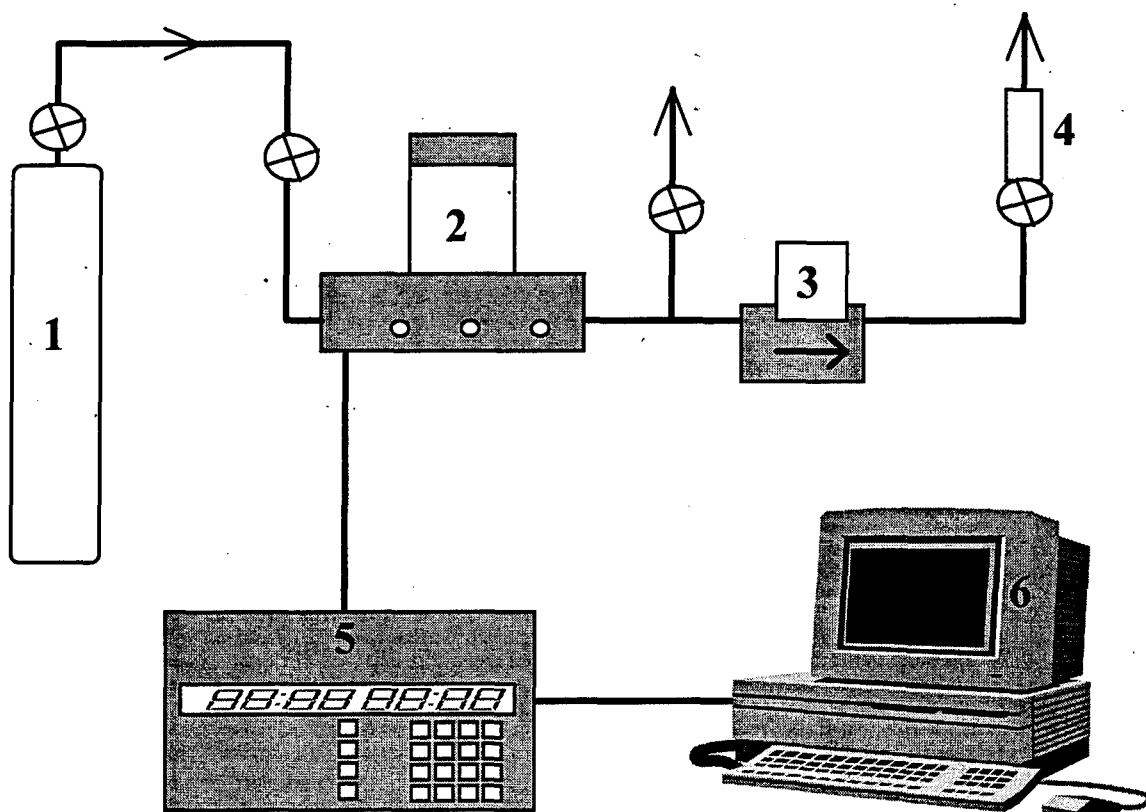


Figure 25. Schematic of experimental setup: 1-Nitrogen cylinder for purge gas; 2-Mettler DSC 27HP; 3-Brooks 5866 Pressure Controller; 4-Rotameter; 5-Mettler TC11 TA Processor; 6-PC running Mettler Graphware TA72 analysis software.

Following the method currently under development by ASTM E37, aliquots (2-20 mg) of each material was weighed and sealed in 40 μ L aluminum crucibles with a lid having a 0.10-0.13 mm laser-drilled orifice (Lasertron, Sun Rise, Florida). Samples were ramped in temperature at 5 K/min, and the phase-change endotherms were recorded. Melting and boiling points were then evaluated using Mettler TA72 GraphWare software, and transferred through the QNX operating system to DOS running graphics/statistics software for display and curve fitting.

The DSC was calibrated with three temperature points over the range of 30-420°C using gallium (MP 29.8°C, purity 99.9999%, Aldrich), bismuth (MP 271.3°C, purity 99.99%, Aldrich), and zinc (MP 419.6°C, purity 99.998%, Aldrich). The true melting points of these standards used in the calibration of the DSC were assumed invariant with pressure.

The protocol for selecting melting and boiling points, and the calibration temperatures, was the maximum in the heat flow-temperature derivative (dQ/dT) curve. Example vaporization scans for naphthalene at 47.6 kPa, decafluorobiphenyl at 343.4 kPa, and biphenyl at 1.034 MPa are shown in Figures 26, 27, and 28, respectively. Note that positive values correspond to an endotherm, or heat being added to the sample. The maximum in the heat flow curve is denoted by the symbol ●, and the maximum first derivative (or slope) in the heat flow curve is denoted by ▲. The maximum first derivative protocol for temperature selection was recommended by Mettler specialists as having a high degree of repeatability, and was therefore used for all calibration and sample runs. Other temperature selection protocols such as onset and peak temperatures should not alter the applicability of the DSC method described in this study, provided the method is used consistently with calibration and sample studies.

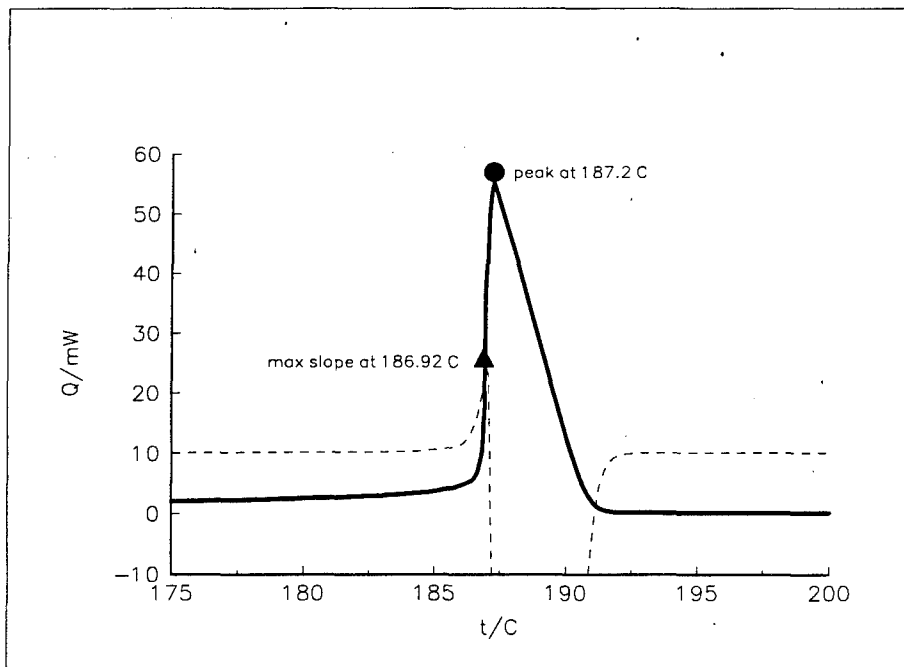


Figure 26. DSC temperature scan ($5^{\circ}\text{C}/\text{min}$) for naphthalene at 47.6 kPa with maximum-slope boiling temperature (\blacktriangle) and peak boiling temperature (\bullet). DSC Q (mW) T (C) scan and dQ/dT curve are represented by the solid and dashed curves, respectively.

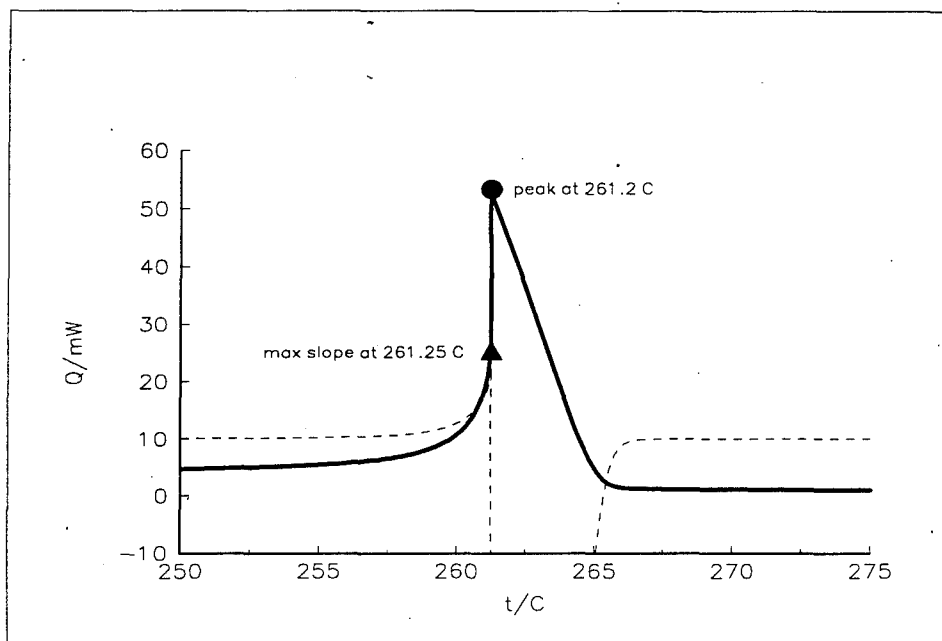


Figure 27. DSC temperature scan ($5^{\circ}\text{C}/\text{min}$) for decafluorobiphenyl at 343.4 kPa with maximum-slope boiling temperature (\blacktriangle) and peak boiling temperature (\bullet). DSC Q (mW) T (C) scan and dQ/dT curve are represented by the solid and dashed curves, respectively.

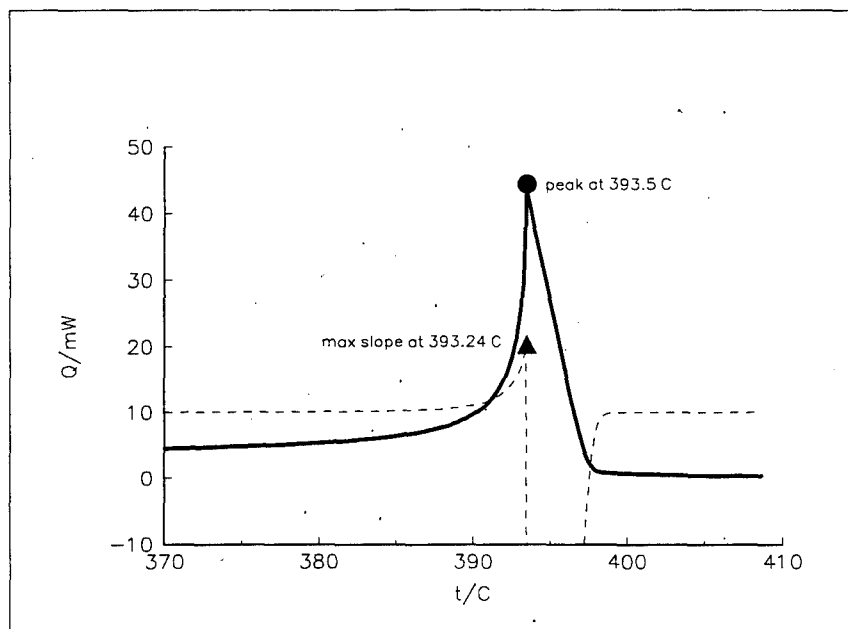


Figure 28. DSC temperature scan (5°C/min) for biphenyl at 1.034 MPa with maximum-slope boiling temperature (▲) and peak boiling temperature (●). DSC Q (mW) T (C) scan and dQ/dT curve are represented by the solid and dashed curves, respectively.

The six candidate working fluids and water were examined using this DSC method to characterize both the melting and boiling points at pressures ranging from 50 kPa to 1.4 MPa. The vaporization data was then curve fitted to the Antoine Equation:

$$\text{Log}_{10} P = a - \frac{b}{T + c}$$

where:

P = pressure (kPa)

T = temperature (K)

a, b, c = fitted constants

using linear-least-squares procedures within DOS-PC Microsoft Excel spreadsheet software, and then with Marquardt-Levenberg (Ref. 75) non-linear least squares regression software (AXUM by TriMetrix, Inc.). The data was fitted to the Antoine equation to minimize the residual error function ϵ in pressure estimates (Ref. 79) defined as:

$$\varepsilon = \sum_{i=1}^N \left(\frac{P_i^{calc} - P_i}{P_i} \right)^2 \cong \sum_{i=1}^N \left(\text{Log} \frac{P_i^{calc}}{P_i} \right)^2 \text{ as } |P_i^{calc} - P_i| \rightarrow 0$$

where N is the number of data points fitted, ε is the residual error function, $P_{i,calc}$ is the pressure estimate from the curve fit, and P_i is the actual pressure data point. Note that the equality in equation (2) is a very close approximation when the relative error $(P_{i,calc} - P_i)/P_i$ is small (i.e., less than 0.15, or 15%). Substituting the Antoine equation into the above equation, the resulting error function equation can be rewritten as:

$$\varepsilon = \sum_{i=1}^N \left(\text{Log} \frac{P_i^{calc}}{P_i} \right)^2 = \sum_{i=1}^N \left(\text{Log} P_i^{calc} - \text{Log} P_i \right)^2 = \sum_{i=1}^N \left(a - \frac{b}{T_i + c} - \text{Log} P_i \right)^2$$

where T_i is the experimental temperature of vaporization corresponding to pressure P_i . Consequently, minimizing the residual of the Antoine equation with P expressed non-linearly as $\text{Log}_{10} P$ results in the constants a, b, and c which minimize the error function ε , or *percent error* of the fit. The specific convergence criterion used for the Marquardt-Levenberg nonlinear regression was a 0.01% or less change in the sum of squared residuals after each iteration relative to the sum of squared residuals at the current iteration of the above equation. The standard deviation percent error ($\sigma_{\%}$) associated with the minimized error function of the above equation can be defined as:

$$\sigma_{\%} = 100 \sqrt{\frac{\varepsilon}{N-1}}$$

with $2\sigma_{\%}$ therefore being a measure of the expected percent error of the fit at 95% confidence.

The complete least squares regression analysis was carried out by first calculating the 'initial' constant values a_0 , b_0 , and c_0 , from a *linear* least squares curve fit of the re-arranged Antoine equation:

$$T \text{ Log}_{10} P = a_0 T - c_0 \text{ Log}_{10} P + (c_0 a_0 - b_0)$$

which is linear in constant coefficients a_0 , b_0 , and c_0 . Note that a linear least squares analysis minimizes the residual of $(T \text{Log}_{10}P)$, not P or $\text{Log}_{10}P$. The values of a_0 , b_0 , and c_0 were then used as starting values for a non-linear regression of the Antoine equation, minimizing the residual of the error function equation to determine the constants a , b , and c of the Antoine equation. Non-linear regression of the Antoine equation leads to values for a , b , and c which differed only slightly from a_0 , b_0 , and c_0 . It should be noted that the minimization of a residual function linear in pressure (i.e., without P_i in the denominator) does not minimize the *percent* error. Accordingly, it was determined that a curve fit based on minimizing the pressure residual (i.e., $P_{i\text{calc}} - P_i$) resulted in over-leveraged high pressure curve-fit estimates at the expense of large relative errors for low pressure estimates (e.g., 10-30%). Thus, for the most accurate curve-fit representation over the full temperature range Mainstream chose to minimize the percent error per the error function equation.

A summary of the non-linear regression results are given in Table 12. The value of $2\sigma\%$ of the fit is given, in addition to the 2σ percent error of the measured pressures relative to DIPPR correlations (Ref. 43). The non-linear Antoine equation curve fits and data points are given for naphthalene, biphenyl, and *o*-terphenyl in Figure 29, decafluorobiphenyl, quinoline, and perfluoro-1,3,5-triphenylbenzene in Figure 30. In Figure 31, several steam table points (Ref. 80) are also given for comparison to the DSC data and Antoine regression curve.

Table 12. Non-linear least squares curve fits to the Antoine equation.

FLUID	Antoine constants			T range (in °C)	2 σ percent errors	
	<i>a</i>	<i>b</i>	<i>c</i>		curve fit	DIPPR ^[43]
biphenyl	6.493	2123.12	-55.39	222-415	1.85	2.60
decafluoro-biphenyl	7.025	2239.78	-34.00	180-335	6.26	-
<i>o</i> -terphenyl	6.718	2639.94	-50.54	303-513	4.10	5.24
naphthalene	6.464	2035.46	-35.02	187-374	1.46	3.10
perfluoro-TPB	7.223	2550.04	-132.18	319-476	16.41	-
quinoline	6.357	1938.13	-65.12	207-395	1.30	2.93
water	6.995	1572.27	-58.18	81-193	2.98	5.46

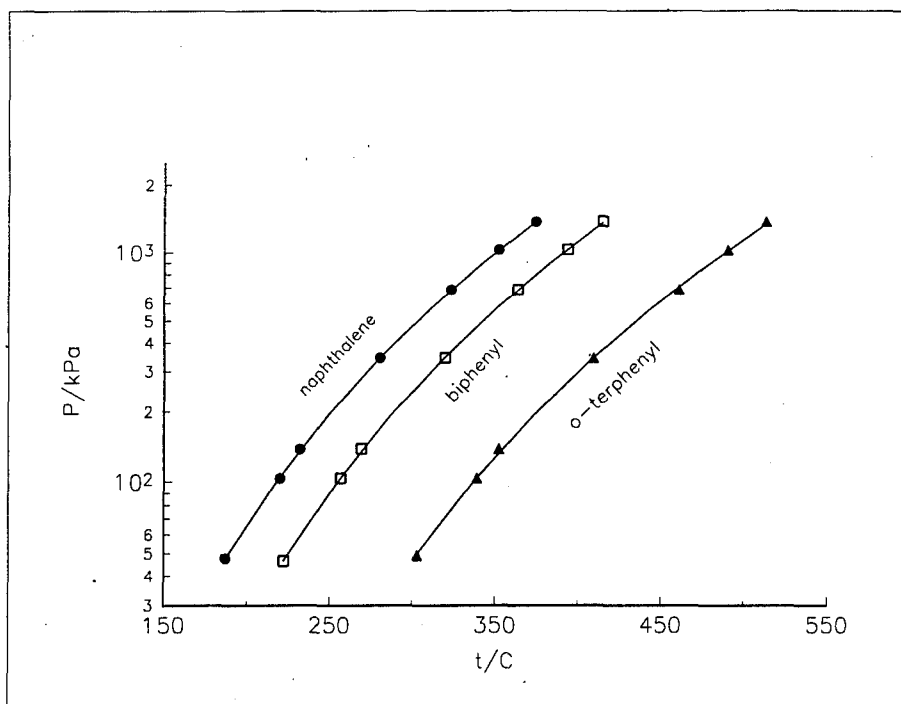


Figure 29. Antoine equation curve fits (solid lines) and DSC pressure-temperature data points for naphthalene (●), biphenyl (□), and *o*-terphenyl (▲).

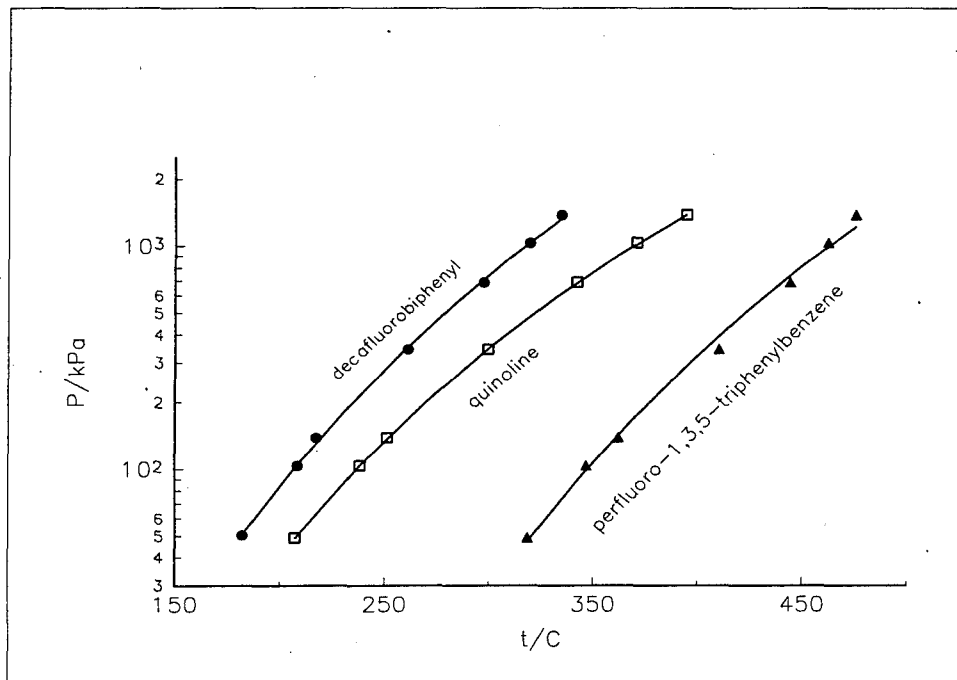


Figure 30. Antoine equation curve fits (solid lines) and DSC pressure-temperature data for decafluorobiphenyl (●), quinoline (□), and perfluoro-1,3,5-triphenylbenzene (▲).

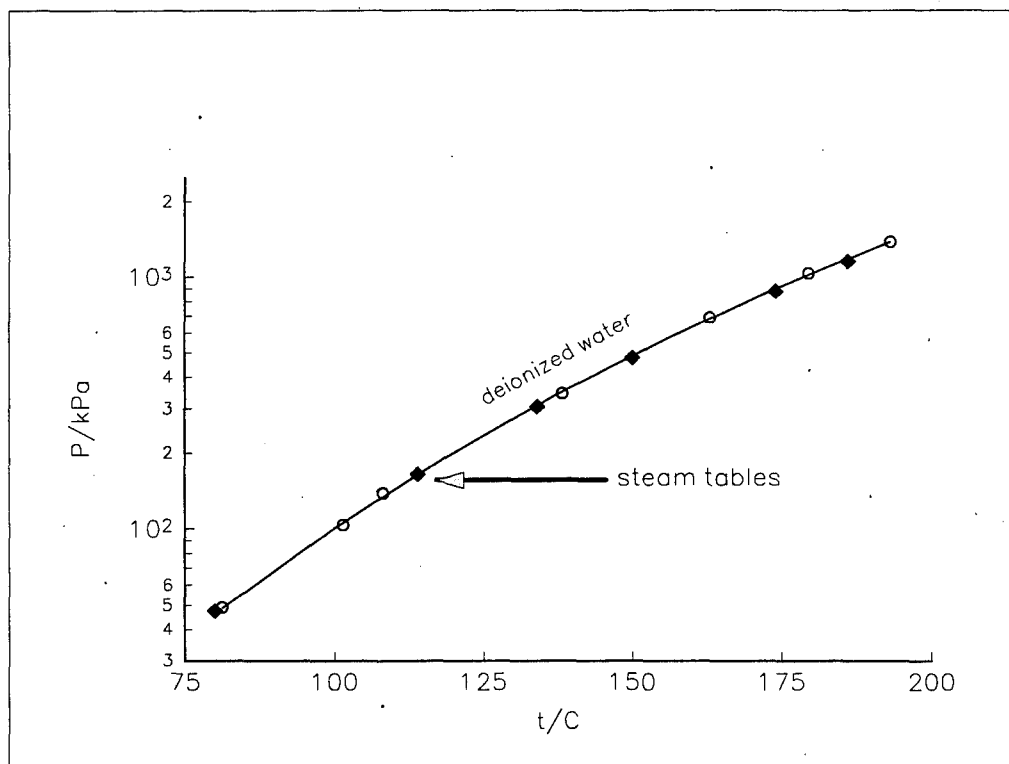


Figure 31. Antoine equation curve fits (solid lines) and DSC pressure-temperature data points for deionized water (○), and selected steam table^[7] pressure-temperature points (◆) for comparison.

As shown in Table 12, the non-linear Antoine curve fits yielded $\pm 2\sigma\%$ errors of 1-7%, excluding the results for perfluoro-1,3,5-triphenylbenzene. Also shown in Table 12, the experimental pressure data fell within 6% ($\pm 2\sigma$) of literature and other correlation values at the same temperatures. The regression errors of the DIPPR correlations for saturated pressure of biphenyl, o-terphenyl, naphthalene, quinoline, and water are reported as $\pm 3\%$, $\pm 10\%$, $\pm 1\%$, $\pm 3\%$, $\pm 0.2\%$, respectively, which are comparable to the standard errors ($\sigma\%$) of the curve fits developed in this study.

Perfluoro-1,3,5-triphenylbenzene was found to decompose at the higher pressures and temperatures of the study as evidenced by a black residue in the aluminum sample crucible after completion of the temperature scan. The temperature scans for perfluoro-1,3,5-triphenylbenzene were also characterized by noisy baselines for pressures exceeding about 343 kPa (corresponding to a boiling point of 410.4°C). Consequently, the Antoine equation may only adequately fit the

data over a limited range at low pressures (and temperatures) for perfluoro-1,3,5-triphenylbenzene. Figure 32 shows a DSC scan for perfluoro-1,3,5-triphenylbenzene at 343 kPa (50 psia) for which this behavior was noted. As shown, the baseline is not smooth and the maxima of the vaporization endotherm are difficult to discern.

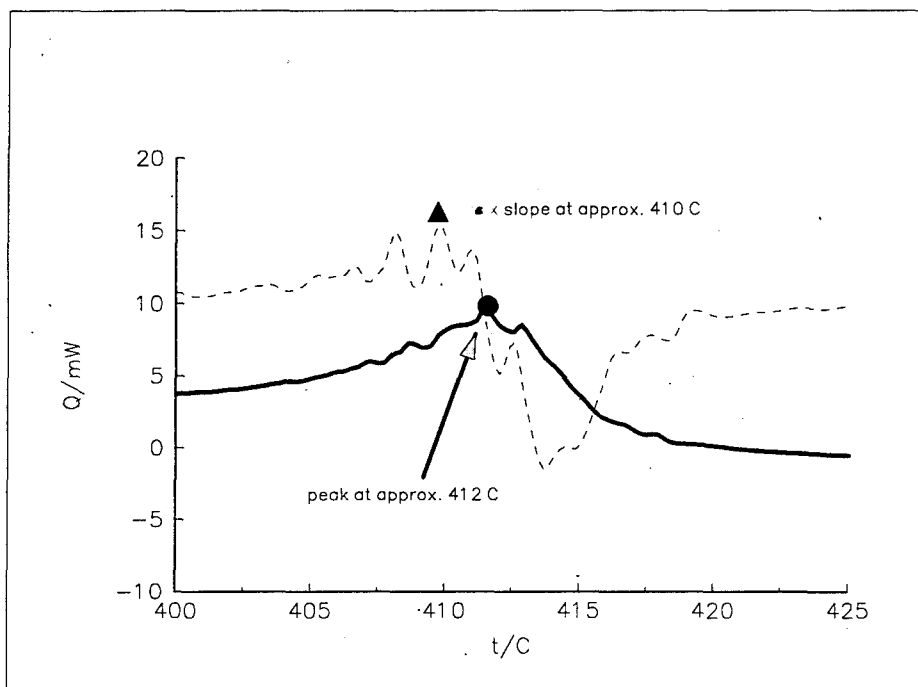


Figure 32. DSC temperature scan (5°C/min) for perfluoro-1,3,5-triphenylbenzene at 343.4 kPa showing noisy baseline and undefined endotherm peak. DSC Q (mW) T (C) scan and dQ/dT curve are represented by the solid and dashed curves, respectively.

Similar baseline noise in DSC scans was encountered for *o*-terphenyl at pressures exceeding 1.03 MPa, which corresponds to a vaporization temperature for the fluid of 492°C or greater. The curve in Figure 30 for perfluoro-1,3,5-triphenylbenzene, and the curve in Figure 29 for *o*-terphenyl, compared to the other materials in Figures 29, 30, and 31, also suggests anomalous behavior of perfluoro-1,3,5-triphenylbenzene and *o*-terphenyl due to more scatter in the data about the Antoine curve fit. These two materials had the highest boiling points among the group of materials studied, so the baseline instabilities and pressure-temperature data scatter are believed to be either directly (e.g., thermal instabilities within the DSC cell) and/or indirectly (e.g., decomposition) related to the high DSC temperatures.

The enthalpy of vaporization was of central interest in this study. Since the DSC does not in itself provide a means to directly measure the enthalpy of vaporization ΔH_{vap} due to mass loss during the process, the exact thermodynamic relationship of Clapeyron (Ref. 80) was used to calculate ΔH_{vap} from pressure-temperature data. The Clapeyron equation is expressed as:

$$\Delta H_{vap} = T (V^v - V^l) \frac{dP}{dT}$$

where:

V^v = vapor molar volume

V^l = liquid molar volume

T = temperature in K

T and P = saturated pressure and temperature (K and kPa, respectively)

The vapor and liquid volumes as a function of temperature were experimentally determined as discussed in this final report, and the derivative in the Clapeyron equation is determined from the Antoine equation. The final expression for ΔH_{vap} , after substituting dP/dT per the Antoine equation, is given as:

$$\Delta H_{vap}(T, P) = 2.303 (V^v - V^l) \frac{b TP}{[T + c]^2}$$

A summary of enthalpy of vaporization results is given in Table 13 for selected temperatures and pressures. Values found in literature (Ref. 43) are also given for comparison at the same temperatures and pressures. As shown in Table 13, the enthalpy of vaporization values predicted from the Antoine curve fit are similar to those found in literature. The regression errors of the DIPPR correlations for the heat of vaporization of biphenyl, o-terphenyl, naphthalene, quinoline, and water are reported as $\pm 5\%$, $\pm 10\%$, $\pm 1\%$, $\pm 5\%$, $\pm 1\%$, respectively. The differences between the curve fit generated values and those calculated from the DIPPR correlations are generally within, or at the limits of, these published regression errors.

Table 13. Enthalpy of vaporization data from Antoine and Clapeyron equations.

Fluid	t in °C	P in MPa	ΔH_{vap} in kJ/mol		% diff.
			curve fit	literature	
biphenyl	351	0.5756	42.19	40.56	4.0
decafluoro-biphenyl	321	1.0629	10.94	-	-
o-terphenyl	351	0.1305	50.62	57.29	11.6
naphthalene	351	1.0209	33.57	32.30	3.9
perfluoro-TPB	362	0.1379	103*	-	-
quinoline	351	0.7764	38.22	38.12	0.3
water	100	0.1007	41.31	40.80	1.3

* value estimated from endotherm area of DSC scan

The melting points of the candidate working fluids were also measured and a summary is given in Table 14. The standard deviation of the melting point over the pressure range of the vaporization experiments ranged from 0.59 to 1.84 °K. This variance has contributions from both pressure variations and inherent DSC system variations. The average melting temperature of the distilled naphthalene of this study was 352.21 ± 0.62 °K (1 standard deviation), compared to the NPL Certificate Value (Ref. 81) of 353.37 °K. Melting points for biphenyl, and o-terphenyl were 340.84 ± 0.59 °K and 328.02 ± 1.84 °K, respectively, over the pressure range of 50 kPa to 1.4 MPa. These compare to literature values (Ref. 43) of 342.27 °K and 329.35 °K, respectively.

Table 14. Comparison of measured melting points to literature values.

Fluid	Experimental			Literature		% diff.
	T_{fus} (in °K)	$T_{\text{fus}} - 1\sigma$ (in °K)	P range (in MPa)	T_{fus} (in °K)	P range (in MPa)	
biphenyl	340.84	± 0.59	0.05-1.4	342.27	0.1	0.4
decafluoro-biphenyl	339.74	± 0.90	0.05-1.4	342.15*	0.1	0.7
o-terphenyl	328.02	± 1.84	0.05-1.4	329.35	0.1	0.4
naphthalene	352.21	± 0.62	0.05-1.4	353.37	0.1	0.3
perfluoro-TPB	422.25	± 0.66	0.05-1.4	-	-	-

* average value reported by Ryan Scientific

Liquid Thermal Conductivity

An effort was made to measure the liquid thermal conductivity of the candidate working fluids. We developed a method for measuring liquid thermal conductivity that is based on a concentric cylinder method described by Briggs (Ref. 82) and Ziebland and Burton (Ref. 31). In this method, a column of working fluid is contained between two coaxial cylinders. The inner cylinder is a heating cylinder and the outer cylinder is the receiving cylinder. By temperature measurement of the cylinder surfaces, the thermal conductivity of the liquid is determined from Fourier's Law. The overall design consists of a thermal conductivity cell and a containment vessel, which will allow the test to be performed under the fluid's own vapor pressure. The cell will be pressurized with nitrogen to prevent fluids from boiling.

The thermal conductivity cell has a testing zone in the middle and two guard zones on the sides. The overall dimensions of the thermal conductivity cell is 1.25" in diameter and 7.75" long. Functionally, it mainly consists of emitting and receiving tubes, and a heater. The length of the test section is 3.000". The outside diameter for the emitting tube is 1.000 ± 0.0005 " (21.336 ± 0.001 mm) and the inside diameter of the receiving tube is 1.094 ± 0.0005 " (27.788 ± 0.01 mm), forming a gap of 0.047" (1.1938 mm) for fluid heat conduction. The inner emitting tube is made out of high conductive copper and has a wall of thickness 0.080" (2.032 mm). The thick wall structure is for meeting the manufacturing requirements and will keep the temperature more uniform in testing. The outer receiving tube is made out of brass in order to have a good surface finish inside the tube. To make measurements more accurately, two low conductivity guard tubes are put on the ends of the testing tube. They are 2-inch long and made out of 304 stainless with only 1/25 of the copper thermal conductivity. This will effectively reduce the axial heat loss through them, thus greatly increasing the accuracy of this instrument. Two end caps made out of Macor glass ceramic (Accuratus Ceramic Corp., NJ), the lowest thermally conductive material at high temperature, hold the cell in integrity. Two-thirds of the total contacting area have been cut to reduce the heat loss further.

Due to the compact size, temperature measurement with thermocouples will be used for this test. With a precision digital multimeter (Hewlett Packard 3478A), a resolution of less than 0.002 K and a measurement accuracy of 0.03-0.05 K for temperature difference can be achieved.

Thermocouples are directly welded on the tubes so that exact wall temperature can be measured. T type thermocouple wires (copper and copper+nickel, gauge #20, .034" in diameter) have been found to have the best TIG welding ability to copper, brass, and stainless steel. Two thermocouples are welded on the inner tube, two on the outer tube, and one each on the guard tube. This configuration allowed for measurement of six individual temperatures and four temperature differences (two each between each guard heater and the main heater). The tubes were machined after thermocouple welding to the final dimensions. The manufacturing tolerances, concentricity, straightness, have been controlled between 0.0005 to 0.001" with a surface finishing of 32. To be consistent, all the thermocouple wires are from the same spool. The thermocouple wires are directly led out of the container through a sealing board so that no error will be introduced from thermocouple wire joints. A Fluke Data Logger system (2620A Data Acquisition Unit) as well as a digital multimeter (Hewlett-Packard 3478A) were used to measure the temperature.

The heater also consists of three zones; a guard zone (8 W), a heater zone (16 W), and a guard zone (8 W). A 24 VDC regulated power supply (Sola 83-24-260-2) has been selected as the power source. The voltage fluctuation at 3 amp current was found to be less than 0.1%. The main heater is controlled by a variable resistor. Two guard heaters are controlled each with two variable resistors, one for rough adjustment and one for fine adjustment. These heaters are manually controlled. The power of the main heater can be obtained through two voltage readings across a reference resistor and the main heater with high accuracy. Though the estimated power required for the main heater is only 3.3 watts, the power of the main heater can be adjusted in a range from 1.7 through 16 watts. The guard heaters can be adjusted from 0.4 to 8 watts.

To perform thermal conductivity measurements, the cell is initially cleaned inserted into the cylindrical container. The container is heated to about 100°C and liquid working fluid is filled into the cell. The cell is then sealed, and the remaining void volume of the cylindrical container

is filled with working fluid. The cylindrical container is then evacuated, cooled (to allow the working fluid to freeze), and pressurized with nitrogen above the vapor pressure of the fluid at the test temperature. The apparatus is then inserted in the constant temperature bath and allowed to reach thermal equilibrium.

Preliminary testing of the thermal conductivity measurement apparatus was performed using toluene as the test fluid. During this testing, electrical grounding problems with the heaters were encountered. Upon disassembly, it was noticed that the fiberglass insulation around the heater wires was torn during assembly of the cell in the cylindrical container, which caused the heater to contact the container causing the grounding problem. Preliminary testing continued with toluene using the apparatus without the outer cylindrical container. Table 15 presents the results of the liquid thermal conductivity measurements made and compares the value for toluene with the value from the DIPPR database (Ref. 43). This table shows that the error in our experimental measurement for toluene was 15.4% compared to the DIPPR value. This error is in the range of error expected from empirical liquid thermal conductivity estimation (Ref. 41).

Table 15. Results of liquid thermal conductivity characterizations.

Fluid	Temperature (°C)	Thermal Conductivity (W/m-K)
toluene	35°C	0.151
		(DIPPR value = 0.13065 - 15.4% error)
biphenyl	305.7	0.114
	313.4	0.145
	321.6	0.291
	330.6	0.270
	340.1	0.275
	349.6	0.283

Table 15 also shows the experimental results for biphenyl between 300°C and 350°C, which show a trend of increasing thermal conductivity with increasing temperature. The experimental data does not agree with the information known on thermal conductivity of liquids, which is that

thermal conductivity decreases with increasing temperature (except for aqueous solutions, water, multi-hydroxy and multi-amine compounds) (Ref. 41). Technical papers on the thermal conductivity of liquid biphenyl up to its normal boiling point (256°C) also confirm the fact that the thermal conductivity of liquid biphenyl decreases with increasing temperature (Refs. 31 and 34). Due to the large error in these measurements, the difficulty with the apparatus and the significant amount of time required for the experiments, no further measurements of liquid thermal conductivity were made. This decision was approved by the Air Force technical monitor.

Figures-of-Merit

The thermophysical property measurements performed in this task can be used to calculate the heat pipe figures-of-merit for the working fluids. Figure 33 is a plot of the liquid transport factor for the working fluids evaluated. This figure shows that quinoline had the highest value of this factor over the temperature range considered, followed by naphthalene, biphenyl, and o-terphenyl. The liquid transport factor of naphthalene dropped below that of biphenyl and o-terphenyl above 375°C. The liquid transport factor for decafluoro-biphenyl was an order of magnitude lower than the other working fluids at 300°C and dropped rapidly with increasing temperature as the critical temperature (367.5°C) was approached. Figure 34 is a plot of the vapor pressure of the working fluids. This figure shows that all of the fluids have reasonable vapor pressures; with decafluorobiphenyl having the highest pressure, followed by naphthalene, quinoline, biphenyl, and o-terphenyl. Figure 35 is a plot of the kinematic viscosity ratio of the working fluids. This figure shows that decafluorobiphenyl had the lowest ratio, followed by naphthalene, biphenyl, quinoline, and o-terphenyl. Figure 36 is a plot of the wicking height factor for the working fluids. This figure shows that o-terphenyl has the highest value of this factor, followed by quinoline, biphenyl, naphthalene, and decafluorobiphenyl.

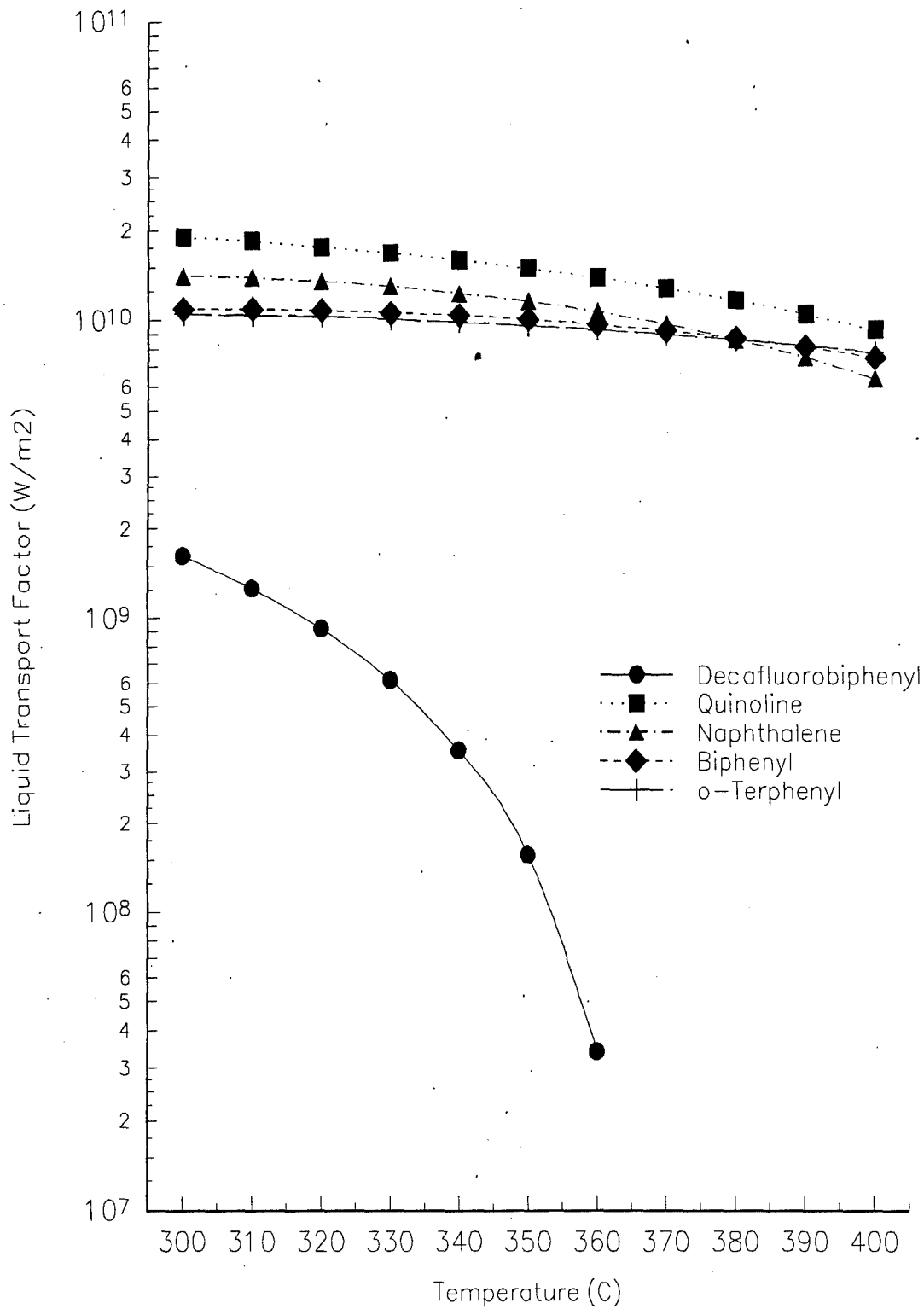


Figure 33. Liquid transport factor of candidate working fluids.

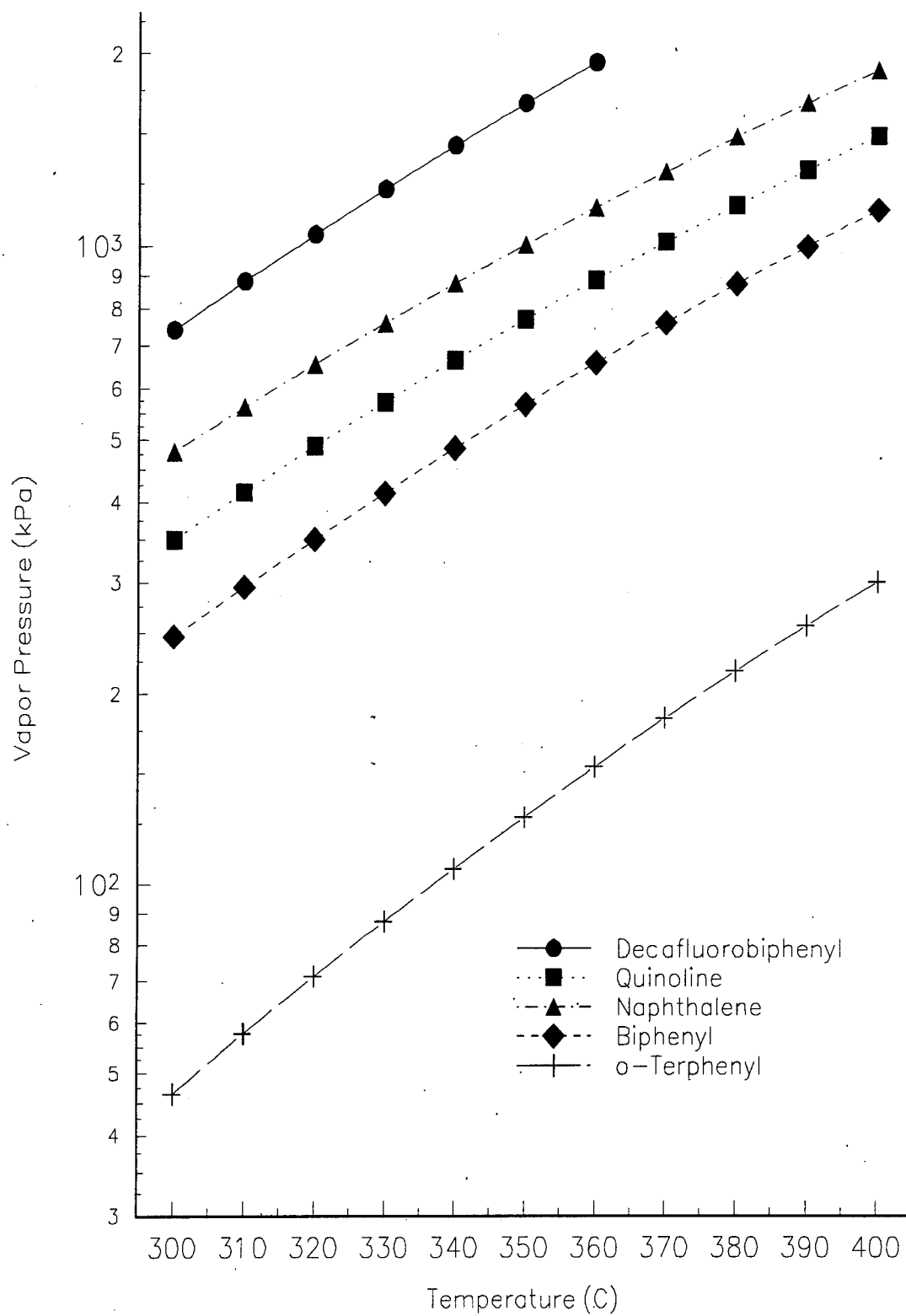


Figure 34. Vapor pressure of candidate working fluids.

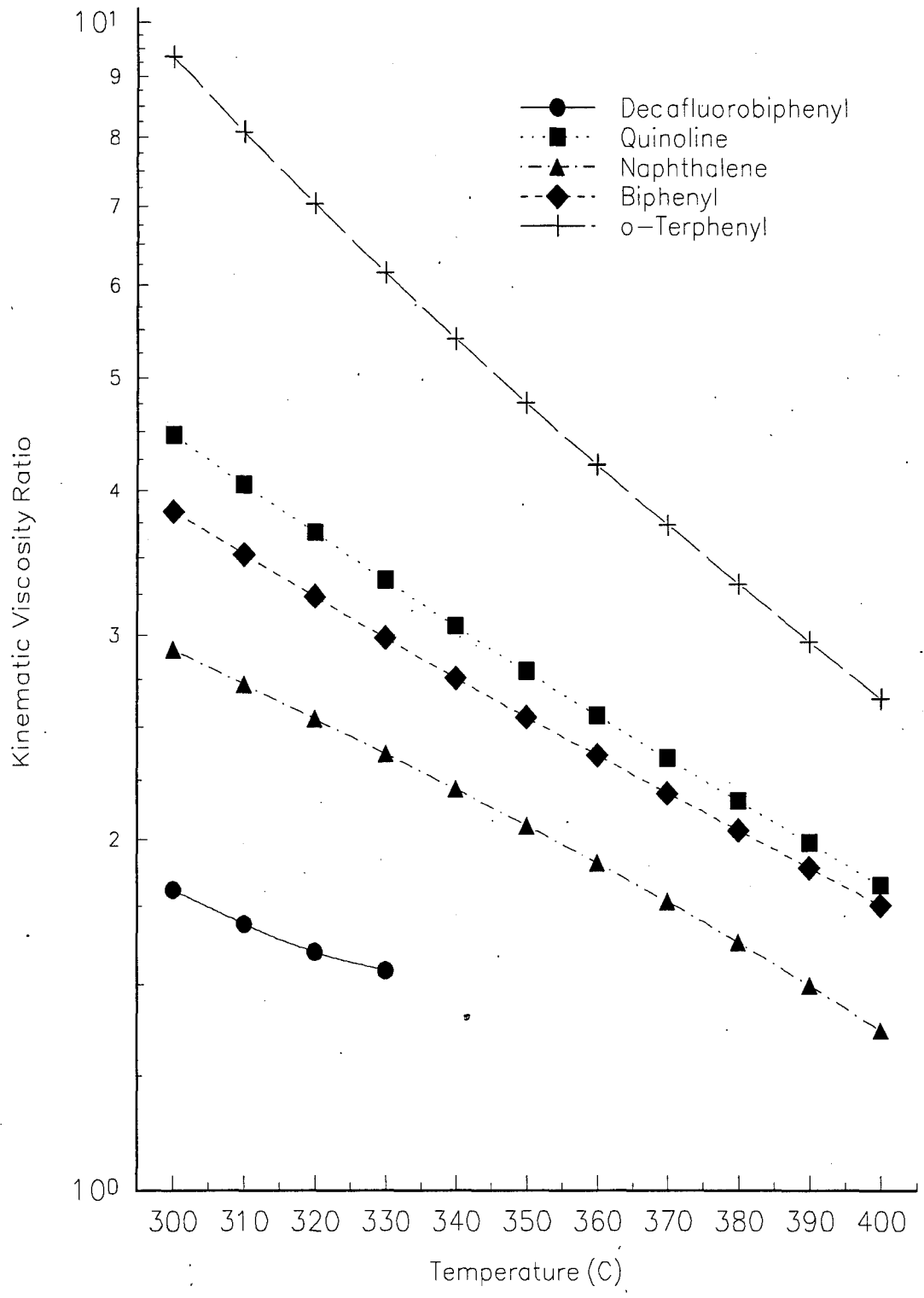


Figure 35. Kinematic viscosity ratio of candidate working fluids.

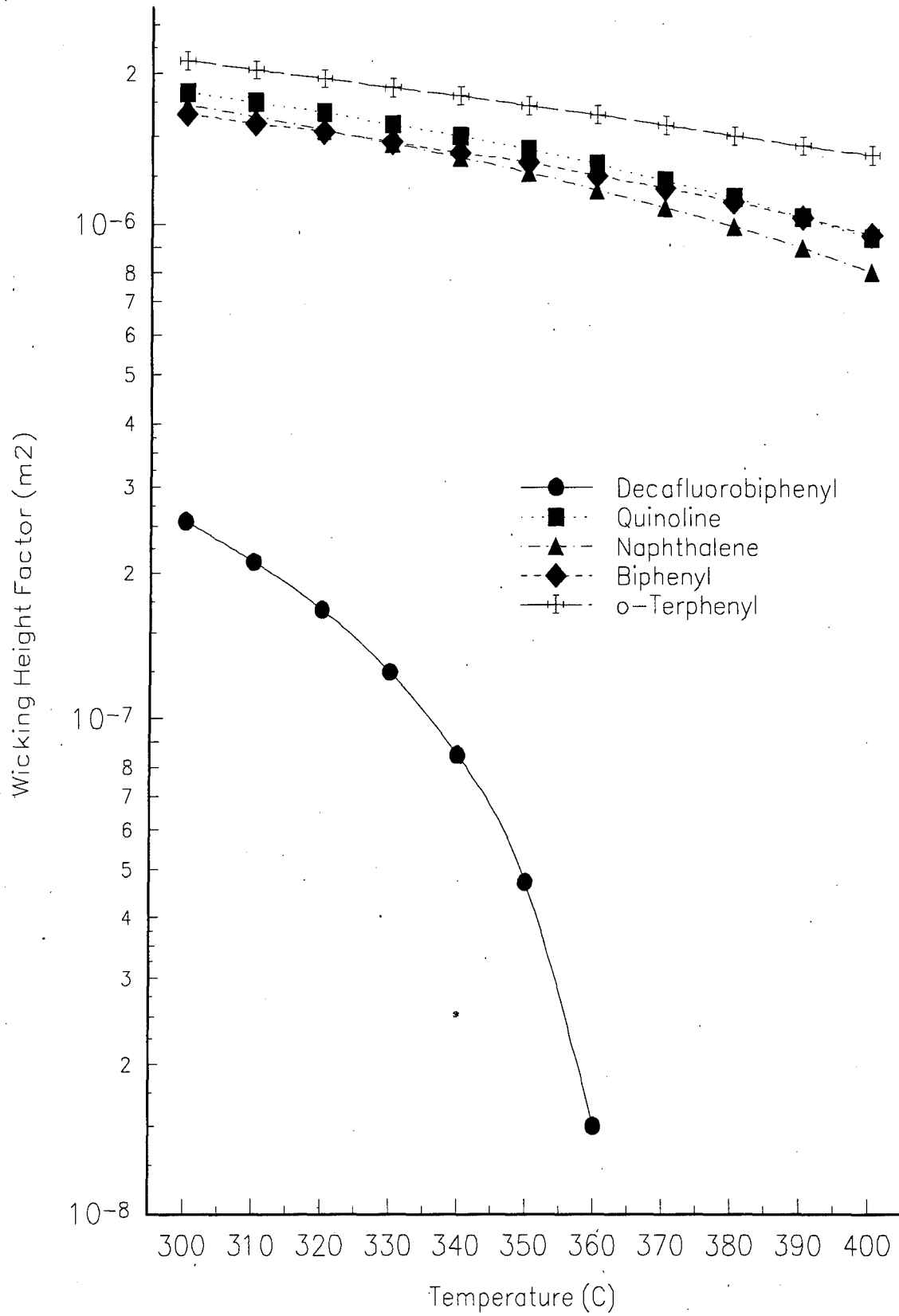


Figure 36. Wicking height factor of candidate working fluids.

TASK 6: CONSTRUCT PROTOTYPE HEAT PIPE

This task involved the design of a heat pipe test stand and the design and fabrication of a prototype heat pipe for fluid performance testing.

Heat Pipe Test Stand Design Concept

The design of the test stand for this task includes a structure that will allow the heat pipe to tilt to a selected angle, heater and data acquisition instrumentation, insulation material, and geometry selection and versatility for various heat pipe geometries. The test stand structure consists of three major sections. They are the main assembly, the heater subassembly, and the angle measuring devices. All the material and equipment used for the heat pipe performance test stand are readily available. The heater geometry depends on the heat pipe diameter.

The main assembly is welded from 1.5" x 1.5" square aluminum (either 6061-T6 or 6063-T4) extrusions. The material is readily available and it is easily machined and welded. There are four height adjustable feet to support the entire structure. The height adjustment is required to provide the test stand a reference horizontal position and eliminate instability. The total dimension of the test stand shall not exceed 3' in length by 1.5' in height. The width of the test stand is approximately 1.5' depending on the heat pipe diameter and the heater subassembly.

The heater subassembly consists of the heater block and insulation. The overall diameter of the heat pipe determines the geometry of the heater block. The heater block is fabricated from standard aluminum round stock, with a band heater on the exterior of the block. The heat pipe is inserted in the center of the heater block. This is the same heater block concept that was used in Task 3. The heaters are connected to a watt meter to provide a constant heat distribution. To reduce the amount of heat loss an insulation material is required to cover the heated section of the heat pipe. The insulation material will be of ceramic type and has a shield to prevent loose ceramic fibers or material to be detached. The heater and insulation is isolated from the main structure. A two-half shell will be used to clamp the heater assembly, this concept enables the

test stand to accept a variety of heat pipe diameters and allows quick change of different heat pipes. A water-cooled calorimeter will be used on the condenser section of the pipe. This calorimeter will be insulated to minimize heat losses. This will allow for a quantitative measurement of the heat being rejected through the condenser section of the heat pipe. Quantifying the heat transport based on the heat supplied to the evaporator will likely result in significant errors due to heat losses in the adiabatic section and heat losses from the evaporator heaters.

The design of the test stand structure includes a pivot point on the heat pipe that will utilize simple geometry to calculate the tilt angle. The tilt angle is easily adjusted using a height gage and allows the heat pipe to tilt to approximately 40° from a reference plane (horizontal plane). The structure is then fixed at a selected tilt angle for testing. The structure has two methods of determining the tilt angle. The visual protractor provides a coarse description of the tilt angle. This visual indication is for approximate inspection purpose only. The height is accurately measured using a cathetometer (the same device used in the surface tension measurements). The cathetometer has tolerances up to 0.0005" (approximately 0.002°). The tilt angle (Θ_{tilt}) is determined from geometry calculations,

PP = length from pivot point to measuring point

DY = change in height of heat pipe at the measured point

$$\Theta_{\text{tilt}} = \tan^{-1}(DY/PP)$$

Since the structure utilizes geometry to calculate the tilt angle, the location of the pivot point with respect to the measured point is critical to provide an accurate tilt angle. The pivot point of the heat pipe can be adjusted due to a tube-in-tube design of the structure. The heat pipe is capable of sliding in a substructure that includes the insulation material and a round enclosure that with the pivot mechanism. This design allows for different heat pipe lengths to be tested and allow ease of operation and replacement of various heat pipes. The test stand has another substructure to support the selected tilt angle position and hold it in place. This reduces the

possibility of damage to a costly height gage during experiment and provides a firm support for the heat pipe.

Design and Fabrication of Prototype Heat Pipe

A heat pipe design was developed by Anthony Gurule of the Orion International Technologies. His design calls for an axial groove stainless steel pipe, 36 inches long, 1 inch OD, with a circular cross section. A total heat input in the evaporator of 55 watts was designed. The evaporator section is 6 inches, the adiabatic section is 24 inches, and the condenser section is 6 inches. The dimensions of the axial grooves vary depending on the fluid selected. A summary of the design is given in Appendix C.

Quotations for commercial heat pipes were solicited from OAO and Dynatherm. OAO proposed fabricating a stainless steel circular cross section heat pipe with a stainless steel fibrous composite wick structure. Dynatherm proposed fabricating axial grooves in planar stainless steel sheet, rolling the sheet into the circular cross section geometry, then welding the seam. The quotations and technical comments from OAO and Dynatherm are provided in Appendix C.

Mainstream also investigated the possibility of fabricating axial groove circular cross section heat pipes from stainless steel for this project in-house. We considered extruding stainless steel tubing, electrical discharge machining (EDM) of stainless round stock, and broaching stainless steel tubing. None of these techniques were deemed suitable for machining axial grooves of 3-foot length in stainless steel tubing. The 1-inch diameter was too small for extruding 3-foot lengths of stainless tubing. The 3-foot length was too long for EDM, however, it could be accomplished in 2, 1.5-foot lengths, which would then have to be welded together (this was deemed unfeasible). The ID was too small for broaching 3-foot lengths of stainless tubing.

After consideration of the various options for manufacturing the heat pipes, the following action was decided upon agreement between the Phillips Lab and Mainstream. Mainstream would fabricate heat pipes with a rectangular cross section, using L-shaped stainless steel angle. The

grooves were fabricated using a slitting saw on an end mill. The groove width fabricated by the slitting saw was 5.08×10^{-4} m (0.020 in.), with a groove depth of 1.02×10^{-3} m (0.040 in.) and a landing area of 3.81×10^{-4} m (0.015 in). The tolerance on the slitting saw's groove width is ± 0.0002 in. and it is capable of providing a surface finish of 32-64. A total of 19 grooves were fabricated on three sides, with 18 grooves on the fourth side, giving a total of 75 grooves. The two fabricated angles were TIG welded together after machining. Mainstream fabricated, filled, and delivered a heat pipe filled with biphenyl.

The machining of rectangular cross section axial grooves has several advantages over techniques used to fabricate circular cross section axial groove heat pipes:

1. The fact that the grooves are machined (using an end mill) rather than extruded reduces the fabrication cost and time. This method also allows fabrication of grooves in stainless steel at a reduced cost and reduced time than other methods (i.e. the proposed Dynatherm approach).
2. Machining results in greater control over tolerances and surface finishes than extrusions.
3. The rectangular cross-section is the preferred geometry over circular cross sections from a heat transfer perspective. The heat pipe must be able to accept and reject waste heat to and from various sources and sinks that typically have flat (planar) surfaces. The rectangular cross section reduces the resistance to heat transfer to planar surfaces compared to circular cross sections. Circular cross-section heat pipes typically have extended flat metal surfaces to mate properly with the heat source and sink. This increases the resistance to heat transfer, and is not required for a rectangular cross-section heat pipe.
4. The modeling of the heat transfer is simpler than for circular cross section heat pipes. Circular cross section heat pipes typically requires extended surface to mate properly with the heat sources. The heat transfer in these surfaces, from the flat surface to the circular cross section is at least two dimensional, and somewhat complicated to model, whereas in a rectangular cross section heat pipe, the heat transfer is essentially 1-dimensional.

TASK 7: HEAT PIPE PERFORMANCE TESTING

The performance of this task was dropped from the project by mutual agreement between Mainstream and the Phillips Lab technical monitor.

TASK 8: PREPARATION OF TWO-PHASE DESIGN MANUAL

This task involves the presentation of the thermophysical properties of the candidate working fluids in the form of tabular data. The tabular data is presented in Appendix D. The following sections are summaries of how the property data was measured, calculated, or predicted.

Vapor Pressure. Vapor pressure measurements were performed using a Mettler TA4270-HPDSC High Pressure DSC, with a 0.005-inch hole laser-drilled in the lid of a crimp-sealed aluminum sample pan. The vaporization temperature/pressure data was fitted to the Antoine equation, which is given below. The fitted constants for each compound are listed in Table 16 as is the average regression error.

$$\log_{10} P = a - \frac{b}{T + c}$$

where:

P = absolute pressure (kPa)

T = absolute temperature (K)

a, b, c = fitted constants

Table 16. Fitted constants for Antoine equation.

Compound	Constant a	Constant b	Constant c	Regression Error
naphthalene	6.464	2035.46	-35.02	0.53%
biphenyl	6.493	2123.12	-55.39	0.81%
decafluorobiphenyl	7.025	2239.78	-34.00	2.71%
o-terphenyl	6.718	2639.94	-50.54	1.57%
quinoline	6.357	1938.13	-65.12	0.56%

Liquid Density. Experimental values of liquid density were determined by measuring the mass of a fluid contained in a constant-volume sample cylinder (volume calibrated with water). The experimental data was then fit to a second-order polynomial to correlate liquid density (g/ml) with absolute temperature (K). Table 17 lists the constants for the polynomial for each of the fluids and gives the average regression error for the data.

$$\rho_l = A + BT + CT^2$$

where:

T = temperature (K)

A, B, C = fitted constants

ρ_l = liquid density (g/ml)

Table 17. Fitted constants for liquid density equation.

Compound	Constant A	Constant B	Constant C	Regression Error
naphthalene	-7.018e-1	5.910e-3	-5.842e-6	0.27%
biphenyl	1.721e+0	-2.051e-3	7.395e-7	0.34%
decafluorobiphenyl	-1.48e+0	1.248e-2	-1.383e-5	0.25%
o-terphenyl	-1.711e-1	3.956e-3	-3.833e-6	0.12%
quinoline	2.755e+0	-4.885e-3	2.739e-6	0.54%

Vapor Density. The vapor densities presented are the saturated vapor density values calculated from the Lee-Kesler generalized thermodynamic correlations (Ref. 59).

Heat of Vaporization. The heat of vaporization of the compounds was calculated over the entire range of vaporization data using the Clapeyron equation. Rearrangement of this equation yields

$$\Delta H_{vap}(T, P) = 2.303 (V^v - V^l) \frac{b TP}{[T + c]^2}$$

where:

ΔH_{vap} = heat of vaporization (kJ/kg)

v_{vap} = specific volume of saturated vapor (l/kg)

v_{liq} = specific volume of saturated liquid (l/kg)

b, c = constants from Antoine equation (Table 16)

T_{sat} = vaporization temperature (K)

P_{sat} = vaporization pressure (kPa)

Surface Tension. The surface tension of the candidate working fluids was measured using the differential capillary rise technique in a closed vessel. The experimental data was then fit to an equation that describes the variation of surface tension with temperature (Ref. 41). Table 18 presents the values of the constants to the equation for each fluid and the average regression error of the fit for each fluid.

$$\sigma = c(1 - T_r)^{4n}$$

where:

n, c = fitted constants

$T_r = T/T_c$

σ = surface tension (dyne/cm)

Table 18. Fitted constants for surface tension equation.

Compound	Constant n	Constant c	Regression Error
naphthalene	0.2875	68.86	0.7%
biphenyl	0.2850	56.11	1.2%
decafluorobiphenyl	0.3475	64.95	3.9%
o-terphenyl	0.3575	75.77	0.7%
quinoline	0.3290	86.98	1.3%

Liquid Viscosity. The experimental values of liquid kinematic viscosity were measured using a modified, closed Cannon-Fenske capillary viscometer. The absolute viscosities were determined from the kinematic viscosities and correlated using the equation below. Table 19 presents the values of the constants of this equation for all fluids and gives the average regression error for each fluid.

$$\ln \mu = A + \frac{B}{T}$$

where:

μ = absolute viscosity (cP) = ν/ρ

A, B = fitted constants

T = temperature (K)

Table 19. Fitted constants for liquid viscosity equation.

Compound	Constant A	Constant B	Regression Error
naphthalene	2663.33	-6.22	0.58%
biphenyl	2772.6	-6.12	1.44%
decafluorobiphenyl	2279.0	-5.616	3.47%
o-terphenyl	2010.5	-4.534	0.90%
quinoline	2296.37	-5.486	0.28%

Vapor Viscosity. The saturated vapor viscosity of the fluids was calculated using the Jossi, Stiel, Thodos pressure correction (Ref. 41) to the Stiel-Thodos correlation (Ref. 83) for decafluorobiphenyl, and the DIPPR correlations (Ref. 43) for the biphenyl, o-terphenyl, quinoline, and naphthalene.

Liquid Thermal Conductivity. The liquid thermal conductivity of the fluids was calculated using the Sato-Riedel method (Ref. 41) for decafluorobiphenyl, and the DIPPR correlations (Ref. 43) for the biphenyl, o-terphenyl, quinoline, and naphthalene.

Liquid Transport Factor. The liquid transport factor (N_l) was calculated using the equation given below.

$$N_l = 1000\Delta H_{vap} \sigma \rho_{liq} / \mu_{liq}$$

Kinematic Viscosity Ratio. The kinematic viscosity ratio was calculated using the equation given below.

$$\text{kinematic viscosity ratio} = (\mu_{vap} \rho_{liq}) / (\mu_{liq} \rho_{vap})$$

Wicking Height Factor. The wicking height factor (H) was calculated using the equation given below.

$$H = \sigma / \rho_l g$$

RECOMMENDATIONS FOR FURTHER WORK

This project resulted in the characterization of the thermal stability characteristics and thermophysical properties of six aromatic hydrocarbons and perfluorocarbons. The most suitable fluids investigated were biphenyl and o-terphenyl. Recommendations for future work in this area are given below.

On this effort Mainstream developed an innovative way to fabricate axial-grooved heat pipes in stainless steel. Stainless steel is the preferred material of construction for this temperature range; but the normal fabrication technique for axial-groove heat pipes, extruding, is not feasible with stainless steel. Mainstream's unique fabrication technique has successfully been used to machine several different groove widths in stainless steel to manufacture axial-groove heat pipes. Further work should concentrate on fine-tuning the technique and establishing the limitations of the technique. Parameters such as minimum groove width, maximum grooves per side, groove width and depth tolerances, and machining finish all need to be established to determine the limitations of this fabrication technique.

Once the fabrication process has been fully investigated and the limitations have been established, the design of the axial-groove heat pipe should be optimized to maximize the performance of the working fluid. The optimization process mainly involves the optimization of the groove pattern and geometry, but also involves analysis of the vapor core and containment characteristics to minimize mass. As an ongoing process, the various heat pipe designs should be optimized in normal gravity to demonstrate the optimum heat pipe design. Once the optimum design is established, zero-gravity flight tests should be pursued with the working fluids.

Concurrent work on all three areas will result in the demonstration of this high-performance, low-mass technology to passively remove heat from the sodium/sulfur battery and transport it over a significant distance to a heat sink. Successful demonstration will be of significant benefit to the Air Force, as well as in the commercial heat exchanger industry.

CONCLUSIONS

This project identified and characterized two-phase heat pipe working fluids in the 300°C to 400°C temperature range for thermal control of the sodium/sulfur battery. Previous work performed by Mainstream and other researchers recommended aromatic hydrocarbons and aromatic perfluorocarbons as compounds with suitable thermal stability and thermophysical property characteristics for use in this temperature range. This project involved the identification, selection, and extensive experimental evaluation of specific compounds from these two chemical families to determine their suitability for this application. As a result of the performance of this effort, several conclusions were made:

1. Six compounds were selected for evaluation based on a survey of property and availability information on aromatic perfluorocarbons and hydrocarbons: naphthalene, quinoline, biphenyl, o-terphenyl, decafluorobiphenyl, and perfluoro-1,3,5-triphenylbenzene. These compounds were procured from chemical manufacturers and were purified by either fractional distillation under vacuum or by multiple crystallizations from suitable solvents.
2. Long-term thermal stability tests were performed on each of these fluids between 325°C and 380°C in stainless steel gravity reflux heat pipes to assess their thermal stability. Based on the results of these tests, the following thermal stability ranking was developed (from most stable to least stable): biphenyl, o-terphenyl, naphthalene, decafluorobiphenyl, quinoline, perfluoro-1,3,5-triphenylbenzene. No decomposition was detected for any of the biphenyl samples tested.
3. Thermophysical property measurements were made for all fluids (except for perfluoro-1,3,5-triphenylbenzene) between 300°C and 400°C. Specific properties measured included liquid density, liquid viscosity, surface tension, vapor pressure, heat of vaporization, critical point, and melting point. The thermophysical properties of the working fluid candidates were then used to calculate the figures-of-merit (i.e. liquid transport factor, vapor pressure, kinematic viscosity ratio) of the fluids in the 300°C-400°C temperature range.

4. An analysis of the thermal stability characteristics and the figures-of-merit of the working fluids evaluated resulted in the recommendation of biphenyl and o-terphenyl as the most suitable working fluids for the 300°C-400°C temperature range. There were no references in the open technical literature regarding performance testing of these fluids in heat pipes. These two fluids also had the highest thermal stability of all fluids tested.
5. A unique fabrication process for stainless steel axial groove heat pipes was developed. The normal method of fabricating axial grooves, extrusion, is not feasible with stainless steel. The fabrication process involved machining the grooves in angle stainless steel, followed by the welding of two angle steel parts together to form a rectangular heat pipe cross section. Two prototype heat pipes were fabricated using this method; one was filled with biphenyl and one with o-terphenyl. This type of fabrication method is less costly and time-consuming than other fabrication methods. The rectangular cross section also has heat transfer benefits over circular cross sections for heat sources and sinks with flat surfaces.
6. Future work in this area should concentrate on three areas: 1) refinement of the axial-groove heat pipe fabrication with stainless steel, 2) optimization of the heat pipe design to maximize the performance of the fluids in the 300°C to 400°C temperature range, and 3) performance testing of biphenyl and o-terphenyl in heat pipes in normal and reduced gravity. Concurrent work on all three areas will result in the demonstration of this technology to passively remove heat from the sodium/sulfur battery and transport it over a significant distance to a heat sink.

REFERENCES

1. Private communication, L. R. Grzyll of Mainstream and R. Vacek of the Phillips Lab, U. S. Air Force, October 1, 1991.
2. Private communication, L. R. Grzyll of Mainstream and S. Vukson of Wright Research and Development Center, U. S. Air Force, August 14, 1990.
3. Private communication, L. R. Grzyll of Mainstream and C. R. Halbach of Space Systems Loral, September 12, 1991.
4. Saaski, E. W. and Tower, L., "Two-Phase Working Fluids for the Temperature Range 100°C-350°C," AIAA 12th Thermophysics Conference Proceedings, Albuquerque, NM, 1977.
5. Saaski, E. W. and Owzarski, P. C., Two-Phase Working Fluids for the Temperature Range 50°C-350°C, NASA CR-135255, June 1977.
6. Saaski, E. W. and Hartl, J. H., Two-Phase Working Fluids for the Temperature Range 50°C-350°C, NASA CR-159847, May 1980.
7. Kenney, D. D. and Feldman, K. T., "Heat Pipe Life Tests at Temperatures Up To 400°C," Proceedings of the 13th Intersociety Energy Conversion and Engineering Conference, 1056-9, 1978.
8. Grzyll, L. R. and Barthel-Rosa, L. P., Investigation of Novel Working Fluids for Spacecraft Heat Pipes, Final Report, Mainstream Engineering Corp., submitted to Air Force Wright Aeronautical Lab, December 1989.
9. Grzyll, L. R., "Investigation of Heat Pipe Working Fluids for Thermal Control of the Sodium/Sulfur Battery," Proceedings of the 26th Intersociety Energy Conversion and Engineering Conference, Vol. 3, 390, 1991.
10. Private communication, L. R. Grzyll of Mainstream and E. K. Brakebill, Fluids Development Manager, Monsanto Chemical Company, January 24, 1990.
11. Curran, H. M., "The Use of Organic Working Fluids in Rankine Engines," Proceedings of the 15th Intersociety Energy Conversion and Engineering Conference, 985-91, 1980.
12. Johns, I. B., McElhill, E. A., and Smith, J. O., "Thermal Stability of Organic Compounds," Industrial and Engineering Chemistry Product Research and Development, 1(1), 2-6, 1962.
13. Johns, I. B., McElhill, E. A., and Smith, J. O., "Thermal Stability of Some Organic Compounds," Journal of Chemical and Engineering Data, 7(1), 277-81, 1962.

14. Stone, J. P., Ewing, C. T., Blachly, C. H., Walker, B. E., and Miller, R. R., "Heat Transfer Studies on a Forced Convection Loop with Biphenyl and Biphenyl Polymers," Industrial and Engineering Chemistry, 50(6), 895-902, 1958.
15. Stone, J. P., Ewing, C. T., and Miller, R. R., "Heat-Transfer Studies on Some Stable Organic Fluids in a Forced Convection Loop," Journal of Chemical and Engineering Data, 7(4), 519-25, 1962.
16. "Clear Way for Organic Coolants?" Chemical Week, 69-71, April 20, 1963.
17. Parrish, C. F. and Grzyll, L. R., Development of Nontoxic Heat Transport Fluids for Habitat Two-Phase Thermal Control Systems, Final Report, Mainstream Engineering Corp., submitted to NASA-JSC, July 1991.
18. Parrish, C. F. and Grzyll, L. R., "Development of Nontoxic Heat Transport Fluids for Habitat Two-Phase Thermal Control Systems," SAE Transactions - Journal of Aerospace, 1993.
19. Rogers, G. C. and Cady, G., "Pyrolysis of Perfluoro-n-pentane," Journal of the American Chemical Society, 73, 3523-4, 1951.
20. Grosse, A. V. and Cady, G. H., "Properties of Fluorocarbons," Industrial and Engineering Chemistry, 39(3), 367-74, 1947.
21. Pummer, W. J. and Wall, L. A., "Preparation and Properties of Aromatic Fluorocarbons," Journal of Chemical and Engineering Data, 6(1), 76-8, 1961.
22. Allen, R. W., "The Maximum Pressure of Naphthalene Vapour," Journal of the Chemical Society, 77, 400-12, 1900.
23. Finck, J. L. and Wilhelm, R. M., "Variation With Pressure of the Boiling Points of Naphthalene, Benzophenone, and Anthracene," Journal of the American Chemical Society, 47, 1577-82, 1925.
24. Spaght, M. E., Thomas, S. B., and Parks, G. S., "Some Heat-Capacity Data on Organic Compounds Obtained With a Radiation Calorimeter," Journal of Physical Chemistry, 36, 882-8, 1932.
25. Andrews, J. N. and Ubbelohde, A. R., "Melting and Crystal Structure: The Melting Parameters of Some Polyphenyls," Proceedings of the Royal Society A, 228, 435-47, 1955.
26. Walker, B. E., Brooks, M. S., Ewing, C. T., and Miller, R. R., "Specific Heat of Biphenyl and Other Polyphenyls," Journal of Chemical and Engineering Data, 3(2), 280-2, 1958.
27. Madison, J. J. and Roberts, R. M., "Pyrolysis of Aromatics and Related Heterocyclics," Industrial and Engineering Chemistry, 50(2), 237-250, February 1958.

28. De Halas, D. R., Kinetics of the Decomposition of Organic Coolants, PhD. Thesis, Oregon State College, June 1960.
29. Blake, E. S., Hammann, W. C., Edwards, J. W., Reichard, T. E., and Ort, M. R., "Thermal Stability as a Function of Chemical Structure," Journal of Chemical and Engineering Data, 6(1), 87-98, January 1961.
30. Maslov, P. G., "Methods of Investigating the Reactivity of Radicals," Russian Journal of Physical Chemistry, 35(7), 762-764, July 1961.
31. Ziebland, H. and Burton, J. T. A., "Transport Properties of Some Organic Heat Transfer Fluids," Journal of Chemical and Engineering Data, 6(4), 579-83, 1961.
32. Horrocks, J. K. and McLaughlin, E., "Non-Steady-State Measurements of the Thermal Conductivities of Liquid Polyphenyls," Proceedings of the Royal Society A, 273, 259-74, 1963.
33. Fowler, L., Trump, W. N., and Vogler, C. E., "Vapor Pressure of Naphthalene," Journal of Chemical and Engineering Data, 13(2), 209-10, 1968.
34. Hedley, W. H., Milnes, M. V., and Yanko, W. H., "Thermal Conductivity and Viscosity of Biphenyl and the Terphenyls," Journal of Chemical and Engineering Data, 15(1), 122-127, 1970.
35. Chang, S. S. and Bestul, A. B., "Heat Capacity and Thermodynamic Properties of o-Terphenyl Crystal, Glass, and Liquid," Journal of Chemical Physics, 56(1), 503-516, 1972.
36. Jasper, J. J., "The Surface Tension of Pure Liquid Compounds," Journal of Physical and Chemical Reference Data, 4(1), 841, 1972.
37. Radchenko, L. G. and Kitaigorodskii, A. I., "The Vapour Pressures and Heats of Sublimation of Naphthalene, Biphenyl, Octafluoronaphthalene, Decafluorobiphenyl, Acenaphthene, and Nitronaphthalene," Russian Journal of Physical Chemistry, 48(11), 1595-1597, 1974.
38. Paul, S. and Back, M. H., "A Kinetic Determination of the Dissociation Energy of the C-O Bond in Anisole," Canadian Journal of Chemistry, 53, 3330-3338, 1975.
39. Yaws, C. L. and Turnbough, A. C., "Benzene and Naphthalene," Chemical Engineering, 107-115, September 1, 1975.
40. "Diphenyl and Terphenyls," Kirk-Othmer Encyclopedia of Chemical Technology, 3rd Ed., Wiley Interscience, 1978.

41. Reid, R. C., Prausnitz, J. M., and Poling, B. E., The Properties of Gases and Liquids, 4th Ed., McGraw-Hill, New York, 1987.
42. Chirico, R. D., Knipmeyer, S. E., Nguyen, A. and Steele, W. V., "The Thermodynamic Properties of Biphenyl," Journal of Chemical Thermodynamics, 21, 1307-1331, 1989.
43. The DIPPR Pure Component Data Compilation, Version 3.0, Technical Database Services, New York, NY, 1989.
44. Aldrich Catalog Handbook of Fine Chemicals, Aldrich Chemical Company, 1992.
45. Hellmann, M., Bilbo, A. J., and Pummer, W. J., "Synthesis and Properties of Fluorinated Polyphenyls," Journal of the American Chemical Society, 77, 3650-1, 1955.
46. Gething, B., Patrick, C. R., Stacey, F. R. S., and Tatlow, J. C., "A New General Route To Aromatic Fluorocarbons," Nature, 183, 588-9, 1959.
47. Wall, L. A., Donadio, R. E., and Pummer, W. J., "Preparation and Thermal Stability of Tetrakis-(pentafluorophenyl)-silane and Tris-(pentafluorophenyl)-phosphine," Journal of the American Chemical Society, 82, 4846-7, 1960.
48. Pummer, W. J. and Wall, L. A., "Preparation and Properties of Aromatic Fluorocarbons," Journal of Chemical and Engineering Data, 6(1), 76-78, January 1961.
49. Cheng, D. C. and McCoubrey, J. C., "The Critical Temperatures of Covalent Fluorides," Journal of the Chemical Society, 4993-4995, 1963.
50. Bloch, F. W. and MacKenzie, D. R., "Radiolysis of Cyclic Fluorocarbons. II. Perfluoroaromatics at Elevated Temperatures," Journal of Physical Chemistry, 73(3), 552-7, 1969.
51. Burdon, J., Knights, J. R., Parsons, I. W., and Tatlow, J. C., "Fluorinations With Potassium Tetrafluorocobaltate(III) - V," Tetrahedron, 30, 3499-3506, 1974.
52. Robota, L. P. and Malichenko, B. F., "Nucleophilic Substitution of Fluorine Atoms in Perfluorinated Aromatic Compounds," Journal of Organic Chemistry of the USSR, 12, 233, 1976.
53. Pozdnyakov, Y. V. and Shteingarts, V. D., "Reaction of Polyfluorinated Aromatic Compounds With Antimony Pentafluoride," Journal of Organic Chemistry of the USSR, 14, 2069-70, 1978.
54. Price, S. J. W. and Sapiano, H. J., "Determination of the H_{298° ($C_{12}F_{10}$, g) From Studies of the Combustion of Decafluorobiphenyl in Oxygen and Calculation of $D(C_6F_5-C_6F_5)$," Canadian Journal of Chemistry, 57, 1468-70, 1979.

55. Bardin, V. V., Furin, G. G., Avramenko, A. A., Krasil'nikov, V. A., Tushin, P. P., Karelin, A. I., and Yakobson, G. G., "Aromatic Fluorine Derivatives. Oxidative Fluorination of Perfluorinated Aromatic Compounds With Vanadium Pentafluoride," Journal of Organic Chemistry of the USSR, 20, 307-11, 1984.
56. Mukherjee, T. and Mittal, J. P., "Energy Transfer from Benzene to Some Aromatic Hydrocarbons and Their Perfluorinated Analogs," Indian Journal of Chemistry, 24A, 1008-14, 1985.
57. Atwal, R. K. and Bolton, R., "Nucleophilic Displacement in Polyhalogenoaromatic Compounds. XIII. Polyfluoroarene Systems," Australian Journal of Chemistry, 40, 241-7, 1987.
58. Sax, I. N., Dangerous Properties of Industrial Materials, 5th Ed., Van Nostrand Reinhold Co., New York, 1979.
59. Lee, B. I. and Kesler M. G., "A Generalized Thermodynamic Correlation Based on Three-Parameter Corresponding States," AIChE Journal, 21, 510-27, 1975.
60. Brennan, P. J. and Kroliczek, E. J., Heat Pipe Design Handbook, prepared for NASA-GSFC, prepared By B&K Engineering, Inc., June 1979.
61. Barbour, A. K., Barbow, G. G., and Tatlow, J. C., "The Fluorination of Hydrocarbons With Cobalt Trifluoride," Journal of Fluorine Chemistry, 2, 127, 1952.
62. Coe, P. L., Habib, R. M., and Tatlow, J. C., "Polyfluorobicyclo[4,4,0] Decanes. Part 1. The Fluorination of Tetralin over Cobalt Trifluoride," Journal of Fluorine Chemistry, 20, 203, 1982.
63. Gethig, B., Patrick, C. R., Stacey, M., and Tatlow, J. C., "A New General Route to Aromatic Perfluorocarbons," Nature, 183, 588, 1959.
64. Hu, C., Long, F., and Xu, Z., "Defluorination of Hexadecafluoro-Bicyclo[4,4,0] Dec-1(6)-Ene: A Facile Synthesis of Perfluoroaromatics," Journal of Fluorine Chemistry, 48, 29-35, 1990.
65. Marsella, J. A., Pez, G. P., and Coughlin, A. M., "Synthesis of Highly Fluorinated Aromatic Compounds," U. S. Patent 5,026,929, June 25, 1991.
66. Pozdnyakovich, Yu. V., Chikova, T. V., Bardin, V. V., and Shteingarts, V. D., "Formation of Polynuclear Aromatic Compounds in the Reaction of Heptafluorobenzonium Ion, Nonafluoro-1-Naphthalenonium Ion, and Octafluoronaphthalene Radical Cation With Polyfluorinated Aromatic Compounds in SbF_5 ," Russian Journal of Organic Chemistry, 687, 1976.

67. Shteingarts, V. D. and Pozdnyakovich, Yu. V., "Action of Electrophilic Agents on Polyfluoroaromatic Compounds. IV. Formation of Polyfluorinated Arenonium Ions by the Reaction of Polyfluorinated Cyclohexadienes with Antimony Pentafluoride," Russian Journal of Organic Chemistry, 744-52, 1971.
68. Edelstein, F. and Haslett, R., Heat Pipe Manufacturing Study, NASA CR-139140, 1974.
69. Chi, S. W., Heat Pipe Theory and Practice, Hemisphere, 1976.
70. Dunn, P. and Reay, D. A., Heat Pipes, Pergamon Press, 1976.
71. Wilson, D. P. and Basu, R. S., "Thermodynamic Properties of a New Stratospherically Safe Working Fluid - Refrigerant 134a," ASHRAE Transactions, 2095-104, 1988.
72. Salvi-Narkhede, M., Wang, B-H., Adcock, J. L., and Van Hook, W., "Vapor Pressures, Liquid Molar Volumes, Vapor Non-Ideality, and Critical Properties of Some Partially-Fluorinated Ethers, Some Perfluoroethers, and of CHF₂Br and CF₃CFHCF₃," Journal of Chemical Thermodynamics, 24, 1065-75, 1992.
73. Phillips, T. W. and Murphy, K. P. Liquid Viscosity of Halocarbons. Journal of Chemical and Engineering Data, 15, 304-307, 1970.
74. Burns, W. G., Morris, B., and Wilkinson, R. W., "An Apparatus for the Viscometry of Organic Liquids at High Temperatures," Journal of Scientific Instruments, 35, 291-3, 1958.
75. Press, W. H., Flannery, B. P., Teukolsky, S. A., and Vetterling, W. T., Numerical Recipes, Cambridge University Press, Cambridge, MA, 1986.
76. Chae, H. B., Schmidt, J. W., and Moldover, M. R., "Alternative Refrigerants R123a, R134, R141b, R142b, and R152a: Critical Temperature, Refractive Index, Surface Tension, and Estimates of Liquid, Vapor, and Critical Densities," Journal of Physical Chemistry, 94, 8840-45, 1990.
77. Lane, J. E., "Correction Terms for Calculating Surface Tension From Capillary Rise," Journal of Colloidal and Interface Science, 42(1), 145-9, 1973.
78. ASTM Project TM-01-05A-9, "Standard Test Method for Determining Vapor Pressure By Thermal Analysis", (provisional method under development by ASTM E37 task group).
79. G. Soave, "Rigorous and Simplified Procedures for Determining the Pure Component Parameters in the Redlich-Kwong-Soave Equation of State," Chemical Engineering Science, 35, 1725, 1980.

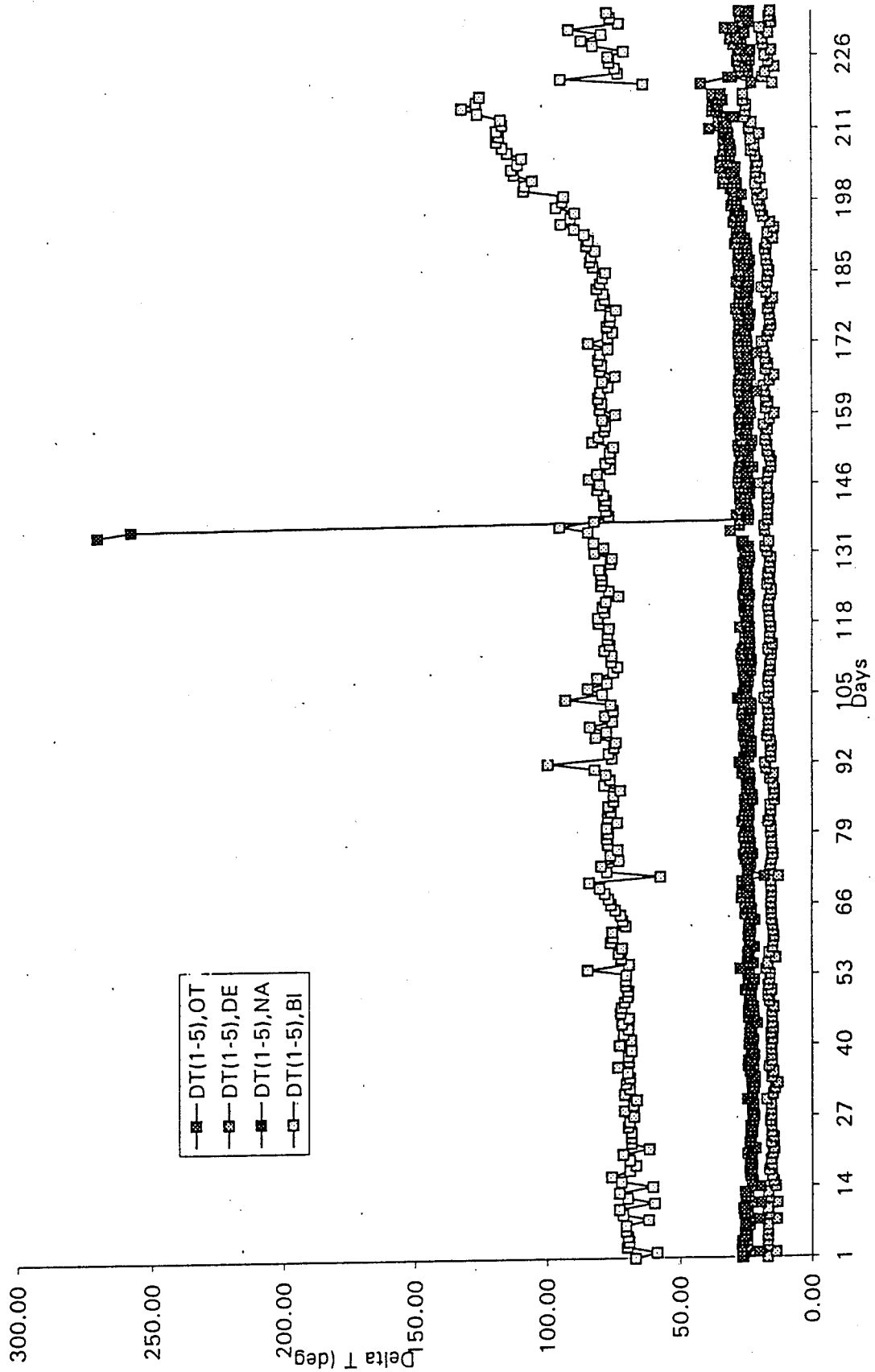
80. J.M. Smith and H.C. Van Ness, Introduction to Chemical Engineering Thermodynamics, 4th ed., McGraw-Hill Book Company, New York, 1987, Chapter 4 and Appendix C.
81. R.J.L. Andon, J.E. Connett, and J.F. Martin, The Enthalpy of Fusion of Indium; Certificate of a Sample for Use as a CRM, NPL Report Chem. 101, 1979.
82. Briggs, D. K. H., "Thermal Conductivity of Liquids," Industrial and Engineering Chemistry, 49(3), 418-21, 1957.
83. Weber, J. H., "Predict the Viscosities of Pure Gases," Chemical Engineering, 111-7, June 18, 1979.

APPENDIX A: GRAVITY REFLUX HEAT PIPE TEST RESULTS

CONTENTS:

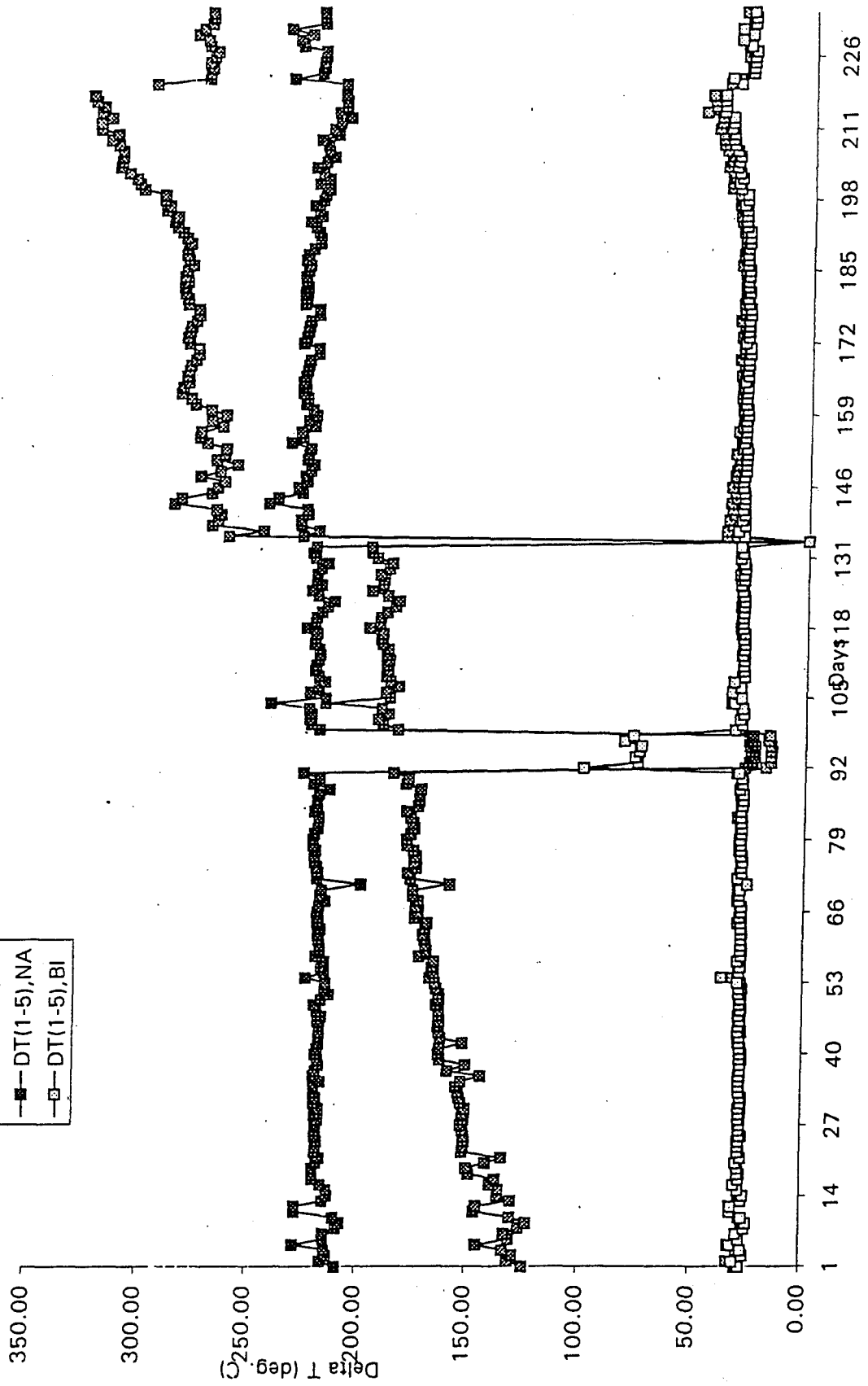
1. Evaporator-Condenser Temperature Profiles
2. Description of Fluid Appearance After Test
3. DSC Analysis Results

Block #1



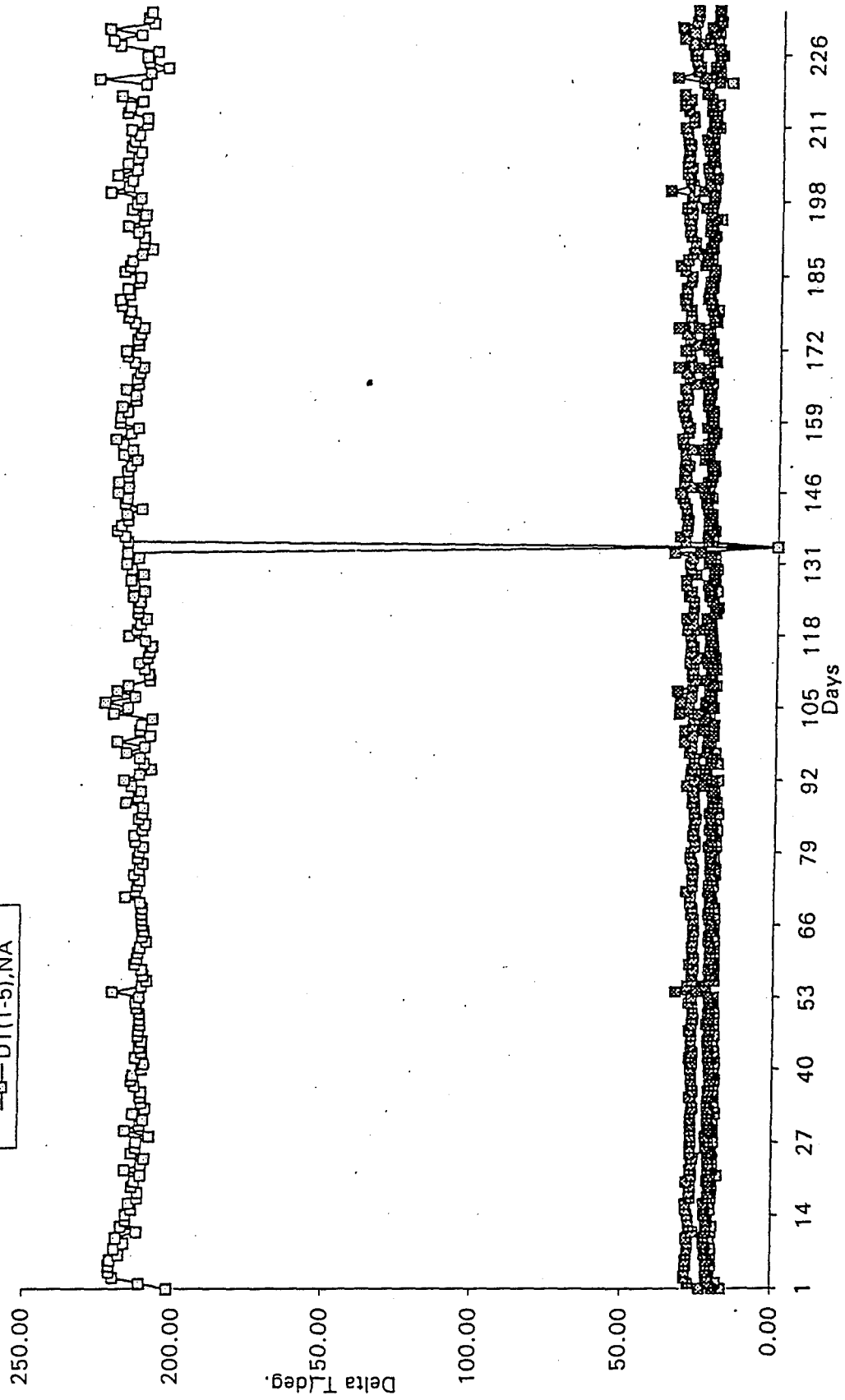
Block #2

- DT(1-5),DE
- DT(1-5),OT
- DT(1-5),NA
- DT(1-5),BI

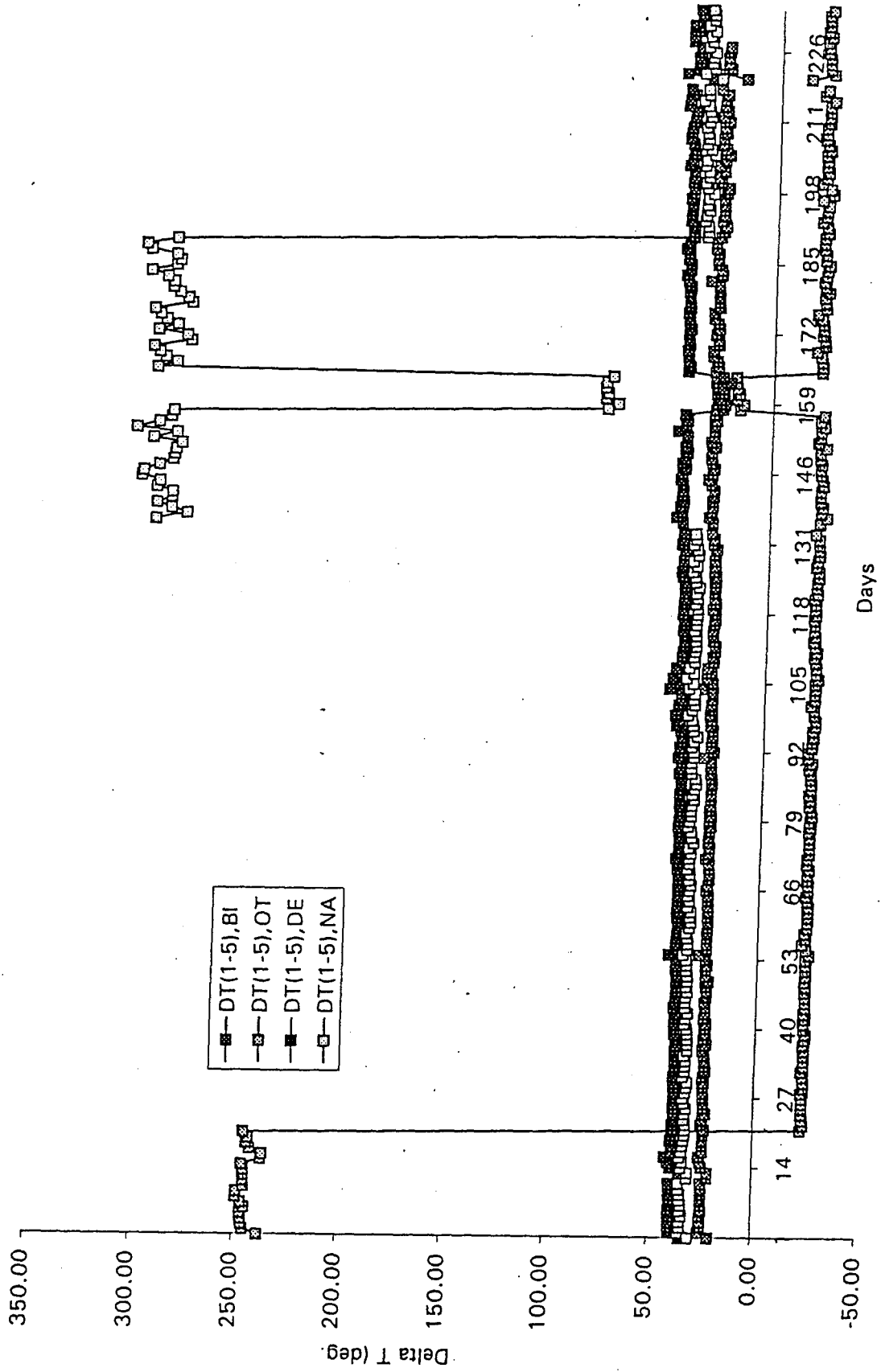


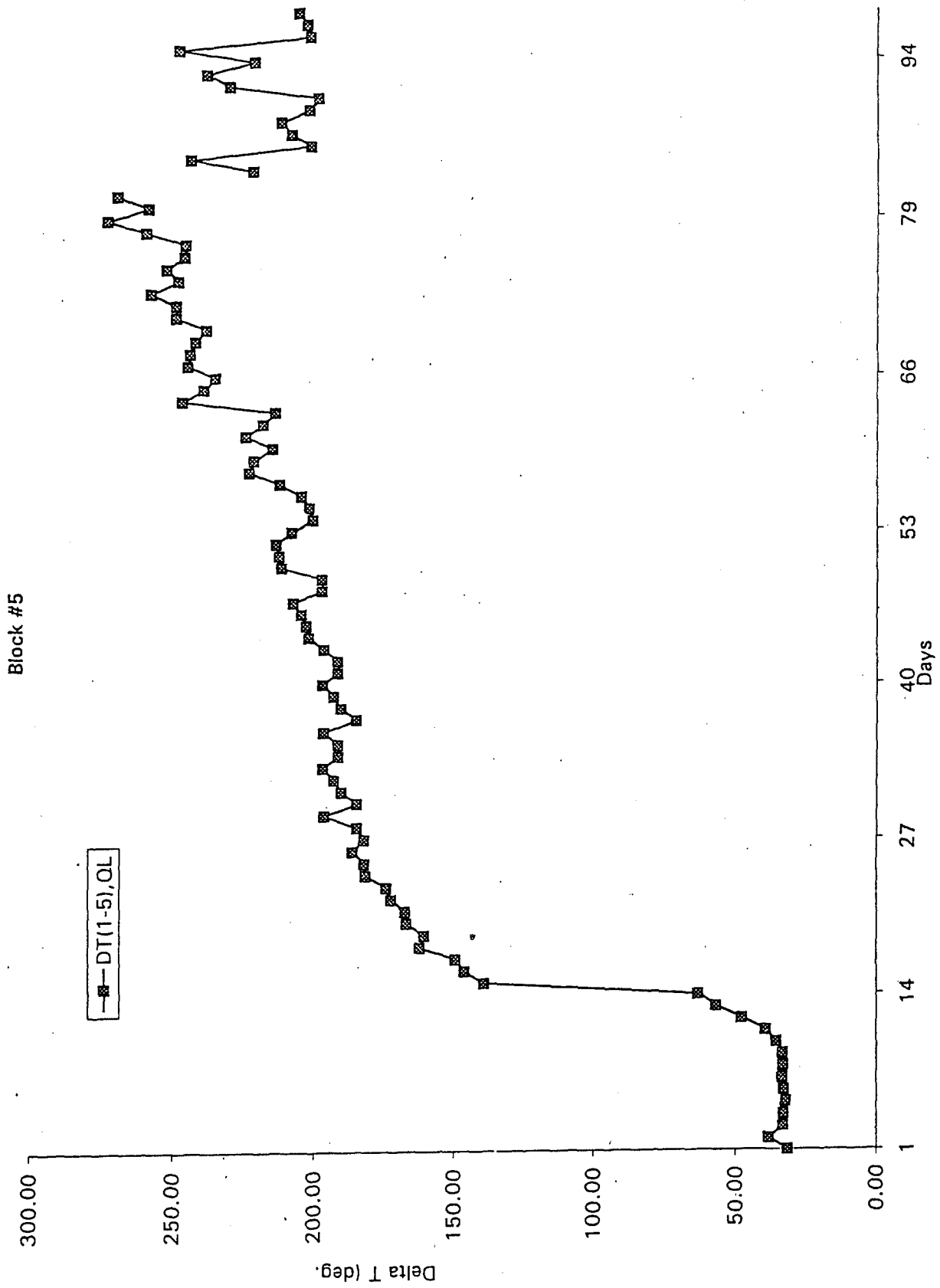
Block #3

- DT(1-5), OT
- DT(1-5), DE
- DT(1-5), BI
- DT(1-5), NA

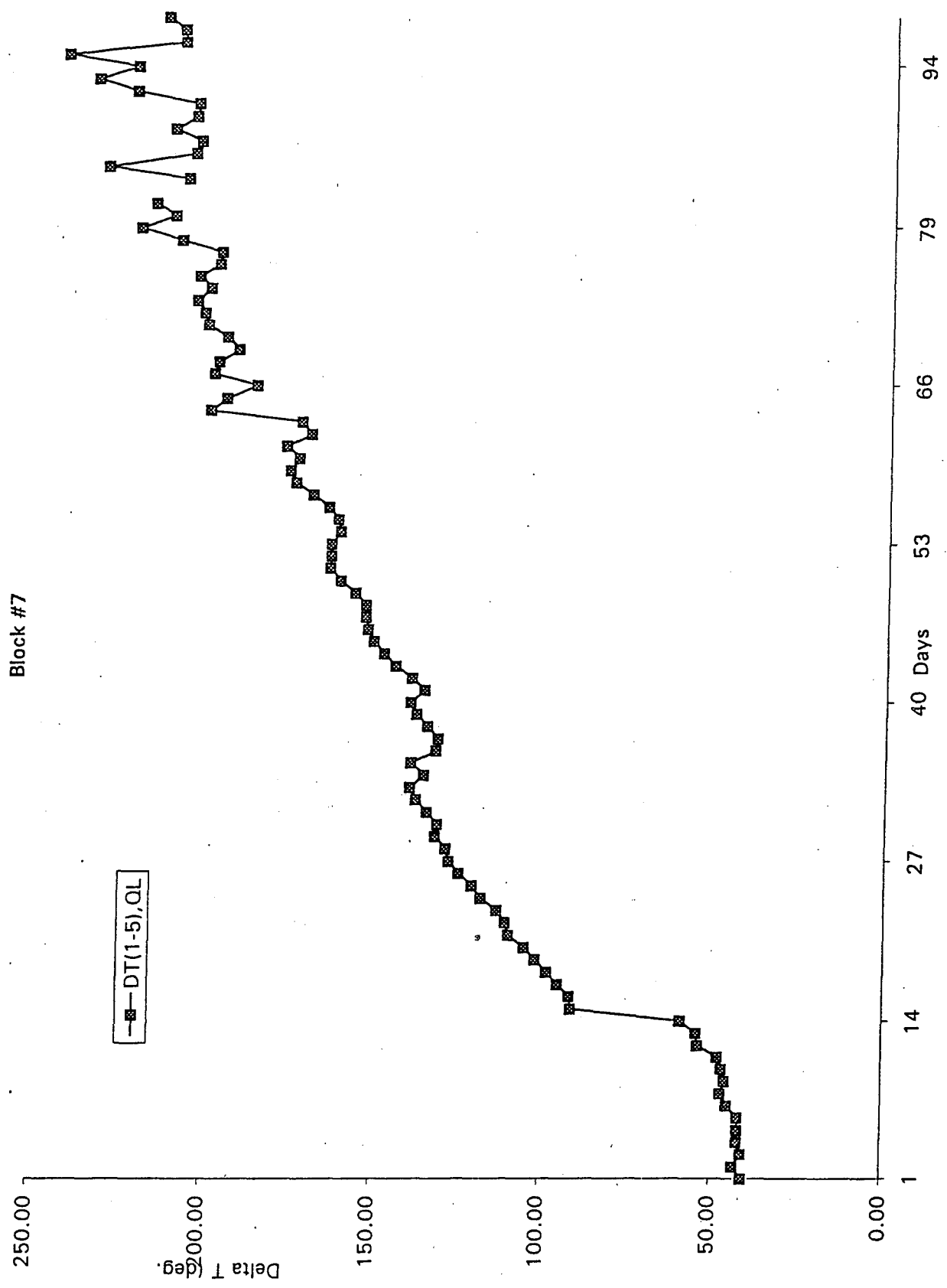


Block #4





Block #7



-■- DT(1-5),OL

GRAVITY REFLUX HEAT PIPE TESTS - FLUID APPEARANCE AFTER TEST

Block #	Test	Pipe #	Fluid	Initial Mass	Duration	Final Mass	Final Appearance	GC Results
1	variable	16	o-terphenyl	4.7 grams	230 days	2.7 grams	light amber/white crystals	no impurities detected
		12	decafluorobiphenyl	8.4 grams		7.9 grams	magenta crystals and needles	no impurities detected
		10	naphthalene	4.4 grams		4.1 grams	white crystals and needles	no impurities detected
		2	biphenyl	2.9 grams		0.8 grams	white crystals and needles	no impurities detected
2	variable	14	decafluorobiphenyl	4.2 grams	230 days	ND	ND	ND
		19	o-terphenyl	4.3 grams		4.3 grams	white crystals	no impurities detected
		9	naphthalene	3.2 grams		2.7 grams	light brown crystals	no impurities detected
		4	biphenyl	2.9 grams		1.2 grams	white crystals and needles	no impurities detected
3	constant	20	o-terphenyl	4.5 grams	230 days	3.9 grams	light amber/white crystals	no impurities detected
		15	decafluorobiphenyl	6.6 grams		6.9 grams	magenta crystals and needles	no impurities detected
		3	biphenyl	3.0 grams		2.5 grams	light amber crystals	no impurities detected
		7	naphthalene	3.2 grams		2.0 grams	light brown crystals	no impurities detected
4	constant	6	biphenyl	2.8 grams	230 days	0.9 grams	white crystals and needles	no impurities detected
		18	o-terphenyl	4.5 grams		4.4 grams	light amber/white crystals	no impurities detected
		13	decafluorobiphenyl	6.0 grams		6.7 grams	magenta crystals and needles	no impurities detected
		8	naphthalene	4.3 grams		3.7 grams	white crystals and needles	no impurities detected
5	variable	17	quinoline	4.4 grams	98 days	1.8 grams	dark brown liquid with solid precipitate	no impurities detected
6	variable	21	quinoline	3.5 grams	81 days	0.2 grams	dark brown liquid with solid precipitate	no impurities detected
		7	quinoline	3.8 grams	98 days	2.4 grams	dark brown liquid with solid precipitate	high-boiler detected
8	constant	23	quinoline	4.5 grams	pipe leaked	ND	ND	ND

DSC THERMAL STABILITY ANALYSIS

Fluid	Block #	Pipe #	Appearance	Melting Pt. (C)	Boiling Pt. (C)
naphthalene	distilled - untested		white crystals	79.45	219.04
naphthalene	2	9	light brown crystals	79.34	221.15
naphthalene	3	7	light brown crystals	79.47	220.77
naphthalene	1	10	white crystals and needles	79.26	219.25
naphthalene	4	8	white crystals and needles	79.77	219.8
biphenyl	distilled - untested		white crystals	68.03	257.88
biphenyl	3	3	light amber crystals	68.13	257.37
biphenyl	1	2	white crystals and needles	68.25	257.51
biphenyl	4	6	white crystals and needles	68.47	256.02
biphenyl	2	4	white crystals and needles	68.29	257.3
o-terphenyl	distilled - untested		white crystals	56.14	339.89
o-terphenyl	3	20	light amber/white crystals	55.85	339.4
o-terphenyl	4	18	light amber/white crystals	55.83	339.96
o-terphenyl	1	16	light amber/chite crystals	55.81	340.16
o-terphenyl	2	19	white crystals	55.8	339.82
ecafluorobipheny	distilled - untested		white crystals	66.94	206.87
ecafluorobipheny	1	12	magenta crystals and needles	67.09	208.17
ecafluorobipheny	3	15	magenta crystals and needles	66.83	207.03
ecafluorobipheny	4	13	magenta crystals and needles	66.69	207.51
ecafluorobipheny	2	14	ND	ND	ND
quinoline	distilled - untested		colorless liquid	N/A	238.42
quinoline	5	17	dark brown liquid/solid	N/A	242.55

APPENDIX B: SURFACE TENSION FORTRAN PROGRAM

PROGRAM ALPHA

```
C
C-----
C THIS PROGRAM COMPUTES THE VALUES FOR "ALPHA" USING DIFFERENTIAL
C CAPILLARY RISE TECHNIQUES AS DESCRIBED BY LANE [1973] AND CHAE
C ET AL. [1990]. THE THREE VALUES GENERATED CAN THEN BE USED TO
C COMPUTE A VALUE FOR THE SURFACE TENSION THROUGH:
C
C      SIGMA = ALPHA^2 * (RHOI-RHOv) * g / 2
C
C THE TWO EQUATIONS
C
C      H(L) = [ALPHA(ij)^2/r(L)]/F(r(L)/ALPHA)   r(L)/ALPHA < 2
C           = [ALPHA(ij)^2 / r(L)] * PHI(r(L)/ALPHA) r(L)/ALPHA > 2
C
C AND
C
C      ALPHA(ij)^2 = r(S)*[dH(ij)+H(L)]*F(r(S)/ALPHA)   r(S)/ALPHA < 2
C                = r(S)*[dH(ij)+H(L)]/PHI(r(S)/ALPHA) r(S)/ALPHA > 2
C
C ARE SOLVED ITERATIVELY FOR EACH OF THE 'ij' SETS: 12, 23, AND 13.
C ABOVE, 'ij' REFERS TO THE 'i' AND 'j' CAPILLARIES, 'L' DESIGNATES
C THE LARGER OF THESE TWO CAPILLARIES, AND 'S' DESIGNATES THE SMALLER.
C THE VALUES DETERMINED FOR ALPHA(ij), ij=12,23,13, CAN THEN BE USED
C TO ESTIMATE THE SURFACE TENSION SIGMA.
C
C NOTE: ALL OUTPUTTED LENGTH UNITS ARE IN mm.
C
C      DWIGHT D. BACK, MAINSTREAM ENGINEERING CORP.
C                      7/13/93
C-----
C
C DEFINE THE EXTERAL FUNCTIONS PER LANE [1973]
C
C      external RATLT2
C      external RATGT2
C
C INITIALIZE THE CAPILLARY RADII
C
C      CHARACTER*8 FILENM, FILEOUT
C      DATA DH12, DH23, DH13, ALPH12, ALPH23, ALPH13/6*0./
C      DATA XOLD/0./
C      DATA RAT12S, RAT12L, RAT23S, RAT23L, RAT13S, RAT13L/6*0./
C      DATA IT12, IT23, IT13/3*0/
C      DATA PHI12, PHI23, PHI13, FUNC12, FUNC23, FUNC13/6*0./
C      errlim = 0.1
C
```



```

WRITE(*,*) 'ENTER INPUT DATA FILE NAME (8 CHAR. MAX):'
READ(*,'(1A)') FILENM
WRITE(*,*) 'ENTER OUTPUT DATA FILE NAME (8 CHAR. MAX):'
READ(*,'(1A)') FILEOUT
C
OPEN(55, FILE=FILEOUT)
OPEN(57, FILE='MISCDAT')
OPEN(56, FILE=FILENM)
C
C THE THREE CAPILLARY RADII USED IN THE STUDY (mm)
C
R1=0.276
R2=0.320
R3=0.574
C
C READ IN THE CAPILLARY HEIGHT DIFFERENCES FROM 'FILENM'
C
WRITE(57,*) 'ENTER delta h between med & small capillary (DH23):'
READ(56,*) DH12
WRITE(57,*) DH12
DH12 = DH12 * 25.4
WRITE(57,*) 'ENTER delta h between med & large capillary (DH12):'
READ(56,*) DH23
WRITE(57,*) DH23
DH23 = DH23 * 25.4
WRITE(57,*) 'ENTER delta h between small & lrg capillary (DH13):'
READ(56,*) DH13
WRITE(57,*) DH13
DH13 = DH13 * 25.4
WRITE(57,*) 'ENTER the TEMPRATURE (C):'
READ(56,*) Temp
WRITE(57,*) Temp
C
C CALCULATE THE INITIAL ALPHA VALUES
C
ALPH12 = SQRT(DH12*R1)
ALPH23 = SQRT(DH23*R2)
ALPH13 = SQRT(DH13*R1)
WRITE(55,105) FILENM
WRITE(*,105) FILENM
WRITE(55,104) ALPH12, ALPH23, ALPH13
WRITE(*,104) ALPH12, ALPH23, ALPH13
C
C ITERATE TO DETERMINE THE VALUE FOR "ALPHA(12)"
C
DO 91 J=1,1000
RAT12L = R2/ALPH12
RAT12S = R1/ALPH12
write(57,*) 'RAT12S, RAT12L=',RAT12S, RAT12L
C
C DETERMINE H12(L)
C
IF(RAT12L .GT. 2.0) THEN
F12L = RATGT2(RAT12L)

```

```

        zh12L = (ALPH12**2 / R2) * F12L
    ELSE
        F12L = RATLT2(RAT12L)
        zh12L = (ALPH12**2 / R2) / F12L
    ENDIF
C
C DETERMINE NEW ALPHA(12)
C
    XOLD = ALPH12
    IF(RAT12S .GT. 2.0) THEN
        F12S = RATGT2(RAT12S)
        ALPH12 = SQRT(R1*(DH12+zh12L)/F12S)
    ELSE
        F12S = RATLT2(RAT12S)
        ALPH12 = SQRT(R1*(DH12+zh12L)*F12S)
    ENDIF
C
C CHECK FOR CONVERGENCE OF ALPHA(12)
C
    IT12 = IT12 + 1
    WRITE(57,*)'XOLD, ALPH12=',XOLD,ALPH12
    ERROR = 100.*(1.-XOLD/ALPH12)
    WRITE(57,*)'LOOP 12: ERROR=',ERROR
    IF(ABS(ERROR) .LE. errlim) GOTO 82
    if((j/50)*50 .eq. j) WRITE(57,*) 'LOOP 12: j='j
91 CONTINUE
82 IF(RAT12L .GT. 2.) PHI12 = F12L
    IF(RAT12L .LE. 2.) FUNC12 = F12L
C
C ITERATE TO DETERMINE THE VALUE FOR "ALPHA(23)"
C
    WRITE(57,*) 'ALPH23=',alph23
C
    DO 92 J=1,1000
        RAT23L = R3/ALPH23
        RAT23S = R2/ALPH23
        write(57,*) 'RAT23S, RAT23L=',RAT23S, RAT23L
C
C DETERMINE H23(L)
C
    IF(RAT23L .GT. 2.0) THEN
        F23L = RATGT2(RAT23L)
        zh23L = (ALPH23**2 / R3) * F23L
    ELSE
        F23L = RATLT2(RAT23L)
        zh23L = (ALPH23**2 / R3) / F23L
    ENDIF
C
C DETERMINE NEW ALPHA(23)
C
    XOLD = ALPH23
    IF(RAT23S .GT. 2.0) THEN
        F23S = RATGT2(RAT23S)
        ALPH23 = SQRT(R2*(DH23+zh23L)/F23S)

```

```

ELSE
    F23S = RATLT2(RAT23S)
    ALPH23 = SQRT(R2*(DH23+zh23L)*F23S)
ENDIF
c
C CHECK FOR CONVERGENCE OF ALPHA(23)
C
    IT23 = IT23 + 1
    WRITE(57,*)'XOLD, ALPH23=',XOLD,ALPH23
    ERROR = 100.*(1.-XOLD/ALPH23)
    WRITE(57,*)'LOOP 23: ERROR=',ERROR
    IF(ABS(ERROR) .LE. errlim) GOTO 83
    if((j/50)*50 .eq. j) WRITE(57,*) 'LOOP 23: j=',J
92 CONTINUE
83 IF(RAT23L .GT. 2.) PHI23 = F23L
    IF(RAT23L .LE. 2.) FUNC23 = F23L
C
C ITERATE TO DETERMINE THE VALUE FOR "ALPHA(13)"
C
    DO 93 J=1,1000
        RAT13L = R3/ALPH13
        RAT13S = R1/ALPH13
        write(57,*) 'RAT13S, RAT13L=',RAT13S, RAT13L
C
C DETERMINE H13(L)
C
    IF(RAT13L .GT. 2.0) THEN
        F13L = RATGT2(RAT13L)
        zh13L = (ALPH13**2 / R3) * F13L
    ELSE
        F13L = RATLT2(RAT13L)
        zh13L = (ALPH13**2 / R3) / F13L
    ENDIF
C
C DETERMINE NEW ALPHA(13)
C
    XOLD = ALPH13
    IF(RAT13S .GT. 2.0) THEN
        F13S = RATGT2(RAT13S)
        ALPH13 = SQRT(R1*(DH13+zh13L)/F13S)
    ELSE
        F13S = RATLT2(RAT13S)
        ALPH13 = SQRT(R1*(DH13+zh13L)*F13S)
    ENDIF
C
C CHECK FOR CONVERGENCE OF ALPHA(13)
C
    IT13 = IT13 + 1
    WRITE(57,*)'XOLD, ALPH13=',XOLD,ALPH13
    ERROR = 100.*(1.-XOLD/ALPH13)
    WRITE(57,*)'LOOP 13: ERROR=',ERROR
    IF(ABS(ERROR) .LE. errlim) GOTO 84
    if((j/50)*50 .eq. j) WRITE(57,*) 'LOOP 13: j=',J
93 CONTINUE

```

```

84  IF(RAT13L .GT. 2.) PHI13 = F13L
      IF(RAT13L .LE. 2.) FUNC13 = F13L
C
C OUTPUT DATA
C
      WRITE(55,106) TEMP, ALPH12, IT12, ALPH23, IT23, ALPH13, IT13
      WRITE(55,107) R1, R2, R3, DH12, DH23, DH13
      WRITE(*,106) TEMP, ALPH12, IT12, ALPH23, IT23, ALPH13, IT13
      WRITE(*,107) R1, R2, R3, DH12, DH23, DH13
      WRITE(55,108)
      WRITE(55,109) FUNC12, PHI12, ALPH12, ZH12L, R2,
1      FUNC23, PHI23, ALPH23, ZH23L, R3,
2      FUNC13, PHI13, ALPH13, ZH13L, R3,
3      (ALPH12+ALPH23+ALPH13)/3.
104  FORMAT(/10X,'INITIAL: ALPH(12)=' ,G10.5,' ALPH(23)=' ,G10.5,
1  ' ALPH(13)=' ,G10.5)
105  FORMAT(/10X,'VALUES FOR ALPHA; DATA FILE: ',1A,/10X,37('*'))
106  FORMAT(/10X,'TEMPERATURE=' ,F7.2,' DEG. C'//10X,'ALPHA(12)=' ,
1  G10.5,' (AFTER ',I4,' ITERATIONS)'//10X,'ALPHA(23)=' ,
2  G10.5,' (AFTER ',I4,' ITERATIONS)'//10X,'ALPHA(13)=' ,
3  G10.5,' (AFTER ',I4,' ITERATIONS)'//)
107  FORMAT(/10X,'CAPILLARY RADII (1,2,3) = ',3(G10.4,' ')/
1  10X,'DELTA HEIGHTS (DH12,DH23,DH23) = ',
2  3(G10.4,' '))
108  FORMAT(///17X,'SUMMARY TABLE FOR EQS. 11 & 12 (LANE)'
1  /17X,37('-')/3X,'ALPHA',3X,2X,'F(R/A)',3X,1X,'PHI(R/A)',
2  2X,3X,'ALPHA',3X,3X,'H(L)',4X,3X,'R(L)'/)
109  FORMAT(4X,'12',8X,5(G10.5,1X)/4X,'23',8X,5(G10.5,1X)/
1  4X,'13',8X,5(G10.5,1X)//17X,'THE AVG. ALPHA IS: ',G10.5)
C
      CLOSE(55)
      CLOSE(56)
      CLOSE(57)
      STOP
      END
C
C FUNCTIONAL FORM FOR "PHI" WHEN (R/A)>2
C
      FUNCTION RATGT2(X)
      DUM = EXP(-1.41222*X+0.66161+0.14681/X+0.37136/X**2)
      DUM = DUM*X**(3./2.)
      RATGT2 = DUM
      RETURN
      END
C
C FUNCTIONAL FORM FOR "F" WHEN (R/A)<2
C
      FUNCTION RATLT2(X)
      DUM = 3327.9*X**2 + 65.263*X**3 - 473.926*X**4 + 663.569*X**5
      DUM = DUM - 300.032*X**6 + 75.1929*X**7 - 7.3163*X**8
      DUM = 1.0 + DUM/1.E4
      RATLT2 = DUM
      RETURN
      END

```

Example Output From FORTRAN Program

VALUES FOR ALPHA; DATA FILE: sign

INITIAL: ALPH(12)=.67259 ALPH(23)=1.2855 ALPH(13)=1.3726

TEMPERATURE= 300.00 DEG. C

ALPHA(12)=1.7956 (AFTER 30 ITERATIONS)

ALPHA(23)=1.9145 (AFTER 10 ITERATIONS)

ALPHA(13)=1.8895 (AFTER 8 ITERATIONS)

CAPILLARY RADII (1,2,3) = .2760 .3200 .5740
DELTA HEIGHTS (DH12,DH23,DH23) = 1.639 5.164 6.827

SUMMARY TABLE FOR EQS. 11 & 12 (LANE)

ALPHA	F(R/A)	PHI(R/A)	ALPHA	H(L)	R(L)
12	.97848	.00000	1.7956	10.279	.32000
23	.97590	.00000	1.9145	6.5340	.57400
13	.97598	.00000	1.8895	6.3623	.57400

THE AVG. ALPHA IS: 1.8665

APPENDIX C: PROTOTYPE HEAT PIPE DESIGNS

CONTENTS:

1. Orion International Heat Pipe Design
2. Dynatherm Quotation/Comments
3. OAO Quotation/Comments

TO: Mary Corrigan, PL/VTPT
 FROM: Anthony Gurule
 SUBJECT: Design of Axial Groove Heat Pipes

21 July 1994

BACKGROUND

I have completed a preliminary design of axial groove heat pipes utilizing the working fluids outlined in Reference 1 and 2. The boundary conditions as to what the heat pipes are to be designed to are extracted from References 1, 3, 4 and 5. The methodology used to design the pipes is taken primarily from Reference 6 with support from References 7 and 8. To provide a feeling of comfort the heat pipe steady state computer code, HTPIPE, was modified to analyze the fluids selected. All calculations are provided as Attachment 1.

PROBLEM DEFINITION

Based on Attachment 2 and Reference 3, 4, and 5 the following was identified as the problem statement. The approach was to design a simple axial groove heat pipe that would allow the characterization and testing of the potential working fluids. The design was to be an axial groove, straight, tubular heat pipe, constructed from readily available material such as stainless steel, with at least an outer diameter of 1 inch. The operating temperature range was 300 to 400 C. A safety design margin of at least 2 was to be incorporated. A total of 55 Watts is inputted at the evaporator end. The heat pipe dimensions shall be; evaporator section, 6 inches in length, adiabatic section, 24 inches, and a condenser section, 6 inches.

WORKING FLUID SELECTION

This effort is designed to characterize and test two-phase working fluids for thermal management of sodium sulfur (NaS) batteries in the temperature range of 300 to 400 C. Several potential fluids have been identified for this application and have been reviewed for merit based on the fluid properties in Attachment 3. In general, when selecting a working fluid several factors should be considered: working pressure, fluid properties, thermal conductivity, compatibility with container material and stability at elevated temperatures. The first three factors are evaluated through the evaluation of the following variables:

- (High) Liquid Transport Factor (LTF) - $\rho_l * \lambda * \sigma / \mu_l$
- (High) Wicking Height (WH) - $\sigma / \rho_l * g$
- (Low) Kinematic Viscosity Ratio (KVR) - ν_v / ν_l
- (Low) Vapor Pressure (VP) - property of fluid

where ρ_l is the density of the liquid, λ is the latent heat of vaporization, σ is surface tension, μ_l is liquid viscosity, g is the gravitational constant, and ν_v and ν_l are the kinematic viscosity of the vapor and liquid respectfully. Based on Attachment 1 the above factors were calculated and summarized below for the top five fluids identified. Only three fluids will be used in the actual test.

	LTF (W/m ²)	WH (m ²)	KVR	VP (kPa)
Biphenyl (C ₁₂ H ₁₀)	1.01E10	1.33E-6	2.55	566.29
O-Terphenyl (C ₁₈ H ₁₄)	9.61E9	1.72E-6	4.76	128.11
Napthalene (C ₁₀ H ₈)	1.16E10	1.27E-6	2.06	1004.34
Decafluorobiphenyl(C ₁₂ F ₁₀)	1.57E8	4.72E-8	1.79	1669.78
Quinoline (C ₉ H ₇ N)	1.49E10	1.41E-6	2.8	768.55

From the above data it seems Biphenyl, O-Terphenyl, and Naphthalene are the top candidate fluids exhibiting the best working fluid properties/characteristics.

As far as the compatibility issue the Material Safety Data Sheets (Attachment 4) do not indicate specifically what (container) materials are incompatible with the fluids. They only indicate that "STRONG OXIDIZING AGENTS" should not come in contact with the fluids. This remains an open issue.

Finally, the issue of thermal stability has been investigated by Mainstream (Reference 2). Based on their analysis, the fluids exhibiting the best to least stability are:

Biphenyl
O-Terphenyl
Decafluorobiphenyl
Naphthalene
Quinolino

In summary, based on the above factors and their fluids properties, three fluids have been identified as candidate working fluids for the heat pipes - they are:

Biphenyl
O-Terphenyl
Naphthalene

The design effort, summarized below, used the three fluids in the calculation of the heat pipe design parameters.

HEAT PIPE DESIGN SUMMARY

The methodology used to design heat pipes for the three candidate working fluids was extracted from References 6, 7, and 8. The methodology or "cook-book" approach provides a general feel as to what needs to be done for the design of an axial groove heat pipe. However, there are some parameters that I still need to investigate such as unforeseen pressure drops that are inherent in axial groove heat pipes. But for now, the following design information should provide a general design guidance for the heat pipes.

The design parameters calculated for the fluids are listed below and pictorially shown in Figure 1. The calculations that were used to derive these design parameters are presented in Attachment 1.

	Effective Pumping Radius (rp) (m)	Groove Width (w) (m)	Groove Depth (s) (m)	Vapor Space Diameter (Dv) (m)	Inner Cell Diameter (Di) (m)	Outer Cell Diameter (Do) (m)	Landing Thickness (lf) (m)	# of Grooves
Biphenyl	1.41E-3	1.41E-3	2.82E-3	2.024E-2	2.589E-2	2.6E-2	7.05E-4	30
O-Terphenyl	1.83E-3	1.83E-3	3.66E-3	1.314E-2	2.048E-2	2.05E-2	9.15E-4	15
Naphthalene	1.35E-2	1.35E-3	2.7E-3	1.94E-2	2.48E-2	2.5E-2	6.75E-4	30

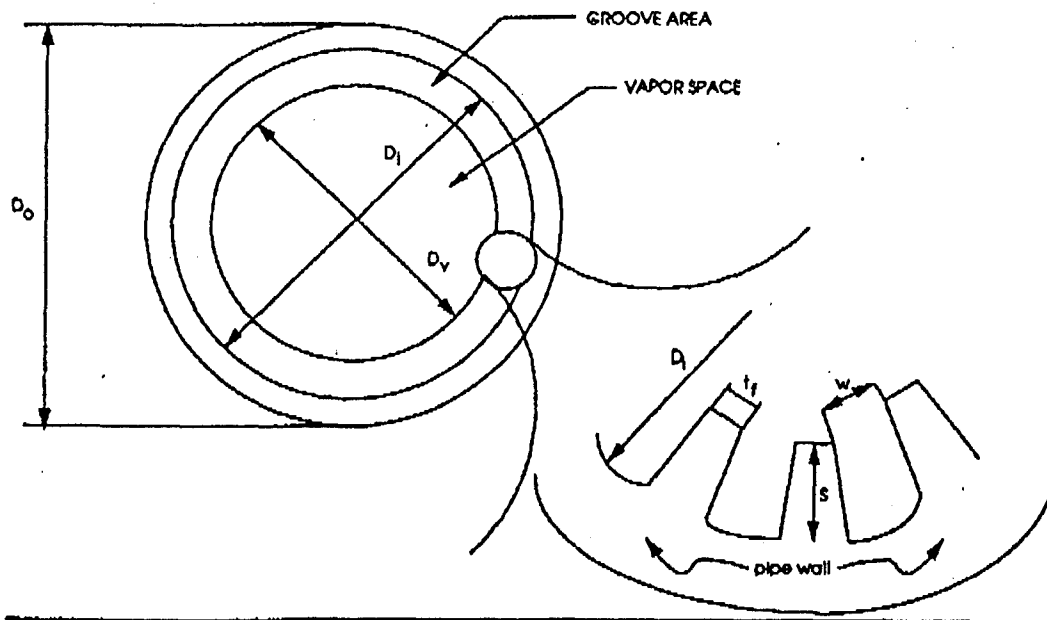


Figure 1. Design Parameters for Axial Groove Heat Pipes.

HTPIPE ANALYSIS

As a check into the design parameters derived for the heat pipes the material properties data file from the heat pipe computer code HTPIPE was modified and computer runs were initiated to arrive at an understanding as to the limitations (sonic, entrainment, and boil) the heat pipes may have. The input file for the HTPIPE computer runs is presented below. Results from the runs are presented in Attachment 5.

HTPIPE INPUT VARIABLES

Type of Run	2	Calculate Limits
Type of Wick	2	Screen Covered Axial Groove (Closest Option)
Working Fluid	*	Fluids Listed Above
Evaporator Length (cm)	15.24	Desired Design
Adiabatic Length (cm)	60.96	Desired Design
Condenser Length (cm)	15.24	Desired Design
Tilt Angle (deg)	0.078	Minimum as Stated in Reference 6
Pipe Inside Radius (cm)	*	See Above Design Parameters
Distribution Screen Thickness (cm)	0.1	Assumed Based on Reference 8
Distance Between Grooves (cm)	*	See Above Design Parameters
1/2 Wire Diameter (cm)	0.0032	Based on 200 Mesh
Depth of Grooves (cm)	*	See Above Design Parameters
Effective Pore Radius (cm)	*	See Above Design Parameters
Number of Grooves	*	See Above Design Parameters
Lowest Evaporator Exit Temperature (K)	573	Desired Design Parameters
Highest Evaporator Exit Temperature (K)	673	Desired Design Parameters
Temperature Increment (K)	10	
Wick Surface Porosity	0.6	Square Mesh
Thermal Conductivity of Pipe Wick ($w/cm K$)	0.705	Aluminum
Nuclear Site Radius	0	Default

The results from the HTPIPE analysis show that all three heat pipes will be well within each envelope with the exception of the boiling limit. At this limit the data shows that the maximum heat input will be very close to the boiling limit.

SUMMARY

A preliminary design analysis was conducted to design three heat pipes using new working fluids developed by Mainstream Engineering. The design parameters from the analysis are presented as well as computer runs that investigate the heat pipe limits. More work has to be conducted to refine the design and incorporate other loss mechanisms not accounted for in the preliminary analysis.

ATTACHMENTS:

- (1) Hand Calculations for the Design of Axial Groove Heat Pipes.
- (2) Memorandum, D. Gluck to M. Corrigan, Subject: Heat Pipes and Test Facility for Sodium Sulfur Battery.
- (3) Heat Pipe Temperature Dependent Fluid Properties Data, Between 300 C and 400 C, Mainstream Engineering Corporation.
- (4) Material Safety Data Sheets for the Working Fluids.
- (5) Results from the HTPIPE computer analyses.

REFERENCES:

- (1) Memorandum, D. Gluck to M. Corrigan, Subject: Heat Pipes and Test Facility for Sodium Sulfur Battery, 2 May 1994.
- (2) R&D Status Report #22, Characterization and Testing of Novel Two-Phase Working Fluids for Spacecraft Thermal Management Systems Operating Between 300 C and 400 C, L.R. Grzyll and N.A. Samad, Mainstream Engineering Corporation, Rockledge, Florida, 6 May 1994.
- (3) DRAFT Internal Report, Thermal Testing of Sodium Sulfur Cells, Capt. Bob Highley, 18 January 1994.
- (4) Sernka, R.P., et. al., Sodium Sulfur Battery Radiator Development (NaSBRD) Final Report, Hughes Aircraft Company Industrial Electronics Group, Torrance, CA., April 1992, WL-TR-92-2013.
- (5) Sernka, R.P., et. al., High Energy Density Rechargeable Battery Interim Report, Hughes Aircraft Company Industrial Electronics Group, Torrance, CA., January 1990, WRDC-TR-89-2131.
- (6) Heat Pipe Design Handbook, Volume #1, B&K Engineering, Inc., Towson, Maryland, N81-70112.
- (7) Heat Pipes, 3rd Edition, P.D. Dunn and D.A. Reay, Pergamon Press, 1982.
- (8) Woloshun, K.A., Merrigan, M.A., and Best E.D., HTPIPE: A Steady-State Heat Pipe Analysis Program, A User's Manual, Los Alamos National Laboratory, Los Alamos New Mexico, November 1988, LA-11324-M.

dynatherm CORPORATION

D-WBB-4221

1 Beaver Court ■ P.O. Box 398
Cockeysville, MD 21030
Telephone (410) 584-7500
FAX (410) 584-7503

September 15, 1994

Orion International Technologies, Inc.
6501 Americas Parkway N.E., Suite #200
Albuquerque, NM 87110

FAXED
9-15-94

ATTN: Anthony Gurule
Staff Engineer

Gentlemen:

Dynatherm is pleased to respond to your verbal request and to submit a quotation for stainless steel heat pipes. This letter is divided into two parts: (1) a discussion of the technical requirements and (2) the quotation for a baseline program as well as for several options.

Discussion of Requirements

The technical requirements are described in memos by Anthony Gurule and Don Gluck; back-up calculations were also provided. A total of twelve (12) heat pipes are required, four (4) each of three (3) different designs. The pipes are intended for operation in the 300 to 400°C temperature range; they are to be fabricated from stainless steel; there are three different groove geometries, each optimized for a different working fluid. The fluids have been identified only by numbers (1, 2, and 3); but it appears that fluid #1 is biphenyl, #2 terphenyl, and #3 naphthalene. Naphthalene has been used extensively in commercial heat pipe heat exchangers, biphenyl is one of the two constituents of Dowtherm A (the other being biphenyl-oxide) which has also been used as a heat pipe working fluid.

We reviewed the analysis leading to the selected heat pipe design and would like to offer a few comments and suggestions. The analysis is based on the models in the B&K edition of the Heat Pipe Design Handbook (the original version of this handbook was written by Dynatherm). The analysis is basically correct but there is a question as to the practicality of the selected designs.

1. The grooves in all three designs have a relatively wide opening (1.35 to 1.83 mm) resulting in very low static heights and consequently, in a design which is very sensitive to orientation. We understand how this design was selected. First, a test orientation of 1.25 mm was chosen and then the "textbook" optimization for the static height was applied:

$$(\tau_p)_{opt} = 4H/3h_c$$

While mathematically correct, it results in a design which will be very difficult to test. It can be shown that the relative error $\Delta(QL)$ due to tolerances in the test orientation Δh is given by:

$$\Delta(QL)/(QL) = |1/(1-\alpha)*\Delta h/h_{stat}|$$

where h_{stat} is the static height and α is the ratio of test orientation to static height ($\alpha = h/h_{stat}$).

Let's look at a typical example: the selected h_{stat} is 1.875 mm, the test orientation 1.25 mm, yielding $\alpha = .667$. Since it will be difficult to level the heat pipe to better than 0.25 mm (0.010"), the above equation predicts an uncertainty of 40% in the measurement of QL! The problem has really two causes: using wide grooves which yield a very low static height and selecting a test point which is at 67% of the static height. By comparison, typical aluminum/ammonia aerospace heat pipes have static heights of 0.5" and are acceptance tested at an elevation of 0.1". The error predicted by the above equation is then only 2.5%.

2. The heat pipe analysis assumes that the grooves are not communicating, otherwise the upper grooves in a 1" diameter pipe would drain. The resulting puddle would make interpretation of the test results very difficult, especially at the very low tilt of 1.25 mm. All manufacturers of grooved heat pipes go through great pains to ensure that the grooves are sealed at the ends and are not communicating. Nevertheless, communication is difficult to eliminate completely. Wide grooves with low capillary pumping capability are more susceptible to the effects of drainage than narrower ones which have a high static height.
3. The wall thickness of the heat pipes was selected purely on the basis of pressure containment resulting in impractical values (e.g. 0.055 mm for design #1). Actual wall thicknesses must be selected on the basis of fabricability.
4. Testing of these heat pipes may prove to be very difficult (aside from the previously mentioned problem with orientation and groove drainage). The design heat load is only 55 Watts at a test temperature of about 350°C. Assuming that the test is done in ambient environment and the adiabatic section (2 ft long) is insulated with 2" insulation, the heat loss is estimated to be about 25 Watts. While the test fixture can be calibrated for heat losses, the extra heat transport requirement must be accounted for. A better approach would be to test in vacuum or to provide a guard heater surrounding the heat pipe in order to eliminate or at least reduce heat losses. Both approaches complicate the test fixture considerably.

Proposal

1. Baseline

The baseline proposal consist of the fabrication and processing of 12 heat pipes in accordance with the designs given in the referenced memos. Since the designs for fluids #1 and #2 are essentially identical, we propose to fabricate only two different groove geometries (4 pipes of one and 8 pipes of the other). The pipes will be fabricated by machining the grooves in the planar configuration and then forming the tubular heat pipes. The material will be type 316 stainless steel. The pipes will be processed (leak testing, cleaning, outgassing) using standard aerospace procedures. They will be charged, in groups of 4, with three different fluids specified by the customer. All heat pipes will be operated in the reflux mode for no less than 8 hours at 350°C. Afterwards, all non-condensable gas will be removed, isothermal operation verified, and the pipes sealed. No performance testing is planned as part of the baseline option.

The price for this baseline program is as follows:

Non-recurring Manufacturing Development	\$16,000
Recurring Price per Heat Pipe	\$1,500
Total Price for 12 Heat Pipes	<u>\$34,000</u>

2. Option 1

Option 1 consists of developing a performance test fixture, calibrating the fixture and testing of selected heat pipes. The test fixture will be designed for operation in an ambient laboratory environment. It will include a guard heater surrounding the evaporator and adiabatic section, and a water cooled calorimeter at the condenser. The fixture will be calibrated for heat losses and for measuring the net heat output at the condenser.

Development of Test Fixture	\$12,000
Performance Test per Heat Pipe	\$1,500
Total (assuming testing of 3 pipes)	<u>\$16,500</u>

3. Option 3

This option would consist of performing an independent optimization of the heat pipe geometry based on requirements established by the customer. We estimate a one month analysis effort for this task.

Heat Pipe Analysis and Design	\$15,000
-------------------------------	----------

Orion International Technologies, Inc.
September 15, 1994
Page 4

D-WBB-4221

We apologize for the late submittal of this proposal and hope that it will still be considered. Please do not hesitate to contact me if you have any questions.

Sincerely,

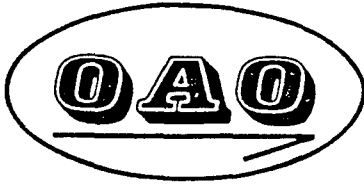
DYNATHERM CORPORATION



Walter B. Bienert
President

WBB:dna

cc: Mary Corrigan-PL/VTPT



7500 Greenway Center • Greenbelt, Maryland 20770-3585
(301) 345-0750

September 21, 1994

Mr. Larry Gryzll
Mainstream Engineering Corporation
Pines Industrial Center
200 Yellow Place
Rockledge, Florida 32955

Subject: High Temperature (300-400°C) Heat Pipe ROM Quotation

Dear Larry:

Thank you for the opportunity to quote the fabrication of heat pipes for high temperature applications in the 300-400°C range. We will utilize a stainless steel system (316L) consisting of threaded tube and composite wick to accommodate the different fluids and provide reasonable transport (~1500 watt-inches). The heat pipes will incorporate external copper saddles for heat addition and removal. We will test the heat pipes prior to charging with the high temperature fluid with Freon 113 or a similar ambient temperature fluid whose transport properties are like those of the high temperature fluids to verify heat pipe performance. Proof pressure tests of the heat pipes will also be conducted. The heat pipes will include an extended fill tube for multiple fill and pinch operations.

Our ROM price for these heat pipes which are assumed to be 2-3 feet long is as follows:

1 Pipe	6 Pipes (3 Fluids)	12 Pipes (4 Fluids)
\$8,000	\$20,000	\$30,000

Delivery of these heat pipes will be within 10 weeks ARO, FOB Greenbelt. This schedule assumes that you provide the working fluids within 6 weeks of award. Please contact me at 301-794-6300 if you have any questions.

Yours truly,

Patrick J. Brennan / jz

Patrick J. Brennan

APPENDIX D: TWO-PHASE DESIGN MANUAL

BIPHENYL

Temp (K)	Temp (C)	Vapor Pressure (kPa)	Heat of Vaporiz. (kJ/kg)	Surface Tension (dynes/cm)	Liquid Density (g/ml)	Vapor Density (g/ml)	Liquid Viscosity (cP)	Vapor Viscosity (cP)	Liquid Thermal Conductivity (W/m-K)	Liquid Transport Factor (W/m ²)	Kinematic Viscosity Ratio	Wicking Height Factor (m ²)
573.15	300	2.47E+02	2.99E+02	1.28E+01	7.88E-01	8.52E-03	2.77E-01	1.15E-02	1.08E-01	1.09E+10	3.84E+00	1.66E-06
574.15	301	2.51E+02	2.99E+02	1.27E+01	7.87E-01	8.67E-03	2.75E-01	1.15E-02	1.08E-01	1.09E+10	3.80E+00	1.65E-06
575.15	302	2.56E+02	2.98E+02	1.27E+01	7.86E-01	8.82E-03	2.73E-01	1.15E-02	1.08E-01	1.09E+10	3.77E+00	1.64E-06
576.15	303	2.60E+02	2.98E+02	1.26E+01	7.85E-01	8.98E-03	2.70E-01	1.16E-02	1.08E-01	1.09E+10	3.74E+00	1.64E-06
577.15	304	2.65E+02	2.97E+02	1.25E+01	7.84E-01	9.13E-03	2.68E-01	1.16E-02	1.07E-01	1.09E+10	3.71E+00	1.63E-06
578.15	305	2.70E+02	2.97E+02	1.25E+01	7.82E-01	9.29E-03	2.66E-01	1.16E-02	1.07E-01	1.09E+10	3.67E+00	1.63E-06
579.15	306	2.75E+02	2.96E+02	1.24E+01	7.81E-01	9.45E-03	2.64E-01	1.16E-02	1.07E-01	1.09E+10	3.64E+00	1.62E-06
580.15	307	2.80E+02	2.96E+02	1.23E+01	7.80E-01	9.61E-03	2.62E-01	1.16E-02	1.07E-01	1.09E+10	3.61E+00	1.61E-06
581.15	308	2.85E+02	2.95E+02	1.23E+01	7.79E-01	9.78E-03	2.59E-01	1.17E-02	1.07E-01	1.09E+10	3.58E+00	1.61E-06
582.15	309	2.90E+02	2.95E+02	1.22E+01	7.78E-01	9.95E-03	2.57E-01	1.17E-02	1.07E-01	1.09E+10	3.55E+00	1.60E-06
583.15	310	2.95E+02	2.95E+02	1.21E+01	7.76E-01	1.01E-02	2.55E-01	1.17E-02	1.07E-01	1.09E+10	3.53E+00	1.59E-06
584.15	311	3.00E+02	2.94E+02	1.21E+01	7.75E-01	1.03E-02	2.53E-01	1.17E-02	1.07E-01	1.09E+10	3.49E+00	1.59E-06
585.15	312	3.05E+02	2.92E+02	1.20E+01	7.74E-01	1.05E-02	2.51E-01	1.17E-02	1.06E-01	1.08E+10	3.45E+00	1.58E-06
586.15	313	3.11E+02	2.94E+02	1.19E+01	7.73E-01	1.06E-02	2.49E-01	1.18E-02	1.06E-01	1.09E+10	3.44E+00	1.57E-06
587.15	314	3.16E+02	2.93E+02	1.18E+01	7.72E-01	1.08E-02	2.47E-01	1.18E-02	1.06E-01	1.09E+10	3.41E+00	1.57E-06
588.15	315	3.22E+02	2.92E+02	1.18E+01	7.71E-01	1.10E-02	2.45E-01	1.18E-02	1.06E-01	1.08E+10	3.37E+00	1.56E-06
589.15	316	3.27E+02	2.91E+02	1.17E+01	7.69E-01	1.12E-02	2.43E-01	1.18E-02	1.06E-01	1.08E+10	3.34E+00	1.56E-06
590.15	317	3.33E+02	2.90E+02	1.17E+01	7.68E-01	1.14E-02	2.41E-01	1.19E-02	1.06E-01	1.08E+10	3.31E+00	1.55E-06
591.15	318	3.39E+02	2.89E+02	1.16E+01	7.67E-01	1.16E-02	2.39E-01	1.19E-02	1.06E-01	1.08E+10	3.28E+00	1.54E-06
592.15	319	3.44E+02	2.91E+02	1.15E+01	7.66E-01	1.17E-02	2.37E-01	1.19E-02	1.06E-01	1.08E+10	3.28E+00	1.54E-06
593.15	320	3.50E+02	2.91E+02	1.15E+01	7.65E-01	1.19E-02	2.36E-01	1.19E-02	1.05E-01	1.08E+10	3.25E+00	1.53E-06
594.15	321	3.56E+02	2.90E+02	1.14E+01	7.63E-01	1.21E-02	2.34E-01	1.19E-02	1.05E-01	1.08E+10	3.22E+00	1.52E-06
595.15	322	3.62E+02	2.89E+02	1.13E+01	7.62E-01	1.23E-02	2.32E-01	1.20E-02	1.05E-01	1.08E+10	3.19E+00	1.52E-06
596.15	323	3.68E+02	2.89E+02	1.13E+01	7.61E-01	1.25E-02	2.30E-01	1.20E-02	1.05E-01	1.08E+10	3.17E+00	1.51E-06
597.15	324	3.75E+02	2.88E+02	1.12E+01	7.60E-01	1.27E-02	2.28E-01	1.20E-02	1.05E-01	1.07E+10	3.14E+00	1.50E-06
598.15	325	3.81E+02	2.88E+02	1.11E+01	7.59E-01	1.29E-02	2.27E-01	1.20E-02	1.05E-01	1.07E+10	3.12E+00	1.50E-06
599.15	326	3.87E+02	2.88E+02	1.11E+01	7.58E-01	1.31E-02	2.25E-01	1.20E-02	1.05E-01	1.07E+10	3.10E+00	1.49E-06
600.15	327	3.94E+02	2.85E+02	1.10E+01	7.56E-01	1.34E-02	2.23E-01	1.21E-02	1.05E-01	1.06E+10	3.05E+00	1.48E-06
601.15	328	4.00E+02	2.85E+02	1.09E+01	7.55E-01	1.36E-02	2.21E-01	1.21E-02	1.04E-01	1.06E+10	3.03E+00	1.48E-06
602.15	329	4.07E+02	2.85E+02	1.09E+01	7.54E-01	1.38E-02	2.20E-01	1.21E-02	1.04E-01	1.06E+10	3.01E+00	1.47E-06
603.15	330	4.14E+02	2.85E+02	1.08E+01	7.53E-01	1.40E-02	2.18E-01	1.21E-02	1.04E-01	1.06E+10	2.99E+00	1.46E-06
604.15	331	4.20E+02	2.85E+02	1.07E+01	7.52E-01	1.42E-02	2.16E-01	1.21E-02	1.04E-01	1.06E+10	2.97E+00	1.46E-06
605.15	332	4.27E+02	2.83E+02	1.07E+01	7.51E-01	1.45E-02	2.15E-01	1.22E-02	1.04E-01	1.05E+10	2.93E+00	1.45E-06
606.15	333	4.34E+02	2.83E+02	1.06E+01	7.49E-01	1.47E-02	2.13E-01	1.22E-02	1.04E-01	1.05E+10	2.91E+00	1.44E-06
607.15	334	4.41E+02	2.83E+02	1.05E+01	7.48E-01	1.49E-02	2.12E-01	1.22E-02	1.04E-01	1.05E+10	2.90E+00	1.44E-06
608.15	335	4.48E+02	2.81E+02	1.05E+01	7.47E-01	1.52E-02	2.10E-01	1.22E-02	1.04E-01	1.05E+10	2.86E+00	1.43E-06
609.15	336	4.56E+02	2.81E+02	1.04E+01	7.46E-01	1.54E-02	2.08E-01	1.22E-02	1.03E-01	1.05E+10	2.85E+00	1.42E-06

BIPHENYL

Temp (K)	Temp (C)	Vapor Pressure (kPa)	Heat of Vaporiz. (kJ/kg)	Surface Tension (dynes/cm)	Liquid Density (g/ml)	Vapor Density (g/ml)	Liquid Viscosity (cP)	Vapor Viscosity (cP)	Liquid Thermal Conductivity (W/m-K)	Liquid Transport Factor (W/m ²)	Kinematic Viscosity Ratio	Wicking Height Factor (m ²)
610.15	337	4.63E+02	2.82E+02	1.03E+01	7.45E-01	1.56E-02	2.07E-01	1.23E-02	1.03E-01	1.05E+10	2.83E+00	1.42E-06
611.15	338	4.70E+02	2.80E+02	1.03E+01	7.44E-01	1.59E-02	2.05E-01	1.23E-02	1.03E-01	1.04E+10	2.80E+00	1.41E-06
612.15	339	4.78E+02	2.80E+02	1.02E+01	7.43E-01	1.61E-02	2.04E-01	1.23E-02	1.03E-01	1.04E+10	2.79E+00	1.40E-06
613.15	340	4.85E+02	2.79E+02	1.01E+01	7.41E-01	1.64E-02	2.02E-01	1.23E-02	1.03E-01	1.04E+10	2.75E+00	1.39E-06
614.15	341	4.93E+02	2.79E+02	1.01E+01	7.40E-01	1.66E-02	2.01E-01	1.23E-02	1.03E-01	1.04E+10	2.74E+00	1.39E-06
615.15	342	5.01E+02	2.78E+02	1.00E+01	7.39E-01	1.69E-02	1.99E-01	1.24E-02	1.03E-01	1.03E+10	2.71E+00	1.38E-06
616.15	343	5.09E+02	2.78E+02	9.94E+00	7.38E-01	1.71E-02	1.98E-01	1.24E-02	1.03E-01	1.03E+10	2.70E+00	1.37E-06
617.15	344	5.17E+02	2.77E+02	9.87E+00	7.37E-01	1.74E-02	1.96E-01	1.24E-02	1.02E-01	1.03E+10	2.67E+00	1.37E-06
618.15	345	5.25E+02	2.76E+02	9.81E+00	7.36E-01	1.77E-02	1.95E-01	1.24E-02	1.02E-01	1.02E+10	2.65E+00	1.36E-06
619.15	346	5.33E+02	2.77E+02	9.74E+00	7.35E-01	1.79E-02	1.94E-01	1.24E-02	1.02E-01	1.02E+10	2.64E+00	1.35E-06
620.15	347	5.41E+02	2.76E+02	9.68E+00	7.33E-01	1.82E-02	1.92E-01	1.25E-02	1.02E-01	1.02E+10	2.61E+00	1.35E-06
621.15	348	5.49E+02	2.75E+02	9.61E+00	7.32E-01	1.85E-02	1.91E-01	1.25E-02	1.02E-01	1.01E+10	2.59E+00	1.34E-06
622.15	349	5.58E+02	2.74E+02	9.55E+00	7.31E-01	1.88E-02	1.89E-01	1.25E-02	1.02E-01	1.01E+10	2.57E+00	1.33E-06
623.15	350	5.66E+02	2.74E+02	9.48E+00	7.30E-01	1.90E-02	1.88E-01	1.25E-02	1.02E-01	1.01E+10	2.56E+00	1.33E-06
624.15	351	5.75E+02	2.74E+02	9.42E+00	7.29E-01	1.93E-02	1.87E-01	1.26E-02	1.02E-01	1.01E+10	2.54E+00	1.32E-06
625.15	352	5.84E+02	2.73E+02	9.35E+00	7.28E-01	1.96E-02	1.85E-01	1.26E-02	1.01E-01	1.00E+10	2.52E+00	1.31E-06
626.15	353	5.93E+02	2.72E+02	9.29E+00	7.27E-01	1.99E-02	1.84E-01	1.26E-02	1.01E-01	9.97E+09	2.50E+00	1.30E-06
627.15	354	6.01E+02	2.71E+02	9.22E+00	7.26E-01	2.02E-02	1.83E-01	1.26E-02	1.01E-01	9.93E+09	2.48E+00	1.30E-06
628.15	355	6.10E+02	2.71E+02	9.16E+00	7.24E-01	2.05E-02	1.82E-01	1.26E-02	1.01E-01	9.89E+09	2.46E+00	1.29E-06
629.15	356	6.20E+02	2.70E+02	9.09E+00	7.23E-01	2.08E-02	1.80E-01	1.27E-02	1.01E-01	9.86E+09	2.44E+00	1.28E-06
630.15	357	6.29E+02	2.70E+02	9.03E+00	7.22E-01	2.11E-02	1.79E-01	1.27E-02	1.01E-01	9.82E+09	2.42E+00	1.28E-06
631.15	358	6.38E+02	2.69E+02	8.96E+00	7.21E-01	2.14E-02	1.78E-01	1.27E-02	1.01E-01	9.79E+09	2.41E+00	1.27E-06
632.15	359	6.48E+02	2.69E+02	8.90E+00	7.20E-01	2.17E-02	1.77E-01	1.27E-02	1.01E-01	9.76E+09	2.39E+00	1.26E-06
633.15	360	6.57E+02	2.69E+02	8.83E+00	7.19E-01	2.20E-02	1.75E-01	1.27E-02	1.00E-01	9.72E+09	2.37E+00	1.25E-06
634.15	361	6.67E+02	2.67E+02	8.77E+00	7.18E-01	2.24E-02	1.74E-01	1.28E-02	1.00E-01	9.65E+09	2.35E+00	1.25E-06
635.15	362	6.77E+02	2.67E+02	8.70E+00	7.17E-01	2.27E-02	1.73E-01	1.28E-02	1.00E-01	9.62E+09	2.33E+00	1.24E-06
636.15	363	6.87E+02	2.66E+02	8.64E+00	7.16E-01	2.30E-02	1.72E-01	1.28E-02	1.00E-01	9.59E+09	2.32E+00	1.23E-06
637.15	364	6.97E+02	2.65E+02	8.57E+00	7.14E-01	2.34E-02	1.71E-01	1.28E-02	1.00E-01	9.52E+09	2.29E+00	1.22E-06
638.15	365	7.07E+02	2.65E+02	8.51E+00	7.13E-01	2.37E-02	1.69E-01	1.28E-02	9.98E-02	9.49E+09	2.28E+00	1.22E-06
639.15	366	7.17E+02	2.65E+02	8.45E+00	7.12E-01	2.40E-02	1.68E-01	1.29E-02	9.97E-02	9.46E+09	2.27E+00	1.21E-06
640.15	367	7.27E+02	2.63E+02	8.38E+00	7.11E-01	2.44E-02	1.67E-01	1.29E-02	9.96E-02	9.39E+09	2.25E+00	1.20E-06
641.15	368	7.38E+02	2.63E+02	8.32E+00	7.10E-01	2.47E-02	1.66E-01	1.29E-02	9.95E-02	9.37E+09	2.23E+00	1.20E-06
642.15	369	7.48E+02	2.62E+02	8.25E+00	7.09E-01	2.51E-02	1.65E-01	1.29E-02	9.93E-02	9.30E+09	2.21E+00	1.19E-06
643.15	370	7.59E+02	2.61E+02	8.19E+00	7.08E-01	2.55E-02	1.64E-01	1.29E-02	9.92E-02	9.24E+09	2.19E+00	1.18E-06
644.15	371	7.70E+02	2.61E+02	8.12E+00	7.07E-01	2.58E-02	1.63E-01	1.30E-02	9.91E-02	9.22E+09	2.18E+00	1.17E-06
645.15	372	7.81E+02	2.60E+02	8.06E+00	7.06E-01	2.62E-02	1.62E-01	1.30E-02	9.90E-02	9.16E+09	2.16E+00	1.17E-06
646.15	373	7.92E+02	2.59E+02	8.00E+00	7.04E-01	2.66E-02	1.61E-01	1.30E-02	9.88E-02	9.10E+09	2.14E+00	1.16E-06

BIPHENYL

Temp (K)	Temp (C)	Vapor Pressure (kPa)	Heat of Vaporiz. (kJ/kg)	Surface Tension (dynes/cm)	Liquid Density (g/ml)	Vapor Density (g/ml)	Liquid Viscosity (cP)	Vapor Viscosity (cP)	Liquid Thermal Conductivity (W/m-K)	Liquid Transport Factor (W/m2)	Kinematic Viscosity Ratio	Wicking Height Factor (m2)
647.15	374	8.03E+02	2.59E+02	7.93E+00	7.03E-01	2.69E-02	1.60E-01	1.30E-02	9.87E-02	9.07E+09	2.13E+00	1.15E-06
648.15	375	8.14E+02	2.58E+02	7.87E+00	7.02E-01	2.73E-02	1.58E-01	1.30E-02	9.86E-02	9.02E+09	2.12E+00	1.14E-06
649.15	376	8.26E+02	2.58E+02	7.81E+00	7.01E-01	2.77E-02	1.57E-01	1.31E-02	9.85E-02	8.96E+09	2.10E+00	1.14E-06
650.15	377	8.37E+02	2.57E+02	7.74E+00	7.00E-01	2.81E-02	1.56E-01	1.31E-02	9.83E-02	8.91E+09	2.08E+00	1.13E-06
651.15	378	8.49E+02	2.56E+02	7.68E+00	6.99E-01	2.85E-02	1.55E-01	1.31E-02	9.82E-02	8.85E+09	2.07E+00	1.12E-06
652.15	379	8.60E+02	2.56E+02	7.62E+00	6.98E-01	2.89E-02	1.54E-01	1.31E-02	9.81E-02	8.80E+09	2.05E+00	1.11E-06
653.15	380	8.72E+02	2.55E+02	7.55E+00	6.97E-01	2.93E-02	1.53E-01	1.31E-02	9.80E-02	8.75E+09	2.04E+00	1.11E-06
654.15	381	8.84E+02	2.54E+02	7.49E+00	6.96E-01	2.97E-02	1.52E-01	1.32E-02	9.78E-02	8.70E+09	2.02E+00	1.10E-06
655.15	382	8.96E+02	2.54E+02	7.43E+00	6.95E-01	3.01E-02	1.51E-01	1.32E-02	9.77E-02	8.64E+09	2.01E+00	1.09E-06
656.15	383	9.09E+02	2.53E+02	7.36E+00	6.94E-01	3.05E-02	1.50E-01	1.32E-02	9.76E-02	8.60E+09	2.00E+00	1.08E-06
657.15	384	9.21E+02	2.52E+02	7.30E+00	6.93E-01	3.10E-02	1.49E-01	1.32E-02	9.75E-02	8.52E+09	1.98E+00	1.08E-06
658.15	385	9.34E+02	2.51E+02	7.24E+00	6.91E-01	3.14E-02	1.48E-01	1.32E-02	9.73E-02	8.47E+09	1.96E+00	1.07E-06
659.15	386	9.46E+02	2.51E+02	7.17E+00	6.90E-01	3.18E-02	1.48E-01	1.33E-02	9.72E-02	8.42E+09	1.95E+00	1.06E-06
660.15	387	9.59E+02	2.50E+02	7.11E+00	6.89E-01	3.23E-02	1.47E-01	1.33E-02	9.71E-02	8.36E+09	1.93E+00	1.05E-06
661.15	388	9.72E+02	2.49E+02	7.05E+00	6.88E-01	3.27E-02	1.46E-01	1.33E-02	9.70E-02	8.30E+09	1.92E+00	1.04E-06
662.15	389	9.85E+02	2.48E+02	6.98E+00	6.87E-01	3.32E-02	1.45E-01	1.33E-02	9.68E-02	8.23E+09	1.91E+00	1.04E-06
663.15	390	9.98E+02	2.48E+02	6.92E+00	6.86E-01	3.36E-02	1.44E-01	1.33E-02	9.67E-02	8.18E+09	1.89E+00	1.03E-06
664.15	391	1.01E+03	2.47E+02	6.86E+00	6.85E-01	3.41E-02	1.43E-01	1.34E-02	9.66E-02	8.12E+09	1.88E+00	1.02E-06
665.15	392	1.02E+03	2.46E+02	6.80E+00	6.84E-01	3.46E-02	1.42E-01	1.34E-02	9.65E-02	8.05E+09	1.86E+00	1.01E-06
666.15	393	1.04E+03	2.46E+02	6.73E+00	6.83E-01	3.50E-02	1.41E-01	1.34E-02	9.63E-02	8.00E+09	1.85E+00	1.01E-06
667.15	394	1.05E+03	2.45E+02	6.67E+00	6.82E-01	3.55E-02	1.40E-01	1.34E-02	9.62E-02	7.94E+09	1.84E+00	9.98E-07
668.15	395	1.07E+03	2.44E+02	6.61E+00	6.81E-01	3.60E-02	1.39E-01	1.34E-02	9.61E-02	7.87E+09	1.82E+00	9.91E-07
669.15	396	1.09E+03	2.43E+02	6.55E+00	6.80E-01	3.65E-02	1.39E-01	1.35E-02	9.60E-02	7.81E+09	1.81E+00	9.83E-07
670.15	397	1.09E+03	2.42E+02	6.48E+00	6.79E-01	3.70E-02	1.38E-01	1.35E-02	9.58E-02	7.74E+09	1.80E+00	9.75E-07
671.15	398	1.11E+03	2.42E+02	6.42E+00	6.78E-01	3.75E-02	1.37E-01	1.35E-02	9.57E-02	7.68E+09	1.78E+00	9.67E-07
672.15	399	1.12E+03	2.41E+02	6.36E+00	6.77E-01	3.80E-02	1.36E-01	1.35E-02	9.56E-02	7.62E+09	1.77E+00	9.59E-07
673.15	400	1.14E+03	2.40E+02	6.30E+00	6.75E-01	3.85E-02	1.35E-01	1.35E-02	9.55E-02	7.56E+09	1.76E+00	9.51E-07

PHYSICAL PROPERTIES

Chemical Formula	C12H10	Critical Temperature	789.26 K	Handling	Irritant
Formula Weight	154.21	Critical Pressure	3847 kPa	Flash Point	Possible Mutagen
CAS Number	92-52-4	Melting Point	340.85 K	Toxicity	385.93 K
		Normal Boiling Point	528.85 K		LD50 (rats): 3280 mg/kg

DECAFLUOROBIPHENYL

Temp (K)	Temp (C)	Vapor Pressure (kPa)	Heat of Vaporiz. (kJ/kg)	Surface Tension (dynes/cm)	Liquid Density (g/ml)	Vapor Density (g/ml)	Liquid Viscosity (cP)	Vapor Viscosity (cP)	Liquid Thermal Conductivity (W/m-K)	Liquid Transport Factor (W/m ²)	Kinematic Viscosity Ratio	Wicking Height Factor (m ²)
573.15	300	7.41E+02	9.82E+01	2.83E+00	1.13E+00	7.19E-02	1.94E-01	2.23E-02	4.10E-02	1.62E+09	1.81E+00	2.56E-07
574.15	301	7.54E+02	9.76E+01	2.78E+00	1.13E+00	7.34E-02	1.93E-01	2.25E-02	4.08E-02	1.58E+09	1.79E+00	2.52E-07
575.15	302	7.68E+02	9.71E+01	2.72E+00	1.12E+00	7.48E-02	1.91E-01	2.27E-02	4.05E-02	1.55E+09	1.78E+00	2.47E-07
576.15	303	7.81E+02	9.66E+01	2.66E+00	1.12E+00	7.63E-02	1.90E-01	2.29E-02	4.03E-02	1.51E+09	1.77E+00	2.43E-07
577.15	304	7.95E+02	9.59E+01	2.60E+00	1.12E+00	7.79E-02	1.89E-01	2.32E-02	4.00E-02	1.48E+09	1.76E+00	2.38E-07
578.15	305	8.09E+02	9.54E+01	2.55E+00	1.11E+00	7.94E-02	1.87E-01	2.34E-02	3.98E-02	1.44E+09	1.75E+00	2.34E-07
579.15	306	8.23E+02	9.48E+01	2.49E+00	1.11E+00	8.10E-02	1.86E-01	2.36E-02	3.95E-02	1.41E+09	1.74E+00	2.29E-07
580.15	307	8.38E+02	9.41E+01	2.43E+00	1.11E+00	8.27E-02	1.85E-01	2.38E-02	3.93E-02	1.37E+09	1.72E+00	2.25E-07
581.15	308	8.52E+02	9.36E+01	2.38E+00	1.10E+00	8.43E-02	1.84E-01	2.41E-02	3.90E-02	1.33E+09	1.71E+00	2.20E-07
582.15	309	8.67E+02	9.29E+01	2.32E+00	1.10E+00	8.60E-02	1.82E-01	2.43E-02	3.88E-02	1.30E+09	1.70E+00	2.16E-07
583.15	310	8.82E+02	9.22E+01	2.27E+00	1.09E+00	8.78E-02	1.81E-01	2.46E-02	3.85E-02	1.26E+09	1.69E+00	2.11E-07
584.15	311	8.97E+02	9.16E+01	2.21E+00	1.09E+00	8.96E-02	1.80E-01	2.48E-02	3.83E-02	1.23E+09	1.68E+00	2.07E-07
585.15	312	9.13E+02	9.10E+01	2.16E+00	1.09E+00	9.14E-02	1.79E-01	2.51E-02	3.80E-02	1.19E+09	1.67E+00	2.02E-07
586.15	313	9.28E+02	9.04E+01	2.10E+00	1.08E+00	9.32E-02	1.78E-01	2.54E-02	3.77E-02	1.16E+09	1.66E+00	1.98E-07
587.15	314	9.44E+02	8.96E+01	2.05E+00	1.08E+00	9.52E-02	1.76E-01	2.57E-02	3.75E-02	1.12E+09	1.65E+00	1.94E-07
588.15	315	9.60E+02	8.89E+01	2.00E+00	1.08E+00	9.71E-02	1.75E-01	2.60E-02	3.72E-02	1.09E+09	1.64E+00	1.89E-07
589.15	316	9.76E+02	8.82E+01	1.94E+00	1.07E+00	9.91E-02	1.74E-01	2.63E-02	3.70E-02	1.06E+09	1.63E+00	1.85E-07
590.15	317	9.93E+02	8.77E+01	1.89E+00	1.07E+00	1.01E-01	1.73E-01	2.66E-02	3.67E-02	1.02E+09	1.62E+00	1.81E-07
591.15	318	1.01E+03	8.70E+01	1.84E+00	1.06E+00	1.03E-01	1.72E-01	2.69E-02	3.64E-02	9.91E+08	1.62E+00	1.76E-07
592.15	319	1.03E+03	8.64E+01	1.79E+00	1.06E+00	1.05E-01	1.71E-01	2.73E-02	3.62E-02	9.59E+08	1.61E+00	1.72E-07
593.15	320	1.04E+03	8.50E+01	1.74E+00	1.06E+00	1.08E-01	1.70E-01	2.76E-02	3.59E-02	9.19E+08	1.59E+00	1.68E-07
595.15	322	1.08E+03	8.39E+01	1.64E+00	1.05E+00	1.12E-01	1.68E-01	2.84E-02	3.53E-02	8.59E+08	1.59E+00	1.59E-07
596.15	323	1.10E+03	8.34E+01	1.59E+00	1.04E+00	1.14E-01	1.66E-01	2.88E-02	3.51E-02	8.30E+08	1.59E+00	1.55E-07
597.15	324	1.11E+03	8.22E+01	1.54E+00	1.04E+00	1.17E-01	1.65E-01	2.92E-02	3.48E-02	7.94E+08	1.57E+00	1.51E-07
598.15	325	1.13E+03	8.17E+01	1.49E+00	1.04E+00	1.19E-01	1.64E-01	2.96E-02	3.45E-02	7.67E+08	1.57E+00	1.46E-07
599.15	326	1.15E+03	8.06E+01	1.44E+00	1.03E+00	1.22E-01	1.63E-01	3.00E-02	3.42E-02	7.33E+08	1.56E+00	1.42E-07
600.15	327	1.17E+03	8.02E+01	1.39E+00	1.03E+00	1.24E-01	1.62E-01	3.05E-02	3.39E-02	7.06E+08	1.56E+00	1.38E-07
601.15	328	1.19E+03	7.91E+01	1.34E+00	1.02E+00	1.27E-01	1.61E-01	3.10E-02	3.36E-02	6.75E+08	1.55E+00	1.34E-07
602.15	329	1.21E+03	7.81E+01	1.29E+00	1.02E+00	1.30E-01	1.60E-01	3.15E-02	3.33E-02	6.44E+08	1.54E+00	1.29E-07
603.15	330	1.23E+03	7.71E+01	1.25E+00	1.02E+00	1.33E-01	1.59E-01	3.21E-02	3.31E-02	6.14E+08	1.54E+00	1.25E-07
604.15	331	1.25E+03	7.61E+01	1.20E+00	1.01E+00	1.36E-01	1.58E-01	3.27E-02	3.28E-02	5.85E+08	1.54E+00	1.21E-07
605.15	332	1.27E+03	7.52E+01	1.16E+00	1.01E+00	1.39E-01	1.57E-01	3.33E-02	3.25E-02	5.57E+08	1.54E+00	1.17E-07
606.15	333	1.29E+03	7.44E+01	1.11E+00	1.00E+00	1.42E-01	1.56E-01	3.40E-02	3.22E-02	5.30E+08	1.54E+00	1.13E-07
607.15	334	1.31E+03	7.35E+01	1.07E+00	9.99E-01	1.45E-01	1.55E-01	3.47E-02	3.19E-02	5.04E+08	1.54E+00	1.09E-07
608.15	335	1.33E+03	7.27E+01	1.02E+00	9.95E-01	1.48E-01	1.54E-01	3.55E-02	3.15E-02	4.79E+08	1.55E+00	1.05E-07
609.15	336	1.35E+03	7.20E+01	9.78E-01	9.90E-01	1.51E-01	1.53E-01	3.63E-02	3.12E-02	4.55E+08	1.55E+00	1.01E-07
610.15	337	1.37E+03	7.07E+01	9.35E-01	9.86E-01	1.55E-01	1.52E-01	3.72E-02	3.09E-02	4.27E+08	1.55E+00	9.68E-08
611.15	338	1.39E+03	6.95E+01	8.92E-01	9.82E-01	1.59E-01	1.52E-01	3.81E-02	3.06E-02	4.02E+08	1.55E+00	9.28E-08
612.15	339	1.41E+03	6.88E+01	8.50E-01	9.77E-01	1.62E-01	1.51E-01	3.92E-02	3.03E-02	3.80E+08	1.57E+00	8.88E-08

DECAFLUOROBIPHENYL

Temp (K)	Temp (C)	Vapor Pressure (kPa)	Heat of Vaporiz. (kJ/kg)	Surface Tension (dynes/cm)	Liquid Density (g/ml)	Vapor Density (g/ml)	Liquid Viscosity (cP)	Vapor Viscosity (cP)	Liquid Thermal Conductivity (W/m-K)	Liquid Transport Factor (W/m ²)	Kinematic Viscosity Ratio	Wicking Height Factor (m ²)
613.15	340	1.44E+03	6.77E+01	8.09E-01	9.73E-01	1.66E-01	1.50E-01	4.02E-02	3.00E-02	3.56E+08	1.57E+00	8.48E-08
614.15	341	1.46E+03	6.66E+01	7.68E-01	9.68E-01	1.70E-01	1.49E-01	4.14E-02	2.96E-02	3.33E+08	1.58E+00	8.09E-08
615.15	342	1.48E+03	6.55E+01	7.28E-01	9.64E-01	1.74E-01	1.48E-01	4.27E-02	2.93E-02	3.11E+08	1.60E+00	7.70E-08
616.15	343	1.50E+03	6.45E+01	6.88E-01	9.59E-01	1.78E-01	1.47E-01	4.41E-02	2.90E-02	2.90E+08	1.62E+00	7.32E-08
617.15	344	1.53E+03	6.31E+01	6.49E-01	9.55E-01	1.83E-01	1.46E-01	4.56E-02	2.86E-02	2.68E+08	1.63E+00	6.94E-08
618.15	345	1.55E+03	6.22E+01	6.11E-01	9.50E-01	1.87E-01	1.45E-01	4.72E-02	2.83E-02	2.48E+08	1.65E+00	6.56E-08
619.15	346	1.57E+03	6.09E+01	5.73E-01	9.45E-01	1.92E-01	1.44E-01	4.90E-02	2.79E-02	2.28E+08	1.67E+00	6.18E-08
620.15	347	1.60E+03	5.97E+01	5.36E-01	9.41E-01	1.97E-01	1.44E-01	5.10E-02	2.76E-02	2.10E+08	1.70E+00	5.81E-08
621.15	348	1.62E+03	5.85E+01	4.99E-01	9.36E-01	2.02E-01	1.43E-01	5.31E-02	2.72E-02	1.92E+08	1.72E+00	5.45E-08
622.15	349	1.65E+03	5.70E+01	4.64E-01	9.31E-01	2.08E-01	1.42E-01	5.55E-02	2.68E-02	1.74E+08	1.75E+00	5.08E-08
623.15	350	1.67E+03	5.56E+01	4.29E-01	9.27E-01	2.14E-01	1.41E-01	5.81E-02	2.65E-02	1.57E+08	1.78E+00	4.72E-08
624.15	351	1.69E+03	5.46E+01	3.95E-01	9.22E-01	2.19E-01	1.40E-01	6.10E-02	2.61E-02	1.42E+08	1.83E+00	4.37E-08
625.15	352	1.72E+03	5.30E+01	3.62E-01	9.17E-01	2.26E-01	1.39E-01	6.43E-02	2.57E-02	1.26E+08	1.87E+00	4.02E-08
626.15	353	1.75E+03	5.17E+01	3.29E-01	9.12E-01	2.32E-01	1.39E-01	6.79E-02	2.53E-02	1.12E+08	1.93E+00	3.68E-08
627.15	354	1.77E+03	5.02E+01	2.98E-01	9.07E-01	2.39E-01	1.38E-01	7.21E-02	2.49E-02	9.85E+07	1.99E+00	3.35E-08
628.15	355	1.80E+03	4.85E+01	2.67E-01	9.02E-01	2.47E-01	1.37E-01	7.68E-02	2.45E-02	8.54E+07	2.05E+00	3.02E-08
629.15	356	1.82E+03	4.69E+01	2.37E-01	8.97E-01	2.55E-01	1.36E-01	8.21E-02	2.40E-02	7.34E+07	2.12E+00	2.70E-08
630.15	357	1.85E+03	4.54E+01	2.09E-01	8.93E-01	2.63E-01	1.35E-01	8.83E-02	2.36E-02	6.25E+07	2.21E+00	2.39E-08
632.15	359	1.91E+03	4.19E+01	1.55E-01	8.83E-01	2.82E-01	1.34E-01	1.04E-01	2.26E-02	4.27E+07	2.43E+00	1.79E-08
633.15	360	1.93E+03	4.02E+01	1.29E-01	8.78E-01	2.92E-01	1.33E-01		2.22E-02	3.43E+07	1.50E-08	
634.15	361	1.96E+03	3.82E+01	1.05E-01	8.73E-01	3.04E-01	1.32E-01		2.16E-02	2.65E+07	1.23E-08	
635.15	362	1.99E+03	3.61E+01	8.29E-02	8.67E-01	3.17E-01	1.32E-01		2.11E-02	1.97E+07	9.75E-09	
636.15	363	2.02E+03	3.40E+01	6.20E-02	8.62E-01	3.31E-01	1.31E-01		2.05E-02	1.39E+07	7.33E-09	
637.15	364	2.05E+03	3.17E+01	4.29E-02	8.57E-01	3.47E-01	1.30E-01		1.99E-02	8.96E+06	5.10E-09	
638.15	365	2.08E+03	2.92E+01	2.60E-02	8.52E-01	3.66E-01	1.29E-01		1.92E-02	4.99E+06	3.11E-09	
639.15	366	2.11E+03	2.66E+01	1.17E-02	8.47E-01	3.87E-01	1.29E-01		1.84E-02	2.06E+06	1.42E-09	
640.15	367	2.13E+03	2.38E+01	1.53E-03	8.42E-01	4.12E-01	1.28E-01		1.74E-02	2.39E+05	1.86E-10	

PHYSICAL PROPERTIES

Chemical Formula	C12F10	Critical Temperature	640.15 K	Handling	Irritant
Formula Weight	334.12	Critical Pressure	2134.9 kPa	Flash Point	No Data
CAS Number	434-90-2	Melting Point	339.75 K	Toxicity	No Data
		Normal Boiling Point	479.65 K		

NAPHTHALENE

Temp (K)	Temp (C)	Vapor Pressure (kPa)	Heat of Vaporiz. (kJ/kg)	Surface Tension (dyne/cm)	Liquid Density (g/ml)	Vapor Density (g/ml)	Liquid Viscosity (cP)	Vapor Viscosity (cP)	Liquid Thermal Conductivity (W/m-K)	Liquid Transport Factor (W/m ²)	Kinematic Viscosity Ratio	Wicking Height Factor (m ²)
573.15	300	4.79E+02	2.94E+02	1.30E+01	7.66E-01	1.48E-02	2.07E-01	1.17E-02	1.25E-01	1.41E+10	2.93E+00	1.73E-06
574.15	301	4.87E+02	2.93E+02	1.29E+01	7.66E-01	1.51E-02	2.06E-01	1.17E-02	1.25E-01	1.41E+10	2.89E+00	1.72E-06
575.15	302	4.95E+02	2.93E+02	1.28E+01	7.65E-01	1.53E-02	2.04E-01	1.18E-02	1.25E-01	1.41E+10	2.88E+00	1.71E-06
576.15	303	5.03E+02	2.91E+02	1.27E+01	7.64E-01	1.56E-02	2.02E-01	1.18E-02	1.25E-01	1.40E+10	2.85E+00	1.70E-06
577.15	304	5.11E+02	2.91E+02	1.27E+01	7.63E-01	1.58E-02	2.01E-01	1.18E-02	1.24E-01	1.40E+10	2.84E+00	1.69E-06
578.15	305	5.19E+02	2.92E+02	1.26E+01	7.62E-01	1.60E-02	1.99E-01	1.18E-02	1.24E-01	1.40E+10	2.83E+00	1.68E-06
579.15	306	5.27E+02	2.90E+02	1.25E+01	7.61E-01	1.63E-02	1.98E-01	1.18E-02	1.24E-01	1.40E+10	2.80E+00	1.67E-06
580.15	307	5.36E+02	2.91E+02	1.24E+01	7.61E-01	1.65E-02	1.96E-01	1.19E-02	1.24E-01	1.40E+10	2.79E+00	1.66E-06
581.15	308	5.44E+02	2.89E+02	1.23E+01	7.60E-01	1.68E-02	1.95E-01	1.19E-02	1.24E-01	1.39E+10	2.76E+00	1.65E-06
582.15	309	5.53E+02	2.88E+02	1.22E+01	7.59E-01	1.71E-02	1.93E-01	1.19E-02	1.24E-01	1.39E+10	2.74E+00	1.64E-06
583.15	310	5.61E+02	2.88E+02	1.21E+01	7.58E-01	1.73E-02	1.92E-01	1.19E-02	1.24E-01	1.39E+10	2.73E+00	1.64E-06
584.15	311	5.70E+02	2.87E+02	1.21E+01	7.57E-01	1.76E-02	1.90E-01	1.20E-02	1.24E-01	1.38E+10	2.71E+00	1.63E-06
585.15	312	5.79E+02	2.86E+02	1.20E+01	7.56E-01	1.79E-02	1.89E-01	1.20E-02	1.24E-01	1.38E+10	2.68E+00	1.62E-06
586.15	313	5.88E+02	2.87E+02	1.19E+01	7.55E-01	1.81E-02	1.87E-01	1.20E-02	1.24E-01	1.38E+10	2.67E+00	1.61E-06
587.15	314	5.97E+02	2.86E+02	1.18E+01	7.54E-01	1.84E-02	1.86E-01	1.20E-02	1.24E-01	1.37E+10	2.65E+00	1.60E-06
588.15	315	6.07E+02	2.85E+02	1.17E+01	7.53E-01	1.87E-02	1.84E-01	1.20E-02	1.24E-01	1.37E+10	2.63E+00	1.59E-06
589.15	316	6.16E+02	2.84E+02	1.16E+01	7.52E-01	1.90E-02	1.83E-01	1.21E-02	1.24E-01	1.36E+10	2.61E+00	1.58E-06
590.15	317	6.25E+02	2.83E+02	1.16E+01	7.51E-01	1.93E-02	1.81E-01	1.21E-02	1.24E-01	1.36E+10	2.59E+00	1.57E-06
591.15	318	6.35E+02	2.84E+02	1.15E+01	7.50E-01	1.95E-02	1.80E-01	1.21E-02	1.24E-01	1.36E+10	2.59E+00	1.56E-06
592.15	319	6.45E+02	2.83E+02	1.14E+01	7.49E-01	1.98E-02	1.79E-01	1.21E-02	1.24E-01	1.35E+10	2.57E+00	1.55E-06
593.15	320	6.54E+02	2.83E+02	1.13E+01	7.48E-01	2.01E-02	1.77E-01	1.21E-02	1.24E-01	1.35E+10	2.55E+00	1.54E-06
594.15	321	6.64E+02	2.82E+02	1.12E+01	7.47E-01	2.04E-02	1.76E-01	1.22E-02	1.24E-01	1.35E+10	2.53E+00	1.53E-06
595.15	322	6.74E+02	2.82E+02	1.11E+01	7.46E-01	2.07E-02	1.75E-01	1.22E-02	1.24E-01	1.34E+10	2.52E+00	1.52E-06
596.15	323	6.84E+02	2.80E+02	1.11E+01	7.45E-01	2.11E-02	1.73E-01	1.22E-02	1.24E-01	1.33E+10	2.49E+00	1.51E-06
597.15	324	6.95E+02	2.79E+02	1.10E+01	7.44E-01	2.14E-02	1.72E-01	1.22E-02	1.24E-01	1.33E+10	2.47E+00	1.50E-06
598.15	325	7.05E+02	2.79E+02	1.09E+01	7.43E-01	2.17E-02	1.71E-01	1.22E-02	1.24E-01	1.32E+10	2.46E+00	1.50E-06
599.15	326	7.16E+02	2.78E+02	1.08E+01	7.42E-01	2.20E-02	1.70E-01	1.23E-02	1.24E-01	1.32E+10	2.44E+00	1.49E-06
600.15	327	7.26E+02	2.78E+02	1.07E+01	7.41E-01	2.23E-02	1.68E-01	1.23E-02	1.24E-01	1.31E+10	2.43E+00	1.48E-06
601.15	328	7.37E+02	2.77E+02	1.06E+01	7.40E-01	2.27E-02	1.67E-01	1.23E-02	1.24E-01	1.30E+10	2.40E+00	1.47E-06
602.15	329	7.48E+02	2.76E+02	1.06E+01	7.39E-01	2.30E-02	1.66E-01	1.23E-02	1.24E-01	1.30E+10	2.39E+00	1.46E-06
603.15	330	7.59E+02	2.76E+02	1.05E+01	7.38E-01	2.33E-02	1.65E-01	1.24E-02	1.23E-01	1.30E+10	2.38E+00	1.45E-06
604.15	331	7.70E+02	2.75E+02	1.04E+01	7.36E-01	2.37E-02	1.63E-01	1.24E-02	1.23E-01	1.29E+10	2.35E+00	1.44E-06
605.15	332	7.81E+02	2.75E+02	1.03E+01	7.35E-01	2.40E-02	1.62E-01	1.24E-02	1.23E-01	1.28E+10	2.34E+00	1.43E-06
606.15	333	7.92E+02	2.73E+02	1.02E+01	7.34E-01	2.44E-02	1.61E-01	1.24E-02	1.23E-01	1.27E+10	2.32E+00	1.42E-06
607.15	334	8.04E+02	2.73E+02	1.01E+01	7.33E-01	2.47E-02	1.60E-01	1.24E-02	1.23E-01	1.27E+10	2.31E+00	1.41E-06
608.15	335	8.15E+02	2.72E+02	1.01E+01	7.32E-01	2.51E-02	1.59E-01	1.25E-02	1.23E-01	1.26E+10	2.29E+00	1.40E-06
609.15	336	8.27E+02	2.72E+02	9.98E+00	7.31E-01	2.54E-02	1.58E-01	1.25E-02	1.23E-01	1.26E+10	2.28E+00	1.39E-06

NAPHTHALENE

Temp (K)	Temp (C)	Vapor Pressure (kPa)	Heat of Vaporiz. (kJ/kg)	Surface Tension (dyne/cm)	Liquid Density (g/ml)	Vapor Density (g/ml)	Liquid Viscosity (cP)	Vapor Viscosity (cP)	Liquid Thermal Conductivity (W/m-K)	Liquid Transport Factor (W/m ²)	Kinematic Viscosity Ratio	Wicking Height Factor (m ²)
610.15	337	8.39E+02	2.71E+02	9.90E+00	7.29E-01	2.58E-02	1.56E-01	1.25E-02	1.23E-01	1.25E+10	2.26E+00	1.39E-06
611.15	338	8.51E+02	2.70E+02	9.82E+00	7.28E-01	2.62E-02	1.55E-01	1.25E-02	1.23E-01	1.24E+10	2.24E+00	1.38E-06
612.15	339	8.63E+02	2.70E+02	9.74E+00	7.27E-01	2.65E-02	1.54E-01	1.25E-02	1.23E-01	1.24E+10	2.23E+00	1.37E-06
613.15	340	8.75E+02	2.69E+02	9.65E+00	7.26E-01	2.69E-02	1.53E-01	1.26E-02	1.23E-01	1.23E+10	2.21E+00	1.36E-06
614.15	341	8.87E+02	2.68E+02	9.57E+00	7.24E-01	2.73E-02	1.52E-01	1.26E-02	1.23E-01	1.22E+10	2.20E+00	1.35E-06
615.15	342	9.00E+02	2.68E+02	9.49E+00	7.23E-01	2.77E-02	1.51E-01	1.26E-02	1.23E-01	1.22E+10	2.18E+00	1.34E-06
616.15	343	9.12E+02	2.67E+02	9.41E+00	7.22E-01	2.81E-02	1.50E-01	1.26E-02	1.23E-01	1.21E+10	2.16E+00	1.33E-06
617.15	344	9.25E+02	2.66E+02	9.33E+00	7.20E-01	2.85E-02	1.49E-01	1.26E-02	1.23E-01	1.20E+10	2.15E+00	1.32E-06
618.15	345	9.38E+02	2.65E+02	9.25E+00	7.19E-01	2.89E-02	1.48E-01	1.27E-02	1.23E-01	1.19E+10	2.13E+00	1.31E-06
619.15	346	9.51E+02	2.65E+02	9.17E+00	7.18E-01	2.93E-02	1.47E-01	1.27E-02	1.23E-01	1.19E+10	2.12E+00	1.30E-06
620.15	347	9.64E+02	2.64E+02	9.08E+00	7.17E-01	2.97E-02	1.46E-01	1.27E-02	1.23E-01	1.18E+10	2.10E+00	1.29E-06
621.15	348	9.77E+02	2.64E+02	9.00E+00	7.15E-01	3.01E-02	1.45E-01	1.27E-02	1.23E-01	1.17E+10	2.09E+00	1.28E-06
622.15	349	9.91E+02	2.63E+02	8.92E+00	7.14E-01	3.05E-02	1.44E-01	1.28E-02	1.23E-01	1.16E+10	2.08E+00	1.28E-06
623.15	350	1.00E+03	2.62E+02	8.84E+00	7.12E-01	3.10E-02	1.43E-01	1.28E-02	1.23E-01	1.15E+10	2.06E+00	1.27E-06
624.15	351	1.02E+03	2.61E+02	8.76E+00	7.11E-01	3.14E-02	1.42E-01	1.28E-02	1.23E-01	1.15E+10	2.04E+00	1.26E-06
625.15	352	1.03E+03	2.61E+02	8.68E+00	7.10E-01	3.18E-02	1.41E-01	1.28E-02	1.23E-01	1.14E+10	2.03E+00	1.25E-06
626.15	353	1.05E+03	2.60E+02	8.60E+00	7.08E-01	3.23E-02	1.40E-01	1.28E-02	1.23E-01	1.13E+10	2.01E+00	1.24E-06
627.15	354	1.06E+03	2.59E+02	8.52E+00	7.07E-01	3.27E-02	1.39E-01	1.29E-02	1.23E-01	1.12E+10	2.00E+00	1.23E-06
628.15	355	1.07E+03	2.58E+02	8.44E+00	7.05E-01	3.32E-02	1.38E-01	1.29E-02	1.22E-01	1.11E+10	1.97E+00	1.22E-06
629.15	356	1.09E+03	2.58E+02	8.36E+00	7.04E-01	3.36E-02	1.37E-01	1.29E-02	1.22E-01	1.10E+10	1.95E+00	1.20E-06
630.15	357	1.10E+03	2.57E+02	8.28E+00	7.03E-01	3.41E-02	1.36E-01	1.29E-02	1.22E-01	1.09E+10	1.94E+00	1.19E-06
631.15	358	1.12E+03	2.56E+02	8.20E+00	7.01E-01	3.46E-02	1.35E-01	1.30E-02	1.22E-01	1.08E+10	1.92E+00	1.18E-06
632.15	359	1.13E+03	2.55E+02	8.12E+00	7.00E-01	3.51E-02	1.34E-01	1.30E-02	1.22E-01	1.07E+10	1.91E+00	1.17E-06
633.15	360	1.15E+03	2.54E+02	8.04E+00	6.98E-01	3.55E-02	1.34E-01	1.30E-02	1.22E-01	1.06E+10	1.90E+00	1.16E-06
634.15	361	1.16E+03	2.54E+02	7.96E+00	6.97E-01	3.60E-02	1.33E-01	1.30E-02	1.22E-01	1.05E+10	1.88E+00	1.16E-06
635.15	362	1.18E+03	2.53E+02	7.88E+00	6.95E-01	3.65E-02	1.32E-01	1.30E-02	1.22E-01	1.04E+10	1.87E+00	1.15E-06
636.15	363	1.19E+03	2.52E+02	7.80E+00	6.94E-01	3.70E-02	1.31E-01	1.30E-02	1.22E-01	1.03E+10	1.85E+00	1.14E-06
637.15	364	1.21E+03	2.51E+02	7.72E+00	6.92E-01	3.75E-02	1.30E-01	1.31E-02	1.22E-01	1.02E+10	1.84E+00	1.13E-06
638.15	365	1.22E+03	2.50E+02	7.64E+00	6.91E-01	3.81E-02	1.29E-01	1.31E-02	1.22E-01	1.02E+10	1.82E+00	1.12E-06
639.15	366	1.24E+03	2.49E+02	7.56E+00	6.89E-01	3.86E-02	1.28E-01	1.31E-02	1.22E-01	1.00E+10	1.81E+00	1.11E-06
640.15	367	1.26E+03	2.48E+02	7.48E+00	6.87E-01	3.91E-02	1.28E-01	1.31E-02	1.22E-01	9.92E+09	1.80E+00	1.10E-06
641.15	368	1.27E+03	2.48E+02	7.40E+00	6.86E-01	3.96E-02	1.27E-01	1.32E-02	1.22E-01	9.81E+09	1.78E+00	1.09E-06
642.15	369	1.29E+03	2.46E+02	7.32E+00	6.84E-01	4.02E-02	1.26E-01	1.32E-02	1.22E-01	9.72E+09	1.77E+00	1.08E-06
643.15	370	1.31E+03	2.46E+02	7.24E+00	6.83E-01	4.07E-02	1.25E-01	1.32E-02	1.22E-01	9.61E+09	1.75E+00	1.07E-06
644.15	371	1.32E+03	2.45E+02	7.16E+00	6.81E-01	4.13E-02	1.24E-01	1.32E-02	1.22E-01	9.49E+09	1.74E+00	1.06E-06
645.15	372	1.34E+03	2.44E+02	7.09E+00	6.79E-01	4.19E-02	1.23E-01	1.32E-02	1.22E-01	9.41E+09	1.73E+00	1.05E-06
646.15	373	1.36E+03	2.43E+02	7.01E+00	6.78E-01	4.24E-02	1.23E-01	1.33E-02	1.22E-01			

NAPHTHALENE

Temp (K)	Temp (C)	Vapor Pressure (kPa)	Heat of Vaporiz. (kJ/kg)	Surface Tension (dyne/cm)	Liquid Density (g/ml)	Vapor Density (g/ml)	Liquid Viscosity (cP)	Vapor Viscosity (cP)	Liquid Thermal Conductivity (W/m-K)	Liquid Transport Factor (W/m ²)	Kinematic Viscosity Ratio	Wicking Height Factor (m ²)
647.15	374	1.37E+03	2.42E+02	6.93E+00	6.76E-01	4.30E-02	1.22E-01	1.33E-02	1.22E-01	9.30E+09	1.71E+00	1.05E-06
648.15	375	1.39E+03	2.41E+02	6.85E+00	6.75E-01	4.36E-02	1.21E-01	1.33E-02	1.22E-01	9.19E+09	1.70E+00	1.04E-06
649.15	376	1.41E+03	2.40E+02	6.77E+00	6.73E-01	4.42E-02	1.20E-01	1.33E-02	1.22E-01	9.08E+09	1.68E+00	1.03E-06
650.15	377	1.42E+03	2.39E+02	6.69E+00	6.71E-01	4.48E-02	1.20E-01	1.33E-02	1.22E-01	8.98E+09	1.67E+00	1.02E-06
651.15	378	1.44E+03	2.38E+02	6.62E+00	6.70E-01	4.54E-02	1.19E-01	1.34E-02	1.22E-01	8.87E+09	1.66E+00	1.01E-06
652.15	379	1.46E+03	2.37E+02	6.54E+00	6.68E-01	4.60E-02	1.18E-01	1.34E-02	1.22E-01	8.77E+09	1.64E+00	9.99E-07
653.15	380	1.48E+03	2.36E+02	6.46E+00	6.66E-01	4.66E-02	1.17E-01	1.34E-02	1.22E-01	8.67E+09	1.63E+00	9.90E-07
654.15	381	1.50E+03	2.35E+02	6.38E+00	6.64E-01	4.73E-02	1.17E-01	1.34E-02	1.21E-01	8.55E+09	1.62E+00	9.80E-07
655.15	382	1.52E+03	2.34E+02	6.30E+00	6.63E-01	4.79E-02	1.16E-01	1.34E-02	1.21E-01	8.44E+09	1.60E+00	9.71E-07
656.15	383	1.53E+03	2.33E+02	6.23E+00	6.61E-01	4.86E-02	1.15E-01	1.35E-02	1.21E-01	8.33E+09	1.59E+00	9.62E-07
657.15	384	1.55E+03	2.32E+02	6.15E+00	6.59E-01	4.92E-02	1.15E-01	1.35E-02	1.21E-01	8.23E+09	1.58E+00	9.52E-07
658.15	385	1.57E+03	2.31E+02	6.07E+00	6.57E-01	4.99E-02	1.14E-01	1.35E-02	1.21E-01	8.11E+09	1.56E+00	9.43E-07
659.15	386	1.59E+03	2.30E+02	6.00E+00	6.56E-01	5.06E-02	1.13E-01	1.35E-02	1.21E-01	7.99E+09	1.55E+00	9.33E-07
660.15	387	1.61E+03	2.29E+02	5.92E+00	6.54E-01	5.12E-02	1.12E-01	1.35E-02	1.21E-01	7.90E+09	1.54E+00	9.24E-07
661.15	388	1.63E+03	2.28E+02	5.84E+00	6.52E-01	5.19E-02	1.12E-01	1.36E-02	1.21E-01	7.78E+09	1.53E+00	9.14E-07
662.15	389	1.65E+03	2.27E+02	5.77E+00	6.50E-01	5.26E-02	1.11E-01	1.36E-02	1.21E-01	7.67E+09	1.51E+00	9.05E-07
663.15	390	1.67E+03	2.26E+02	5.69E+00	6.48E-01	5.34E-02	1.10E-01	1.36E-02	1.21E-01	7.55E+09	1.50E+00	8.96E-07
664.15	391	1.69E+03	2.25E+02	5.61E+00	6.46E-01	5.41E-02	1.10E-01	1.36E-02	1.21E-01	7.44E+09	1.48E+00	8.86E-07
665.15	392	1.71E+03	2.24E+02	5.54E+00	6.45E-01	5.48E-02	1.09E-01	1.37E-02	1.21E-01	7.33E+09	1.47E+00	8.77E-07
666.15	393	1.73E+03	2.23E+02	5.46E+00	6.43E-01	5.56E-02	1.08E-01	1.37E-02	1.21E-01	7.21E+09	1.46E+00	8.67E-07
667.15	394	1.75E+03	2.22E+02	5.39E+00	6.41E-01	5.63E-02	1.08E-01	1.37E-02	1.21E-01	7.10E+09	1.45E+00	8.57E-07
668.15	395	1.77E+03	2.20E+02	5.31E+00	6.39E-01	5.71E-02	1.07E-01	1.37E-02	1.21E-01	6.98E+09	1.43E+00	8.48E-07
669.15	396	1.79E+03	2.19E+02	5.23E+00	6.37E-01	5.79E-02	1.06E-01	1.37E-02	1.21E-01	6.86E+09	1.42E+00	8.38E-07
670.15	397	1.81E+03	2.18E+02	5.16E+00	6.35E-01	5.86E-02	1.06E-01	1.38E-02	1.21E-01	6.76E+09	1.41E+00	8.29E-07
671.15	398	1.83E+03	2.17E+02	5.08E+00	6.33E-01	5.94E-02	1.05E-01	1.38E-02	1.21E-01	6.65E+09	1.40E+00	8.19E-07
672.15	399	1.85E+03	2.16E+02	5.01E+00	6.31E-01	6.03E-02	1.05E-01	1.38E-02	1.21E-01	6.52E+09	1.38E+00	8.09E-07
673.15	400	1.88E+03	2.15E+02	4.93E+00	6.29E-01	6.11E-02	1.04E-01	1.38E-02	1.21E-01	6.41E+09	1.37E+00	8.00E-07

PHYSICAL PROPERTIES

Chemical Formula	C10H8	Critical Temperature	748.35 K	Handling	Irritant
Formula Weight	128.17	Critical Pressure	4051 kPa	Flash Point	Possible Carcinogen
CAS Number	91-20-3	Melting Point	353.15 K	Toxicity	353.15 K
		Normal Boiling Point	492.35 K		Toxic

QUINOLINE

Temp (K)	Temp (C)	Vapor Pressure (kPa)	Heat of Vaporiz. (kJ/kg)	Surface Tension (dyne/cm)	Liquid Density (g/ml)	Vapor Density (g/ml)	Liquid Viscosity (cP)	Vapor Viscosity (cP)	Liquid Thermal Conductivity (W/m-K)	Liquid Transport Factor (W/m ²)	Kinematic Viscosity Ratio	Wicking Height Factor (m ²)
573.15	300	3.50E+02	3.33E+02	1.53E+01	8.55E-01	1.03E-02	2.28E-01	1.23E-02	8.97E-02	1.91E+10	4.48E+00	1.83E-06
574.15	301	3.56E+02	3.31E+02	1.52E+01	8.53E-01	1.05E-02	2.26E-01	1.23E-02	8.94E-02	1.90E+10	4.43E+00	1.82E-06
575.15	302	3.62E+02	3.30E+02	1.51E+01	8.51E-01	1.07E-02	2.25E-01	1.23E-02	8.92E-02	1.89E+10	4.37E+00	1.81E-06
576.15	303	3.68E+02	3.28E+02	1.50E+01	8.50E-01	1.09E-02	2.23E-01	1.24E-02	8.90E-02	1.88E+10	4.32E+00	1.80E-06
577.15	304	3.75E+02	3.30E+02	1.49E+01	8.48E-01	1.10E-02	2.22E-01	1.24E-02	8.88E-02	1.89E+10	4.31E+00	1.80E-06
578.15	305	3.81E+02	3.29E+02	1.48E+01	8.46E-01	1.12E-02	2.20E-01	1.24E-02	8.86E-02	1.88E+10	4.26E+00	1.79E-06
579.15	306	3.88E+02	3.28E+02	1.47E+01	8.45E-01	1.14E-02	2.19E-01	1.24E-02	8.84E-02	1.87E+10	4.21E+00	1.78E-06
580.15	307	3.94E+02	3.27E+02	1.46E+01	8.43E-01	1.16E-02	2.17E-01	1.24E-02	8.81E-02	1.86E+10	4.17E+00	1.77E-06
581.15	308	4.01E+02	3.26E+02	1.45E+01	8.41E-01	1.18E-02	2.16E-01	1.25E-02	8.79E-02	1.85E+10	4.12E+00	1.77E-06
582.15	309	4.08E+02	3.25E+02	1.45E+01	8.39E-01	1.20E-02	2.14E-01	1.25E-02	8.77E-02	1.84E+10	4.08E+00	1.76E-06
583.15	310	4.14E+02	3.25E+02	1.44E+01	8.38E-01	1.22E-02	2.13E-01	1.25E-02	8.75E-02	1.84E+10	4.04E+00	1.75E-06
584.15	311	4.21E+02	3.24E+02	1.43E+01	8.36E-01	1.24E-02	2.11E-01	1.25E-02	8.73E-02	1.83E+10	4.00E+00	1.74E-06
585.15	312	4.28E+02	3.23E+02	1.42E+01	8.34E-01	1.26E-02	2.10E-01	1.26E-02	8.71E-02	1.82E+10	3.96E+00	1.73E-06
586.15	313	4.36E+02	3.23E+02	1.41E+01	8.33E-01	1.28E-02	2.08E-01	1.26E-02	8.68E-02	1.82E+10	3.92E+00	1.72E-06
587.15	314	4.43E+02	3.22E+02	1.40E+01	8.31E-01	1.30E-02	2.07E-01	1.26E-02	8.66E-02	1.81E+10	3.89E+00	1.72E-06
588.15	315	4.50E+02	3.22E+02	1.39E+01	8.29E-01	1.32E-02	2.06E-01	1.26E-02	8.64E-02	1.80E+10	3.85E+00	1.71E-06
589.15	316	4.57E+02	3.22E+02	1.38E+01	8.28E-01	1.34E-02	2.04E-01	1.26E-02	8.62E-02	1.80E+10	3.82E+00	1.70E-06
590.15	317	4.65E+02	3.21E+02	1.37E+01	8.26E-01	1.36E-02	2.03E-01	1.27E-02	8.60E-02	1.79E+10	3.79E+00	1.69E-06
591.15	318	4.72E+02	3.21E+02	1.36E+01	8.24E-01	1.38E-02	2.02E-01	1.27E-02	8.58E-02	1.79E+10	3.76E+00	1.68E-06
592.15	319	4.80E+02	3.18E+02	1.35E+01	8.23E-01	1.41E-02	2.00E-01	1.27E-02	8.55E-02	1.77E+10	3.70E+00	1.68E-06
593.15	320	4.88E+02	3.18E+02	1.34E+01	8.21E-01	1.43E-02	1.99E-01	1.27E-02	8.53E-02	1.76E+10	3.67E+00	1.67E-06
594.15	321	4.96E+02	3.18E+02	1.33E+01	8.19E-01	1.45E-02	1.98E-01	1.27E-02	8.51E-02	1.75E+10	3.64E+00	1.66E-06
595.15	322	5.04E+02	3.18E+02	1.32E+01	8.18E-01	1.47E-02	1.96E-01	1.28E-02	8.49E-02	1.74E+10	3.61E+00	1.65E-06
596.15	323	5.12E+02	3.16E+02	1.31E+01	8.16E-01	1.50E-02	1.95E-01	1.28E-02	8.47E-02	1.73E+10	3.56E+00	1.64E-06
597.15	324	5.20E+02	3.16E+02	1.30E+01	8.15E-01	1.52E-02	1.94E-01	1.28E-02	8.45E-02	1.73E+10	3.54E+00	1.63E-06
598.15	325	5.28E+02	3.16E+02	1.30E+01	8.13E-01	1.54E-02	1.93E-01	1.28E-02	8.42E-02	1.71E+10	3.47E+00	1.62E-06
599.15	326	5.37E+02	3.14E+02	1.29E+01	8.11E-01	1.57E-02	1.91E-01	1.28E-02	8.40E-02	1.71E+10	3.45E+00	1.61E-06
600.15	327	5.45E+02	3.14E+02	1.28E+01	8.10E-01	1.59E-02	1.90E-01	1.29E-02	8.38E-02	1.69E+10	3.40E+00	1.60E-06
601.15	328	5.54E+02	3.13E+02	1.27E+01	8.08E-01	1.62E-02	1.89E-01	1.29E-02	8.36E-02	1.69E+10	3.38E+00	1.59E-06
602.15	329	5.62E+02	3.13E+02	1.26E+01	8.07E-01	1.64E-02	1.88E-01	1.29E-02	8.34E-02	1.68E+10	3.34E+00	1.58E-06
603.15	330	5.71E+02	3.11E+02	1.25E+01	8.05E-01	1.67E-02	1.87E-01	1.29E-02	8.32E-02	1.68E+10	3.32E+00	1.57E-06
604.15	331	5.80E+02	3.12E+02	1.24E+01	8.03E-01	1.69E-02	1.85E-01	1.29E-02	8.29E-02	1.67E+10	3.32E+00	1.57E-06
605.15	332	5.89E+02	3.10E+02	1.23E+01	8.02E-01	1.72E-02	1.84E-01	1.30E-02	8.27E-02	1.66E+10	3.28E+00	1.57E-06
606.15	333	5.98E+02	3.11E+02	1.22E+01	8.00E-01	1.74E-02	1.83E-01	1.30E-02	8.25E-02	1.66E+10	3.26E+00	1.56E-06
607.15	334	6.07E+02	3.09E+02	1.21E+01	7.99E-01	1.77E-02	1.82E-01	1.30E-02	8.23E-02	1.65E+10	3.23E+00	1.55E-06
608.15	335	6.16E+02	3.08E+02	1.20E+01	7.97E-01	1.80E-02	1.81E-01	1.30E-02	8.21E-02	1.63E+10	3.19E+00	1.54E-06
609.15	336	6.26E+02	3.08E+02	1.19E+01	7.96E-01	1.82E-02	1.80E-01	1.31E-02	8.19E-02	1.63E+10	3.17E+00	1.53E-06

QUINOLINE

Temp (K)	Temp (C)	Vapor Pressure (kPa)	Heat of Vaporiz. (kJ/kg)	Surface Tension (dyne/cm)	Liquid Density (g/ml)	Vapor Density (g/ml)	Liquid Viscosity (cP)	Vapor Viscosity (cP)	Liquid Thermal Conductivity (W/m-K)	Liquid Transport Factor (W/m ²)	Kinematic Viscosity Ratio	Wicking Height Factor (m ²)
610.15	337	6.35E+02	3.07E+02	1.19E+01	7.94E-01	1.85E-02	1.79E-01	1.31E-02	8.16E-02	1.62E+10	3.14E+00	1.52E-06
611.15	338	6.45E+02	3.06E+02	1.18E+01	7.93E-01	1.88E-02	1.78E-01	1.31E-02	8.14E-02	1.61E+10	3.11E+00	1.51E-06
612.15	339	6.54E+02	3.05E+02	1.17E+01	7.91E-01	1.91E-02	1.76E-01	1.31E-02	8.12E-02	1.60E+10	3.08E+00	1.51E-06
613.15	340	6.64E+02	3.06E+02	1.16E+01	7.89E-01	1.93E-02	1.75E-01	1.31E-02	8.10E-02	1.59E+10	3.06E+00	1.50E-06
614.15	341	6.74E+02	3.05E+02	1.15E+01	7.88E-01	1.96E-02	1.74E-01	1.32E-02	8.08E-02	1.58E+10	3.03E+00	1.49E-06
615.15	342	6.84E+02	3.04E+02	1.14E+01	7.86E-01	1.99E-02	1.73E-01	1.32E-02	8.06E-02	1.57E+10	3.01E+00	1.48E-06
616.15	343	6.94E+02	3.03E+02	1.13E+01	7.85E-01	2.02E-02	1.72E-01	1.32E-02	8.03E-02	1.56E+10	2.98E+00	1.47E-06
617.15	344	7.05E+02	3.02E+02	1.12E+01	7.83E-01	2.05E-02	1.71E-01	1.32E-02	8.01E-02	1.55E+10	2.95E+00	1.46E-06
618.15	345	7.15E+02	3.02E+02	1.11E+01	7.82E-01	2.08E-02	1.70E-01	1.32E-02	7.99E-02	1.54E+10	2.93E+00	1.45E-06
619.15	346	7.25E+02	3.01E+02	1.10E+01	7.80E-01	2.11E-02	1.69E-01	1.33E-02	7.97E-02	1.53E+10	2.90E+00	1.44E-06
620.15	347	7.35E+02	3.00E+02	1.10E+01	7.79E-01	2.14E-02	1.68E-01	1.33E-02	7.95E-02	1.53E+10	2.88E+00	1.43E-06
621.15	348	7.47E+02	3.00E+02	1.09E+01	7.77E-01	2.17E-02	1.67E-01	1.33E-02	7.93E-02	1.52E+10	2.85E+00	1.43E-06
622.15	349	7.58E+02	2.98E+02	1.08E+01	7.76E-01	2.21E-02	1.66E-01	1.33E-02	7.90E-02	1.50E+10	2.82E+00	1.42E-06
623.15	350	7.69E+02	2.98E+02	1.07E+01	7.75E-01	2.24E-02	1.65E-01	1.33E-02	7.88E-02	1.49E+10	2.79E+00	1.41E-06
624.15	351	7.80E+02	2.97E+02	1.06E+01	7.73E-01	2.27E-02	1.64E-01	1.34E-02	7.86E-02	1.48E+10	2.77E+00	1.40E-06
625.15	352	7.91E+02	2.97E+02	1.05E+01	7.72E-01	2.30E-02	1.63E-01	1.34E-02	7.84E-02	1.47E+10	2.75E+00	1.39E-06
626.15	353	8.02E+02	2.95E+02	1.04E+01	7.70E-01	2.34E-02	1.62E-01	1.34E-02	7.82E-02	1.46E+10	2.72E+00	1.38E-06
627.15	354	8.14E+02	2.95E+02	1.03E+01	7.69E-01	2.37E-02	1.61E-01	1.34E-02	7.80E-02	1.45E+10	2.70E+00	1.37E-06
628.15	355	8.25E+02	2.94E+02	1.02E+01	7.67E-01	2.40E-02	1.60E-01	1.35E-02	7.77E-02	1.44E+10	2.68E+00	1.36E-06
629.15	356	8.37E+02	2.93E+02	1.02E+01	7.66E-01	2.44E-02	1.59E-01	1.35E-02	7.75E-02	1.43E+10	2.65E+00	1.35E-06
630.15	357	8.49E+02	2.93E+02	1.01E+01	7.64E-01	2.47E-02	1.59E-01	1.35E-02	7.73E-02	1.42E+10	2.63E+00	1.34E-06
631.15	358	8.61E+02	2.91E+02	9.99E+00	7.63E-01	2.51E-02	1.58E-01	1.35E-02	7.71E-02	1.41E+10	2.61E+00	1.34E-06
632.15	359	8.73E+02	2.91E+02	9.90E+00	7.61E-01	2.54E-02	1.57E-01	1.35E-02	7.69E-02	1.40E+10	2.59E+00	1.33E-06
633.15	360	8.85E+02	2.90E+02	9.81E+00	7.60E-01	2.58E-02	1.56E-01	1.36E-02	7.67E-02	1.39E+10	2.56E+00	1.32E-06
634.15	361	8.97E+02	2.89E+02	9.73E+00	7.59E-01	2.62E-02	1.55E-01	1.36E-02	7.64E-02	1.38E+10	2.54E+00	1.31E-06
635.15	362	9.09E+02	2.89E+02	9.64E+00	7.57E-01	2.65E-02	1.54E-01	1.36E-02	7.62E-02	1.37E+10	2.52E+00	1.30E-06
636.15	363	9.22E+02	2.88E+02	9.55E+00	7.56E-01	2.69E-02	1.53E-01	1.36E-02	7.60E-02	1.36E+10	2.50E+00	1.29E-06
637.15	364	9.35E+02	2.87E+02	9.47E+00	7.54E-01	2.73E-02	1.52E-01	1.36E-02	7.58E-02	1.34E+10	2.47E+00	1.28E-06
638.15	365	9.47E+02	2.86E+02	9.38E+00	7.53E-01	2.77E-02	1.51E-01	1.37E-02	7.56E-02	1.33E+10	2.45E+00	1.27E-06
639.15	366	9.60E+02	2.86E+02	9.30E+00	7.52E-01	2.80E-02	1.51E-01	1.37E-02	7.54E-02	1.33E+10	2.44E+00	1.26E-06
640.15	367	9.74E+02	2.85E+02	9.21E+00	7.50E-01	2.84E-02	1.50E-01	1.37E-02	7.51E-02	1.31E+10	2.42E+00	1.25E-06
641.15	368	9.87E+02	2.84E+02	9.12E+00	7.49E-01	2.88E-02	1.49E-01	1.37E-02	7.49E-02	1.30E+10	2.40E+00	1.24E-06
642.15	369	1.00E+03	2.83E+02	9.04E+00	7.48E-01	2.92E-02	1.48E-01	1.37E-02	7.47E-02	1.29E+10	2.38E+00	1.23E-06
643.15	370	1.01E+03	2.82E+02	8.95E+00	7.46E-01	2.96E-02	1.47E-01	1.38E-02	7.45E-02	1.28E+10	2.36E+00	1.22E-06
644.15	371	1.03E+03	2.82E+02	8.87E+00	7.45E-01	3.00E-02	1.46E-01	1.38E-02	7.43E-02	1.27E+10	2.34E+00	1.22E-06
645.15	372	1.04E+03	2.80E+02	8.79E+00	7.43E-01	3.05E-02	1.46E-01	1.38E-02	7.41E-02	1.26E+10	2.31E+00	1.21E-06
646.15	373	1.05E+03	2.79E+02	8.70E+00	7.42E-01	3.09E-02	1.45E-01	1.38E-02	7.38E-02	1.25E+10	2.29E+00	1.20E-06

QUINOLINE

Temp (K)	Temp (C)	Vapor Pressure (kPa)	Heat of Vaporiz. (kJ/kg)	Surface Tension (dyne/cm)	Liquid Density (g/ml)	Vapor Density (g/ml)	Liquid Viscosity (cP)	Vapor Viscosity (cP)	Liquid Thermal Conductivity (W/m-K)	Liquid Transport Factor (W/m ²)	Kinematic Viscosity Ratio	Wicking Height Factor (m ²)
647.15	374	1.07E+03	2.79E+02	8.62E+00	7.41E-01	3.13E-02	1.44E-01	1.38E-02	7.36E-02	1.24E+10	2.27E+00	1.19E-06
648.15	375	1.08E+03	2.78E+02	8.53E+00	7.39E-01	3.17E-02	1.43E-01	1.39E-02	7.34E-02	1.23E+10	2.26E+00	1.18E-06
649.15	376	1.10E+03	2.77E+02	8.45E+00	7.38E-01	3.22E-02	1.42E-01	1.39E-02	7.32E-02	1.21E+10	2.23E+00	1.17E-06
650.15	377	1.11E+03	2.76E+02	8.37E+00	7.37E-01	3.26E-02	1.42E-01	1.39E-02	7.30E-02	1.20E+10	2.22E+00	1.16E-06
651.15	378	1.13E+03	2.75E+02	8.28E+00	7.35E-01	3.31E-02	1.41E-01	1.39E-02	7.28E-02	1.19E+10	2.20E+00	1.15E-06
652.15	379	1.14E+03	2.74E+02	8.20E+00	7.34E-01	3.35E-02	1.40E-01	1.39E-02	7.25E-02	1.18E+10	2.18E+00	1.14E-06
653.15	380	1.16E+03	2.73E+02	8.12E+00	7.33E-01	3.40E-02	1.39E-01	1.40E-02	7.23E-02	1.17E+10	2.16E+00	1.13E-06
654.15	381	1.17E+03	2.73E+02	8.03E+00	7.32E-01	3.44E-02	1.39E-01	1.40E-02	7.21E-02	1.16E+10	2.15E+00	1.12E-06
655.15	382	1.19E+03	2.72E+02	7.95E+00	7.30E-01	3.49E-02	1.38E-01	1.40E-02	7.19E-02	1.14E+10	2.13E+00	1.11E-06
656.15	383	1.20E+03	2.71E+02	7.87E+00	7.29E-01	3.54E-02	1.37E-01	1.40E-02	7.17E-02	1.13E+10	2.11E+00	1.10E-06
657.15	384	1.22E+03	2.70E+02	7.79E+00	7.28E-01	3.58E-02	1.36E-01	1.41E-02	7.15E-02	1.12E+10	2.09E+00	1.09E-06
658.15	385	1.23E+03	2.69E+02	7.71E+00	7.26E-01	3.63E-02	1.36E-01	1.41E-02	7.12E-02	1.11E+10	2.07E+00	1.08E-06
659.15	386	1.25E+03	2.68E+02	7.62E+00	7.25E-01	3.68E-02	1.35E-01	1.41E-02	7.10E-02	1.10E+10	2.06E+00	1.07E-06
660.15	387	1.26E+03	2.67E+02	7.54E+00	7.24E-01	3.73E-02	1.34E-01	1.41E-02	7.08E-02	1.09E+10	2.04E+00	1.06E-06
661.15	388	1.28E+03	2.66E+02	7.46E+00	7.23E-01	3.78E-02	1.34E-01	1.41E-02	7.06E-02	1.07E+10	2.02E+00	1.05E-06
662.15	389	1.30E+03	2.66E+02	7.38E+00	7.21E-01	3.83E-02	1.33E-01	1.42E-02	7.04E-02	1.06E+10	2.01E+00	1.04E-06
663.15	390	1.31E+03	2.65E+02	7.30E+00	7.20E-01	3.88E-02	1.32E-01	1.42E-02	7.02E-02	1.05E+10	1.99E+00	1.03E-06
664.15	391	1.33E+03	2.63E+02	7.22E+00	7.19E-01	3.94E-02	1.32E-01	1.42E-02	6.99E-02	1.04E+10	1.97E+00	1.02E-06
665.15	392	1.35E+03	2.62E+02	7.14E+00	7.18E-01	3.99E-02	1.31E-01	1.42E-02	6.97E-02	1.03E+10	1.95E+00	1.02E-06
666.15	393	1.36E+03	2.62E+02	7.06E+00	7.16E-01	4.04E-02	1.30E-01	1.42E-02	6.95E-02	1.02E+10	1.94E+00	1.01E-06
667.15	394	1.38E+03	2.60E+02	6.98E+00	7.15E-01	4.10E-02	1.30E-01	1.43E-02	6.93E-02	1.00E+10	1.92E+00	9.96E-07
668.15	395	1.40E+03	2.60E+02	6.90E+00	7.14E-01	4.15E-02	1.29E-01	1.43E-02	6.91E-02	9.93E+09	1.91E+00	9.86E-07
669.15	396	1.41E+03	2.58E+02	6.82E+00	7.13E-01	4.21E-02	1.28E-01	1.43E-02	6.89E-02	9.80E+09	1.89E+00	9.76E-07
670.15	397	1.43E+03	2.58E+02	6.74E+00	7.11E-01	4.26E-02	1.28E-01	1.43E-02	6.86E-02	9.69E+09	1.88E+00	9.67E-07
671.15	398	1.45E+03	2.57E+02	6.66E+00	7.10E-01	4.32E-02	1.27E-01	1.43E-02	6.84E-02	9.57E+09	1.86E+00	9.57E-07
672.15	399	1.47E+03	2.56E+02	6.58E+00	7.09E-01	4.38E-02	1.26E-01	1.44E-02	6.82E-02	9.44E+09	1.84E+00	9.47E-07
673.15	400	1.48E+03	2.55E+02	6.50E+00	7.08E-01	4.43E-02	1.26E-01	1.44E-02	6.80E-02	9.35E+09	1.83E+00	9.38E-07

PHYSICAL PROPERTIES

Chemical Formula	C9H7N	Critical Temperature	782.15 K	Handling	Irritant
Formula Weight	129.16	Critical Pressure	4660 kPa		Light-Sensitive
CAS Number	91-22-5	Melting Point	258.25 K		Possible Carcinogen
Flash Point	374.26 K	Normal Boiling Point	510.75 K	Toxicity	LD50 (rats): 460 mg/kg

o-TERPHENYL

Temp (K)	Temp (C)	Vapor Pressure (kPa)	Heat of Vaporiz. (kJ/kg)	Surface Tension (dyne/cm)	Liquid Density (g/ml)	Vapor Density (g/ml)	Liquid Viscosity (cP)	Vapor Viscosity (cP)	Liquid Thermal Conductivity (W/m-K)	Liquid Transport Factor (W/m2)	Kinematic Viscosity Ratio	Wicking Height Factor (m2)
573.15	300	4.64E+01	2.60E+02	1.74E+01	8.37E-01	2.27E-03	3.58E-01	9.09E-03	1.08E-01	1.05E+10	9.36E+00	2.12E-06
574.15	301	4.74E+01	2.60E+02	1.73E+01	8.37E-01	2.32E-03	3.56E-01	9.11E-03	1.08E-01	1.05E+10	9.22E+00	2.11E-06
575.15	302	4.85E+01	2.58E+02	1.72E+01	8.36E-01	2.38E-03	3.54E-01	9.12E-03	1.08E-01	1.05E+10	9.06E+00	2.10E-06
576.15	303	4.95E+01	2.58E+02	1.71E+01	8.36E-01	2.43E-03	3.52E-01	9.14E-03	1.08E-01	1.05E+10	8.93E+00	2.09E-06
577.15	304	5.06E+01	2.58E+02	1.70E+01	8.35E-01	2.48E-03	3.50E-01	9.16E-03	1.08E-01	1.05E+10	8.82E+00	2.08E-06
578.15	305	5.18E+01	2.57E+02	1.70E+01	8.35E-01	2.54E-03	3.48E-01	9.17E-03	1.07E-01	1.05E+10	8.67E+00	2.07E-06
579.15	306	5.29E+01	2.57E+02	1.69E+01	8.34E-01	2.59E-03	3.46E-01	9.19E-03	1.07E-01	1.05E+10	8.57E+00	2.07E-06
580.15	307	5.41E+01	2.56E+02	1.68E+01	8.34E-01	2.65E-03	3.44E-01	9.20E-03	1.07E-01	1.04E+10	8.43E+00	2.06E-06
581.15	308	5.53E+01	2.55E+02	1.67E+01	8.33E-01	2.71E-03	3.41E-01	9.22E-03	1.07E-01	1.04E+10	8.30E+00	2.05E-06
582.15	309	5.65E+01	2.55E+02	1.67E+01	8.33E-01	2.76E-03	3.39E-01	9.24E-03	1.07E-01	1.04E+10	8.21E+00	2.04E-06
583.15	310	5.77E+01	2.55E+02	1.66E+01	8.32E-01	2.82E-03	3.37E-01	9.25E-03	1.07E-01	1.04E+10	8.09E+00	2.03E-06
584.15	311	5.89E+01	2.54E+02	1.65E+01	8.32E-01	2.88E-03	3.35E-01	9.27E-03	1.07E-01	1.04E+10	7.98E+00	2.02E-06
585.15	312	6.02E+01	2.53E+02	1.64E+01	8.31E-01	2.95E-03	3.33E-01	9.28E-03	1.07E-01	1.04E+10	7.84E+00	2.02E-06
586.15	313	6.15E+01	2.53E+02	1.63E+01	8.31E-01	3.01E-03	3.32E-01	9.30E-03	1.07E-01	1.04E+10	7.74E+00	2.01E-06
587.15	314	6.28E+01	2.53E+02	1.63E+01	8.30E-01	3.07E-03	3.30E-01	9.31E-03	1.07E-01	1.04E+10	7.64E+00	2.00E-06
588.15	315	6.42E+01	2.52E+02	1.62E+01	8.30E-01	3.14E-03	3.28E-01	9.33E-03	1.06E-01	1.03E+10	7.52E+00	1.99E-06
589.15	316	6.55E+01	2.52E+02	1.61E+01	8.29E-01	3.20E-03	3.26E-01	9.35E-03	1.06E-01	1.03E+10	7.43E+00	1.98E-06
590.15	317	6.69E+01	2.51E+02	1.60E+01	8.29E-01	3.27E-03	3.24E-01	9.36E-03	1.06E-01	1.03E+10	7.32E+00	1.98E-06
591.15	318	6.83E+01	2.51E+02	1.60E+01	8.28E-01	3.34E-03	3.22E-01	9.38E-03	1.06E-01	1.03E+10	7.22E+00	1.97E-06
592.15	319	6.97E+01	2.50E+02	1.59E+01	8.27E-01	3.41E-03	3.20E-01	9.39E-03	1.06E-01	1.03E+10	7.12E+00	1.96E-06
593.15	320	7.12E+01	2.50E+02	1.58E+01	8.27E-01	3.48E-03	3.18E-01	9.41E-03	1.06E-01	1.03E+10	7.02E+00	1.95E-06
594.15	321	7.27E+01	2.49E+02	1.57E+01	8.26E-01	3.55E-03	3.17E-01	9.43E-03	1.06E-01	1.02E+10	6.93E+00	1.94E-06
595.15	322	7.42E+01	2.49E+02	1.57E+01	8.26E-01	3.62E-03	3.15E-01	9.44E-03	1.06E-01	1.02E+10	6.84E+00	1.94E-06
596.15	323	7.57E+01	2.49E+02	1.56E+01	8.25E-01	3.69E-03	3.13E-01	9.46E-03	1.06E-01	1.02E+10	6.76E+00	1.93E-06
597.15	324	7.73E+01	2.48E+02	1.55E+01	8.24E-01	3.77E-03	3.11E-01	9.47E-03	1.06E-01	1.02E+10	6.68E+00	1.92E-06
598.15	325	7.89E+01	2.47E+02	1.54E+01	8.24E-01	3.85E-03	3.09E-01	9.49E-03	1.05E-01	1.02E+10	6.56E+00	1.91E-06
599.15	326	8.05E+01	2.47E+02	1.54E+01	8.23E-01	3.92E-03	3.08E-01	9.50E-03	1.05E-01	1.02E+10	6.48E+00	1.90E-06
600.15	327	8.21E+01	2.47E+02	1.53E+01	8.23E-01	4.00E-03	3.06E-01	9.52E-03	1.05E-01	1.01E+10	6.40E+00	1.90E-06
601.15	328	8.38E+01	2.47E+02	1.52E+01	8.22E-01	4.08E-03	3.04E-01	9.54E-03	1.05E-01	1.01E+10	6.31E+00	1.89E-06
602.15	329	8.55E+01	2.46E+02	1.51E+01	8.21E-01	4.16E-03	3.03E-01	9.55E-03	1.05E-01	1.01E+10	6.23E+00	1.88E-06
603.15	330	8.72E+01	2.45E+02	1.51E+01	8.21E-01	4.25E-03	3.01E-01	9.57E-03	1.05E-01	1.01E+10	6.14E+00	1.87E-06
604.15	331	8.90E+01	2.45E+02	1.50E+01	8.20E-01	4.33E-03	2.99E-01	9.58E-03	1.05E-01	1.01E+10	6.06E+00	1.86E-06
605.15	332	9.07E+01	2.45E+02	1.49E+01	8.19E-01	4.41E-03	2.98E-01	9.60E-03	1.05E-01	1.00E+10	5.99E+00	1.86E-06
606.15	333	9.26E+01	2.44E+02	1.48E+01	8.19E-01	4.50E-03	2.96E-01	9.61E-03	1.05E-01	1.00E+10	5.91E+00	1.85E-06
607.15	334	9.44E+01	2.44E+02	1.48E+01	8.18E-01	4.59E-03	2.94E-01	9.63E-03	1.05E-01	9.99E+09	5.83E+00	1.84E-06
608.15	335	9.63E+01	2.43E+02	1.47E+01	8.17E-01	4.68E-03	2.93E-01	9.65E-03	1.04E-01	9.97E+09	5.75E+00	1.83E-06
609.15	336	9.82E+01	2.43E+02	1.46E+01	8.16E-01	4.77E-03	2.91E-01	9.66E-03	1.04E-01	9.95E+09	5.68E+00	1.83E-06

o-TERPHENYL

Temp (K)	Temp (C)	Vapor Pressure (kPa)	Heat of Vaporiz. (kJ/kg)	Surface Tension (dyne/cm)	Liquid Density (g/ml)	Vapor Density (g/ml)	Liquid Viscosity (cP)	Vapor Viscosity (cP)	Liquid Thermal Conductivity (W/m-K)	Liquid Transport Factor (W/m ²)	Kinematic Viscosity Ratio	Wicking Height Factor (m ²)
610.15	337	1.00E+02	2.43E+02	1.45E+01	8.16E-01	4.86E-03	2.90E-01	9.68E-03	1.04E-01	9.93E+09	5.61E+00	1.82E-06
611.15	338	1.02E+02	2.42E+02	1.45E+01	8.15E-01	4.95E-03	2.88E-01	9.69E-03	1.04E-01	9.92E+09	5.54E+00	1.81E-06
612.15	339	1.04E+02	2.42E+02	1.44E+01	8.14E-01	5.05E-03	2.87E-01	9.71E-03	1.04E-01	9.88E+09	5.46E+00	1.80E-06
613.15	340	1.06E+02	2.42E+02	1.43E+01	8.13E-01	5.14E-03	2.85E-01	9.72E-03	1.04E-01	9.87E+09	5.40E+00	1.80E-06
614.15	341	1.08E+02	2.41E+02	1.42E+01	8.13E-01	5.24E-03	2.84E-01	9.74E-03	1.04E-01	9.84E+09	5.33E+00	1.79E-06
615.15	342	1.10E+02	2.41E+02	1.42E+01	8.12E-01	5.34E-03	2.82E-01	9.76E-03	1.04E-01	9.82E+09	5.26E+00	1.78E-06
616.15	343	1.12E+02	2.40E+02	1.41E+01	8.11E-01	5.44E-03	2.81E-01	9.77E-03	1.04E-01	9.79E+09	5.19E+00	1.77E-06
617.15	344	1.14E+02	2.40E+02	1.40E+01	8.10E-01	5.54E-03	2.79E-01	9.79E-03	1.04E-01	9.77E+09	5.13E+00	1.77E-06
618.15	345	1.17E+02	2.39E+02	1.39E+01	8.10E-01	5.65E-03	2.78E-01	9.80E-03	1.03E-01	9.74E+09	5.06E+00	1.76E-06
619.15	346	1.19E+02	2.39E+02	1.39E+01	8.09E-01	5.75E-03	2.76E-01	9.82E-03	1.03E-01	9.72E+09	5.00E+00	1.75E-06
620.15	347	1.21E+02	2.39E+02	1.38E+01	8.08E-01	5.86E-03	2.75E-01	9.83E-03	1.03E-01	9.69E+09	4.94E+00	1.74E-06
621.15	348	1.23E+02	2.38E+02	1.37E+01	8.07E-01	5.97E-03	2.73E-01	9.85E-03	1.03E-01	9.66E+09	4.87E+00	1.74E-06
622.15	349	1.26E+02	2.38E+02	1.37E+01	8.06E-01	6.08E-03	2.72E-01	9.87E-03	1.03E-01	9.63E+09	4.81E+00	1.73E-06
623.15	350	1.28E+02	2.37E+02	1.36E+01	8.06E-01	6.19E-03	2.70E-01	9.88E-03	1.03E-01	9.61E+09	4.76E+00	1.72E-06
624.15	351	1.30E+02	2.37E+02	1.35E+01	8.05E-01	6.30E-03	2.69E-01	9.90E-03	1.03E-01	9.59E+09	4.70E+00	1.71E-06
625.15	352	1.33E+02	2.37E+02	1.34E+01	8.04E-01	6.42E-03	2.68E-01	9.91E-03	1.03E-01	9.55E+09	4.64E+00	1.71E-06
626.15	353	1.35E+02	2.36E+02	1.34E+01	8.03E-01	6.53E-03	2.66E-01	9.93E-03	1.03E-01	9.53E+09	4.59E+00	1.70E-06
627.15	354	1.38E+02	2.36E+02	1.33E+01	8.02E-01	6.65E-03	2.65E-01	9.94E-03	1.03E-01	9.50E+09	4.53E+00	1.69E-06
628.15	355	1.40E+02	2.36E+02	1.32E+01	8.01E-01	6.77E-03	2.64E-01	9.96E-03	1.02E-01	9.47E+09	4.47E+00	1.68E-06
629.15	356	1.43E+02	2.35E+02	1.32E+01	8.01E-01	6.89E-03	2.62E-01	9.98E-03	1.02E-01	9.44E+09	4.42E+00	1.68E-06
630.15	357	1.46E+02	2.35E+02	1.31E+01	8.00E-01	7.02E-03	2.61E-01	9.99E-03	1.02E-01	9.41E+09	4.36E+00	1.67E-06
631.15	358	1.48E+02	2.34E+02	1.30E+01	7.99E-01	7.14E-03	2.60E-01	1.00E-02	1.02E-01	9.38E+09	4.31E+00	1.66E-06
632.15	359	1.51E+02	2.34E+02	1.29E+01	7.98E-01	7.27E-03	2.58E-01	1.00E-02	1.02E-01	9.35E+09	4.26E+00	1.65E-06
633.15	360	1.54E+02	2.34E+02	1.29E+01	7.97E-01	7.40E-03	2.57E-01	1.00E-02	1.02E-01	9.32E+09	4.21E+00	1.65E-06
634.15	361	1.57E+02	2.33E+02	1.28E+01	7.96E-01	7.53E-03	2.56E-01	1.01E-02	1.02E-01	9.29E+09	4.16E+00	1.64E-06
635.15	362	1.59E+02	2.33E+02	1.27E+01	7.95E-01	7.66E-03	2.54E-01	1.01E-02	1.02E-01	9.26E+09	4.11E+00	1.63E-06
636.15	363	1.62E+02	2.32E+02	1.27E+01	7.94E-01	7.80E-03	2.53E-01	1.01E-02	1.02E-01	9.22E+09	4.06E+00	1.63E-06
637.15	364	1.65E+02	2.32E+02	1.26E+01	7.93E-01	7.93E-03	2.52E-01	1.01E-02	1.02E-01	9.20E+09	4.01E+00	1.62E-06
638.15	365	1.68E+02	2.32E+02	1.25E+01	7.92E-01	8.07E-03	2.51E-01	1.01E-02	1.02E-01	9.16E+09	3.96E+00	1.61E-06
639.15	366	1.71E+02	2.31E+02	1.24E+01	7.92E-01	8.21E-03	2.49E-01	1.01E-02	1.01E-01	9.13E+09	3.92E+00	1.60E-06
640.15	367	1.74E+02	2.31E+02	1.24E+01	7.91E-01	8.35E-03	2.48E-01	1.01E-02	1.01E-01	9.10E+09	3.87E+00	1.60E-06
641.15	368	1.77E+02	2.31E+02	1.23E+01	7.90E-01	8.49E-03	2.47E-01	1.02E-02	1.01E-01	9.07E+09	3.83E+00	1.59E-06
642.15	369	1.80E+02	2.30E+02	1.22E+01	7.89E-01	8.64E-03	2.46E-01	1.02E-02	1.01E-01	9.03E+09	3.78E+00	1.58E-06
643.15	370	1.83E+02	2.30E+02	1.22E+01	7.88E-01	8.79E-03	2.45E-01	1.02E-02	1.01E-01	8.99E+09	3.73E+00	1.57E-06
644.15	371	1.87E+02	2.29E+02	1.21E+01	7.87E-01	8.94E-03	2.43E-01	1.02E-02	1.01E-01	8.96E+09	3.69E+00	1.57E-06
645.15	372	1.90E+02	2.29E+02	1.20E+01	7.86E-01	9.09E-03	2.42E-01	1.02E-02	1.01E-01	8.93E+09	3.65E+00	1.56E-06
646.15	373	1.93E+02	2.29E+02	1.19E+01	7.85E-01	9.24E-03	2.41E-01	1.02E-02	1.01E-01	8.90E+09	3.61E+00	1.55E-06

o-TERPHENYL

Temp (K)	Temp (C)	Vapor Pressure (kPa)	Heat of Vaporiz. (kJ/kg)	Surface Tension (dyne/cm)	Liquid Density (g/ml)	Vapor Density (g/ml)	Liquid Viscosity (cP)	Vapor Viscosity (cP)	Liquid Thermal Conductivity (W/m-K)	Liquid Transport Factor (W/m ²)	Kinematic Viscosity Ratio	Wicking Height Factor (m ²)
647.15	374	1.96E+02	2.28E+02	1.19E+01	7.84E-01	9.40E-03	2.40E-01	1.03E-02	1.01E-01	8.86E+09	3.56E+00	1.55E-06
648.15	375	2.00E+02	2.28E+02	1.18E+01	7.83E-01	9.56E-03	2.39E-01	1.03E-02	1.01E-01	8.82E+09	3.52E+00	1.54E-06
649.15	376	2.03E+02	2.27E+02	1.17E+01	7.82E-01	9.72E-03	2.38E-01	1.03E-02	1.00E-01	8.78E+09	3.48E+00	1.53E-06
650.15	377	2.07E+02	2.27E+02	1.17E+01	7.81E-01	9.88E-03	2.37E-01	1.03E-02	1.00E-01	8.75E+09	3.44E+00	1.53E-06
651.15	378	2.10E+02	2.28E+02	1.16E+01	7.80E-01	1.00E-02	2.35E-01	1.03E-02	1.00E-01	8.75E+09	3.42E+00	1.52E-06
652.15	379	2.14E+02	2.27E+02	1.15E+01	7.79E-01	1.02E-02	2.34E-01	1.03E-02	1.00E-01	8.69E+09	3.37E+00	1.51E-06
653.15	380	2.17E+02	2.26E+02	1.15E+01	7.78E-01	1.04E-02	2.33E-01	1.03E-02	1.00E-01	8.62E+09	3.32E+00	1.50E-06
654.15	381	2.21E+02	2.27E+02	1.14E+01	7.77E-01	1.05E-02	2.32E-01	1.04E-02	9.99E-02	8.64E+09	3.30E+00	1.50E-06
655.15	382	2.25E+02	2.26E+02	1.13E+01	7.75E-01	1.07E-02	2.31E-01	1.04E-02	9.98E-02	8.58E+09	3.26E+00	1.49E-06
656.15	383	2.29E+02	2.25E+02	1.13E+01	7.74E-01	1.09E-02	2.30E-01	1.04E-02	9.97E-02	8.53E+09	3.21E+00	1.48E-06
657.15	384	2.32E+02	2.24E+02	1.12E+01	7.73E-01	1.11E-02	2.29E-01	1.04E-02	9.96E-02	8.47E+09	3.17E+00	1.48E-06
658.15	385	2.36E+02	2.23E+02	1.11E+01	7.72E-01	1.13E-02	2.28E-01	1.04E-02	9.95E-02	8.42E+09	3.13E+00	1.47E-06
659.15	386	2.40E+02	2.25E+02	1.11E+01	7.71E-01	1.14E-02	2.27E-01	1.04E-02	9.94E-02	8.44E+09	3.12E+00	1.46E-06
660.15	387	2.44E+02	2.24E+02	1.10E+01	7.70E-01	1.16E-02	2.26E-01	1.05E-02	9.93E-02	8.39E+09	3.08E+00	1.46E-06
661.15	388	2.48E+02	2.23E+02	1.09E+01	7.69E-01	1.18E-02	2.25E-01	1.05E-02	9.92E-02	8.34E+09	3.04E+00	1.45E-06
662.15	389	2.52E+02	2.23E+02	1.08E+01	7.68E-01	1.20E-02	2.24E-01	1.05E-02	9.91E-02	8.29E+09	3.00E+00	1.44E-06
663.15	390	2.56E+02	2.22E+02	1.08E+01	7.67E-01	1.22E-02	2.23E-01	1.05E-02	9.90E-02	8.25E+09	2.97E+00	1.43E-06
664.15	391	2.61E+02	2.22E+02	1.07E+01	7.66E-01	1.24E-02	2.22E-01	1.05E-02	9.89E-02	8.21E+09	2.93E+00	1.43E-06
665.15	392	2.65E+02	2.21E+02	1.06E+01	7.64E-01	1.26E-02	2.21E-01	1.05E-02	9.88E-02	8.16E+09	2.90E+00	1.42E-06
666.15	393	2.69E+02	2.21E+02	1.06E+01	7.63E-01	1.28E-02	2.20E-01	1.06E-02	9.88E-02	8.12E+09	2.87E+00	1.41E-06
667.15	394	2.73E+02	2.21E+02	1.05E+01	7.62E-01	1.30E-02	2.19E-01	1.06E-02	9.87E-02	8.08E+09	2.83E+00	1.41E-06
668.15	395	2.78E+02	2.20E+02	1.04E+01	7.61E-01	1.32E-02	2.18E-01	1.06E-02	9.86E-02	8.04E+09	2.80E+00	1.40E-06
669.15	396	2.82E+02	2.20E+02	1.04E+01	7.60E-01	1.34E-02	2.17E-01	1.06E-02	9.85E-02	8.01E+09	2.77E+00	1.39E-06
670.15	397	2.87E+02	2.20E+02	1.03E+01	7.59E-01	1.36E-02	2.16E-01	1.06E-02	9.84E-02	7.97E+09	2.74E+00	1.39E-06
671.15	398	2.91E+02	2.20E+02	1.02E+01	7.57E-01	1.38E-02	2.15E-01	1.06E-02	9.83E-02	7.94E+09	2.72E+00	1.38E-06
672.15	399	2.96E+02	2.20E+02	1.02E+01	7.56E-01	1.40E-02	2.14E-01	1.06E-02	9.82E-02	7.90E+09	2.69E+00	1.37E-06
673.15	400	3.01E+02	2.18E+02	1.01E+01	7.55E-01	1.43E-02	2.13E-01	1.07E-02	9.81E-02	7.81E+09	2.64E+00	1.37E-06

PHYSICAL PROPERTIES

Chemical Formula	C18H14	Critical Temperature	890.35 K	Handling	Irritant
Formula Weight	230.31	Critical Pressure	3901 kPa	Flash Point	435.93 K
CAS Number	84-15-1	Melting Point	327.35 K	Toxicity	Toxic
		Normal Boiling Point	611.05 K		

DISTRIBUTION LIST

AUL/LSE Bldg 1405 - 600 Chennault Circle Maxwell AFB, AL 36112-6424	1 cy
DTIC/OCP 8725 John J. Kingman Rd Ste 944 FT Belvoir, VA 22060-6218	2 cys
AFSAA/SAI 1580 Air Force Pentagon Washington, DC 20330-1580	1 cy
PL/SUL Kirtland AFB, NM 87117-5776	2 cys
PL/HO Kirtland AFB, NM 87117-5776	1 cy
Official Record Copy	
PL/VTPT/Larry Crawford	5 cys
Dr. R. V. Wick PL/VT Kirtland, AFB, NM 87117-5776	1 cy